



UNIVERSITEIT • STELLENBOSCH • UNIVERSITY  
jou kennisvenoot • your knowledge partner

# Synthesis of Mixed Metal Oxides for use as Selective Oxidation Catalysts

by Jim Sipho Mlotshweni

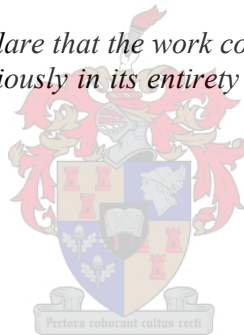
Thesis presented in partial fulfillment of  
the requirements for the degree Masters in Science Engineering  
(Chemical Engineering) at Stellenbosch University

Study leader: Dr. L. H. Callanan

March 2007

# Declaration

*I, the undersigned, hereby declare that the work contained in this thesis is my own original work and that I have not previously in its entirety or in part submitted it at any university for a degree.*



.....  
Signature

.....  
Date

## Abstract

The synthesis of mixed metal oxides, specifically the need and ability to successfully and accurately control the particle size, their stability and the reactivity of these nanoparticles is required, so as to allow the attachment of catalyst nanoparticle to the surface of a substrate or to other particles without leading to coalescence of the catalyst particle and hence to loss of their size induced properties. However, the synthesis of mixed metal oxides is a complex problem. Though various methods of preparing these types of oxides have been reported and applied, such methods they rarely produced pure forms and have often been recorded as having been contaminated with other phases. Often the particle sizes are too large in the micrometer range, and the size distribution is overly wide. Moreover, even if particles of nanometer size are formed, they tend to aggregate or agglomerate.

In the current research, microemulsions were used to synthesize the nanoparticles. Such microemulsion consists of water droplets encapsulated by surfactant molecules in a pool of oil, comprising: water in oil (w/o) or reverse micelles. Reverse micelles in the nanometer size range are thermodynamically stable and optically transparent in the solution. They are believed to be highly dynamic structures whose components rearrange themselves over time and space through interaction or collision, coalescing and redispersing. However, the advantage of this method over using the standard method is that the particle size can largely be controlled, and a narrow size distribution obtained.

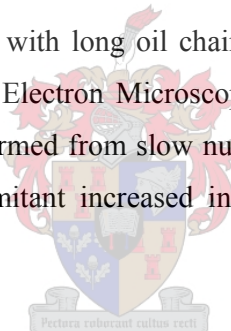
The aim of the research was to investigate the feasibility of using the reverse micelle technique for the synthesis of mixed metal oxides - specifically  $\alpha$ -bismuth molybdate ( $\alpha$ - $\text{Bi}_2\text{Mo}_3\text{O}_{12}$ ) with a controlled and desirable particle size and a narrow size distribution. Such investigation was done firstly by optimizing several parameters, including, amongst others, micelles stability during synthesis; the effect of surfactant type and oil chain length; and the effect of solution salinities. The method employed for this type of analysis was titration analysis and Dynamic Light Scattering (DLS). Secondly, the following factors were hypothesized as affecting the particle size and size distribution:

## Abstract

---

temperature; nucleation and growth; stirring; bismuth molybdate salt ratio and concentrations; and supporting of the catalyst particle. The method employed in the analysis was Transmission Electron Microscopy (TEM). Thirdly, taking into consideration all the aforementioned factors affecting particle size and size distribution, the catalyst particle was synthesized. The anticipated results regarding nanometer-sized particles can potentially apply to the study of the size-dependent effects on material properties as well as catalyst in the reactions of (amm)oxidation reactions; enabling the study of internal kinetic reactions.

The titration analysis showed that the micelles stability is independent of temperature, agitating, aging of salts and the pH of the aqueous phase. Further, the system comprising of CTAB formed micelles which proved stable at higher surfactant concentrations. Consistent with the titration analysis, a Malvern Zetasizer analysis showed that the ternary system consisting of brij 35, together with long oil chain lengths, resulted in substantially more stable micelles. Transmission Electron Microscopy showed that smaller particles with a narrow size distribution are formed from slow nucleation and exhibit a moderate increase in temperature with a concomitant increased in stirring rate. The XRD confirmed the presence of pure  $\alpha$ - $\text{Bi}_2\text{Mo}_3\text{O}_{12}$ .



# Opsomming

Die sintese van gemengde metaaloksiede – in die besonder die behoefte en vermoë om die partikelgrootte, die stabiliteit daarvan en die reaktiwiteit van hierdie nanopartikels met sukses en akkuraatheid te beheer – is noodsaaklik vir die vashegting van 'n katalisator-nanopartikel aan die oppervlak van 'n substraat of aan ander partikels sonder dat dit tot samesmelting van die katalisatorpartikel en sodoende tot die verlies van hulle groottegeïnduseerde eienskappe lei. Die sintese van gemengde metaaloksiede is egter 'n komplekse probleem. Alhoewel verskeie metodes vir die bereiding van hierdie soorte oksiede gerapporteer en toegepas is, het sodanige metodes selde suiwer vorme gelewer en is kontaminasie met ander fases dikwels gerapporteer. Die partikelgroottes is dikwels te groot in die mikrometerreikwydte, en die grootteverdeling is te wyd. Bowendien, selfs al word partikels van nanometer-grootte gevorm, is hulle geneig om te aggregeer of agglomereer.

In die huidige navorsing is mikroëmsulsies gebruik om die nanopartikels te sintetiseer. Sodanige mikroëmsulsies bestaan uit waterdruppels gekapsel met surfaktant-molekules in 'n poel olie, wat water in olie (w/o) of omgekeerde miselle vorm. Omgekeerde miselle in die nanometergrootte-reikwydte is termodinamies stabiel en opties deursigtig in die oplossing. Hulle is vermoedelik hoogs dinamiese strukture waarvan die komponente hulself oor tyd en ruimte heen herrangskik deur middel van interaksie of botsing, samesmelting en herverspreiding. Die voordeel van hierdie metode bo die standaardmetode is egter dat die partikelgrootte in 'n groot mate beheer kan word, en 'n smal grootteverdeling verkry kan word.

Die doel van die huidige navorsing was om die haalbaarheid van die gebruik van die omgekeerdemisel-tegniek vir die sintese van gemengde metaaloksiede (in die besonder  $\alpha$ -bismut-molibdaat  $\alpha\text{-Bi}_2\text{Mo}_3\text{O}_{12}$ ) met 'n beheerde en gewenste partikelgrootte en 'n smal grootteverdeling te ondersoek. Sodanige ondersoek is gedoen deur eerstens verskeie parameters te optimaliseer, met inbegrip van onder andere miselstabiliteit tydens sintese,

## Opsomming

---

die invloed van die soort surfaktant en lengte van die olieketting, en die invloed van die soutgehalte van oplossings. Titrasië-analise en dinamiese ligstrooiing (DLS) is vir hierdie soort analise gebruik. Tweedens is daar gehipotetiseer dat die volgende faktore partikelgrootte en grootteverdeling beïnvloed: temperatuur; kernvorming en groei; roering; bismut-molibdaat-sout-verhouding en die konsentrasies daarvan; en ondersteuning van die katalisatorpartikel. Transmissie-elektronmikroskopie (TEM) is vir dié analise gebruik. Dertens is die katalisatorpartikel gesintetiseer, met inagneming van al die bogenoemde faktore wat partikelgrootte en grootteverdeling beïnvloed. Die verwagte resultate ten opsigte van nanometergrootte partikels kan moontlik van toepassing wees op die studie van die grootte-afhanklike invloed op materiaaleienskappe asook as katalisators in (amm)oksidasië reaksies, wat die studie van interne kinetiese reaksies moontlik maak.

Die titrasië-analise het getoon dat miselstabiliteit onafhanklik van temperatuur, roering, die veroudering van soute en die pH van die waterige fase is. Voorts het die surfaktant CTAB miselle gevorm wat teen hoër surfaktantkonsentrasies stabiel is. In ooreenstemming met die titrasië-analise het 'n Malvern-Zetasizer-analise getoon dat die ternêre stelsel, bestaande uit brij 35, tesame met lang oliekettinglengtes, aansienlik meer stabiele miselle tot gevolg gehad het. Transmissie-elektronmikroskopie het getoon dat kleiner partikels met 'n smal grootteverdeling deur stadige kernvorming gevorm word en 'n matige toename in temperatuur met 'n gepaardgaande toename in roerspoed toon. X-straaldiffraksië het die teenwoordigheid van suiwer  $\alpha$ - $\text{Bi}_2\text{Mo}_3\text{O}_{12}$  bevestig.

# Acknowledgement

The author wishes to acknowledge and thank the following individuals and companies for their valuable contribution for the realization of this study:

- ♦ My supervisor **Dr L. H. Callanan** for advice, support and encouragement.
- ♦ The **NRF** and the **University of Stellenbosch (US)** for financial contribution.
- ♦ The **department of polymer science** at US for assisting me with the use of Malvern Zetiser HSA1000, and for their advise, support and encouragements.
- ♦ The **Electron Microscopy Unit (EMU)** at the University of Cape Town (UCT), specifically **M. A. Jaffer** for assisting with Transmission Electron Microscopy (TEM).
- ♦ **Peter van Vuuren**, for laying a foundation for me to advance this research.
- ♦ **Dr. Remy Bucher** at Ithemba labs, for running an X-Ray Diffraction (XRD) sample on my behalf.
- ♦ **Dr. W. Banda** for assisting with Statistica in analyzing stability diagrams.
- ♦ **F. Kamper and J. Steyl** for timeously organizing most materials and chemicals used in this project.
- ♦ **H. J. Botha** for organizing on my behalf all analytical equipment used in this project.
- ♦ **T. Jansen and J. Celliers** at department of biochemistry at US for assisting with the usage of the centrifuge.
- ♦ The people of the **main lab** in department of process engineering at US for support, encouragement and for always being friendly and supportive, specifically **V. Carolissen** for organizing some of the material used in this project.
- ♦ **Academic and non-academic** staff in the Department of Process Engineering at US for their contribution and assistance whenever required.
- ♦ My **colleagues** for all the great time we share together during social Fridays.
- ♦ My **family**, especially my mom **L. N. Motshweni** and my only sister **W. N. Motshweni** and my brother **E. M. Motshweni** for their patience, moral support and encouragement and for caring.
- ♦ My landlord **Mr. J. Thyse** for providing a home far away from home.
- ♦ Last but not the least, the **almighty God** for everything.

# Dedication

*In remembrance of my beloved grandmother **Maria Jiyane** (1896 - 2004); who watches over me still.*





---

# Table of Contents

## CHAPTER 1: INTRODUCTION

1.1 Introduction	2
1.2 Background Relevance	3
1.3 Methodology	
<b>1.3.1 Reverse micelle technique</b>	5
<b>1.3.2 Advantages and disadvantages of microemulsion</b>	6
1.4 Research question	6
1.5 Objective of this study	7

## CHAPTER 2: LITERATURE REVIEW

2.1 REVERSE MICROEMULSION TECHNIQUE	
<b>2.1.1 Definition</b>	9
<b>2.1.2 Appearance</b>	9
<b>2.1.3 Formation of a nanoparticle</b>	16
<b>2.1.4 Microemulsion dynamics</b>	21
<b>2.1.5 Factors affecting the particle size</b>	26
<b>2.1.6 Methods (and mechanism) of emulsification</b>	38
<b>2.1.7 Monte Carlo Simulation</b>	38
<b>2.1.8 Hypothesis</b>	45
2.2 HYPOTHESIS	47

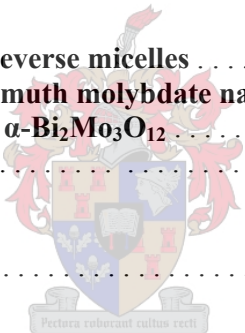
## CHAPTER 3: EXPERIMENTAL

3.1 OPTIMIZATION OF THE REVERSE MICELLE TECHNIQUE	
<b>3.1.1 Titration analysis</b>	42
<b>3.1.2 Malvern Zetasizer 1000 HSA analysis</b>	43
3.2 SYNTHESIS OF $\alpha$ -BISMUTH MOLYBDATE NANOPARTICLE	
<b>3.2.1 Preparation of Decane-Brij 35 mixture</b>	44
<b>3.2.2 Preparation of salt solution</b>	44
<b>3.2.3 Investigation into various factors</b>	45
3.3 SYNTHESIS OF A PURE $\alpha$ - $\text{Bi}_2\text{Mo}_3\text{O}_{12}$	47
3.4 ANALYTICAL TECHNIQUE	
<b>3.4.1 Analyzing by means of Malvern Zetasizer</b>	49
<b>3.4.2 Analysis on Transmission Electron Microscopy (TEM)</b>	49
<b>3.4.3 Analyzing by way of SEM</b>	59
<b>3.4.4 Analyzing by way of XRD</b>	59

## CHAPTER 4: RESULTS AND DISCUSSION

4.1 OPTIMIZATION OF REVERSE MICELLE	
<b>4.1.1 Titration analysis</b>	
4.1.1.1 Stability in a mixture of Brij 35 and hexane	52
4.1.1.2 Stability in a mixture of CTAB in pentanol and hexane	60
4.1.1.3 Stability in a mixture of brij 35 and decane	66

4.1.1.4 Stability in a mixture of CTAB in pentanol and decane . . . . .	70
4.1.1.5 Other observations . . . . .	74
4.1.1.6 Final composition . . . . .	74
<b>4.1.2 Malvern Zetisizer analysis</b>	
4.1.2.1 Stability in a mixture of Brij 35 and decane . . . . .	75
4.1.2.2 Stability in a mixture of CTAB in pentanol and decane . . . . .	82
4.1.2.3 Final composition . . . . .	86
<b>4.2 SYNTHESIS OF <math>\alpha</math>-BISMUTH MOLYBDATE NANOPARTICLES</b>	
<b>4.2.1 Effect of salt concentration on catalyst particle</b> . . . . .	87
<b>4.2.2 Effect of nucleation and growth</b> . . . . .	90
<b>4.2.3 Effect of temperature</b> . . . . .	93
<b>4.2.4 Effect of stirring</b> . . . . .	96
<b>4.2.5 Effect of salt ratio</b> . . . . .	99
<b>4.2.6 Effect of support and solvent used</b> . . . . .	101
<b>4.2.7 Operating window</b> . . . . .	103
<b>4.3 SYNTHESIS OF A PURE <math>\alpha</math>-Bi<sub>2</sub>Mo<sub>3</sub>O<sub>12</sub></b> . . . . .	104
<b>CHAPTER 5: CONCLUSION AND RECOMMENDATIONS</b>	
<b>5.1 CONCLUSION</b>	
5.1.1 Optimization of reverse micelles . . . . .	108
5.1.2 Synthesis of $\alpha$ -bismuth molybdate nanoparticle. . . . .	109
5.1.3 Synthesis of pure $\alpha$ -Bi <sub>2</sub> Mo <sub>3</sub> O <sub>12</sub> . . . . .	110
<b>5.2 RECOMMENDATIONS</b> . . . . .	111
<b>CHAPTER 6: REFERENCE</b>	
<b>REFERENCES</b> . . . . .	113
<b>CHAPTER 7: APPENDIX</b>	
APPENDIX A: MISCELLANEOUS FIGURES . . . . .	121
APPENDIX B: MISCELLANEOUS TABLES . . . . .	132
APPENDIX D1: EXPERIMENTAL DATA (TITRATION ANALYSIS) . . . . .	133
APPENDIX D2: EXPERIMENTAL DATA (MALVERN ZETASIZER) . . . . .	137
APPENDIX D3: EXPERIMENTAL DATA (PARTICLE SIZE DISTRIBUTION) . . . . .	152
APPENDIX D4: EXPERIMENTAL DATA (SYNTHESIS OF PURE $\alpha$ -Bi <sub>2</sub> Mo <sub>3</sub> O <sub>12</sub> ) . . . . .	157



# Symbols used

## ABBREVIATIONS

<b>AOT</b>	Sodium bis(2-ethylhexyl) sulfosuccinate
<b>CMC</b>	Critical Micelle Concentration
<b>CTAB</b>	Cetyltrimethylammonium Bromide
<b>DSC</b>	Differential Scanning Calorimetry
<b>DLS</b>	Dynamic Light Scattering
<b>HLB</b>	Hydrophobic- Lipophilic Balance
<b>NMR</b>	Nuclear Magnetic Resonance
<b>mm</b>	Millimeter
<b>o/w</b>	Oil in Water
<b>EO</b>	Ethylene oxide
<b>PEG</b>	Polyethelene glycol
<b>PFPE</b>	Perfluoroethercarboxylic ether
<b>PIT</b>	phase inversion temperature
<b>POE</b>	Polyoxyethylene
<b>R</b>	Principle radii for spherical droplet
<b>SANS</b>	Small Angle Neutron Scattering
<b>SAXS</b>	Small Angle X-ray Scattering
<b>SDS</b>	Sodium Dodecyl Sulphate
<b>SEM</b>	Scanning Electron Microscopy
<b>SLS</b>	Sodium Lauryl Sulfate
<b>T</b>	Temperature
<b>TEOS</b>	Tetraethylorthosilicate
<b>TEM</b>	Transmission Electron Microscopy
<b>TRFQ</b>	Time Resolve Fluorescence Quenching
<b>XRD</b>	X-Ray diffraction
<b>w/o</b>	Water in Oil

## NOMENCLATURE

<b>V</b>	Volts
<b>K</b>	Kilo (Thousand)
<b>H</b>	Mean curvature
<b>A</b>	Ampere
<b>E</b>	Activation energy
<b>k</b>	Rate constant
<b>k<sub>0</sub></b>	Pre exponential factor
<b>P<sub>A</sub></b>	Partial pressure of the reactant A
<b>P<sub>B</sub></b>	Partial pressure of the reactant B
<b>x,y</b>	Order of the reaction
<b>D</b>	Diffusion coefficient
<b>K</b>	Scattering vector
<b>n</b>	Refractive index
<b>nm</b>	Nanometer
<b>G</b>	Gibbs energy
<b>B</b>	Background value
<b>D</b>	Diffusivity of the dispersed phase
<b>V<sub>m</sub></b>	Molar volume of the disperse phase
<b>I</b>	Intensity
<b>I<sub>0</sub></b>	Intensity at zero
<b>A</b>	Amplitude
<b>B</b>	Baseline of infinite time
<b>Q</b>	Scattering
<b>D</b>	Particle diffusion coefficient
<b>h</b>	Plank's constant
<b>m<sub>e</sub></b>	Rest mass
<b>v</b>	Velocity of the electron
<b>W<sub>0</sub></b>	Water to surfactant ratio
<b>P<sub>0</sub></b>	Alcohol to surfactant ratio

## Nomenclature

---

$\mu$	Micro
$\Delta$	Change
$A$	Interfacial area
$\Delta S$	Change in Entropy
$p$	Laplace pressure
$\gamma$	Interfacial or surface tension
$\tau$	Correlation delay time
$g^{(1)}(\tau)$	Normalized correlation function of the scattered electric field
$G^{(2)}(\tau)$	Photocount correlation function
$\Gamma$	Surface excess (number of moles adsorbed per unit area)
$\lambda$	Wavelength of light
$\theta$	Scattering angle
$\eta$	Viscosity of the medium
$c^{eq}$	Dimensionless solubility of the bulk disperse phase in the medium
$\varepsilon$	Interfacial dilation module
$c(r)$	Solubility surrounding a particle radius $r$
$c(\infty)$	Bulk phase solubility
$\mu$	Chemical potential
$\mu^0$	Standard chemical potential
$a$	Activity
$w$	Ostwald ripening rate

# Chapter 1

## Introduction

*Chapter layout:* In this chapter a general introduction into the topic of this research is presented and a general background including the relevance of the research to current development is presented. In addition to an explanation of the preference for the chosen methodology, the way in which the thesis has been organised is revealed.



A journey of a thousand miles begin with single step [Lao-tzu]

## 1.1 Introduction

The synthesis of mixed metal oxides nanoparticles has attracted much interest from various research groups. The reason for this is that such nanoparticles have found a wide range of applications in many critical areas of modern technology such as in catalysis, ceramic processing, solar energy conversion processes, oil recovery, pharmaceutical applications, and photographic technology [Liu *et al.* (1998); Tomsic *et al.* (2004)] Mixed metal oxides, specifically bismuth-molybdate oxides have a chemical formula  $\text{Bi}_2\text{O}_3 \cdot n(\text{MoO}_3)$  where  $n$  could be 1, 2 or 3, corresponding to  $\gamma\text{-Bi}_2\text{MoO}_6$ ,  $\beta\text{-Bi}_2\text{Mo}_2\text{O}_9$  and  $\alpha\text{-Bi}_2\text{Mo}_3\text{O}_{12}$  respectively. The catalyst corresponding to the alpha phase is the most active catalyst [Ghule *et al.* (2004)]. This study will therefore focus on such a catalyst, in light of its importance and centrality in the (amm)oxidation of alkanes and alkenes to form olefins.

The synthesis of mixed metal nanoparticles is, however, a complex problem, because, firstly, mixed metal oxides are significantly more complex than are metal - based catalysts [Wachs (2004)]. Due to the former complexity, there is a need to develop new spectroscopic methods that allow for the analysis of solid material. Secondly, composition control must be achieved in addition to size and size distribution control [Zhang & Chang (2003)]. Various research groups [Eriksson *et al.* (2004); Ghule *et al.* (2004); Liscieski (2004)] have reported that many different approaches have already been explored for the preparation of such catalyst types including amongst others sol-gel, solid state reactions, spray drying, and coprecipitation and impregnation techniques. However, such methods have proved to be inefficient, as they rarely produce pure forms of the solid material which is often contaminated with the other phases. While the particle sizes are also too large, often being in the micrometer range, the particle distribution is also too wide [Ghule *et al.* (2004)]. In addition, other studies [Bai *et al.* (2005)] have found that even if particle of nanometre are formed, they tend to agglomerate, which influences the application of the nanoparticle's properties. In other instances [Holmberg (2004)] it was found that the nanoparticle formed were often amorphous. Significant scope therefore exists for development within this relatively new and evolving field of research.

## 1.2 Background and Relevance

Selective catalytic oxidation and (amm)oxidation processes of hydrocarbons comprise approximately one-quarter of the value produced by all catalytic process worldwide [Grasselli *et al.* (1999)]. One of the most important processes is the amm(oxidation) of propylene to acrylonitrile; which is a versatile petrochemical intermediate. By means of this process some five billion kilograms of acrylonitrile is produced in terms of the SOHIO/BP process [Grasselli *et al.* (1999)]. Not only are such processes of great commercial importance, but also they present an opportunity for significant fundamental research to take place.

Correlating the physicochemical properties of a catalyst with its catalytic performance, such as activity and selectivity, remains a key goal in selective oxidation reaction studies. The amm(oxidation) reaction of propene with oxygen and/or ammonia over a bismuth molybdate catalyst to form acrolein or acrylonitrile is often used as a test case for selective oxidation, due to the relatively simple kinetics involved. The stoichiometry of the two reactions is as follows:



The kinetic equation for the rate of reaction would be as follows:

$$-r = kP_A^x P_B^y \quad 1.1$$

$$k = k_0 \exp(-E/RT) \quad 1.2$$

Where **k**– rate constant,

**P<sub>A</sub>** – partial pressure of the reactant **A**, **P<sub>B</sub>** –partial pressure of the reactant **B**

**x,y** – order of the reaction

**k<sub>0</sub>** – pre exponential factor

**E** – activation energy

**R** – universal gas constant

and **T** – absolute temperature



The catalytic reaction of a reactant to form products consists of the following steps: the transportation of the reactant from the bulk fluid to the solid–fluid interface; the diffusion of the reactants from the boundary layer to the catalyst surface; the adsorption of reactant into the catalyst surface; the surface chemical reaction; the desorption of products from the catalyst surface; the diffusion of products from the catalyst interior to the boundary layer; and the transportation of the resulting into the bulk fluid [Hanna (2004)].

Krenzke *et al.* (1980) have argued that the propene is oxidised by means of framework oxygen atoms. The reaction rate decreases as the catalyst is steadily more depleted of framework oxygen, resulting in the need for the catalyst to be re-oxidised in order to refill the lattice oxygen in the bismuth molybdate catalyst, meaning that the kinetics of the oxidation of propene to form acrolein is controlled by the kinetics of the re-oxidation of the *bismuth-molybdate* catalyst. Moreover, since it is easier to obtain high reaction selectivity at low conversion than at high conversion, Grasselli *et al.* (2005) have stressed the importance of high catalyst selectivity also being achieved at a reasonable or acceptably high conversion, since the catalyst is to be developed for commercial use. A commercial catalyst must also have a sufficient high activity in order to be economically viable.

In addition, the preparation of high-quality nanocrystal of a desired size is a prerequisite for investigating and utilising their size-determined properties [Schevchenko *et al.* (2003)]. Therefore, relatively simple and reproducible approaches for the synthesis of crystalline nanoparticles of controlled size are of core technological interest. Further, an equally intriguing phenomenon to that of size and size distribution control is that of controlling the morphology of the particles formed [Holmberg (2004)]. The structure of the particles obtained has been postulated to be governed by the structure of the template involved, namely the spherical water droplet, the elongated droplet or the rodlike water channel. In addition, controlling particle morphology is known to be a complex process, requiring a basic understanding of the interactions between solid-state chemistry, the mechanisms and kinetics of interfacial reactions and solution chemistry. Searching for methods by which to synthesise small crystals with controlled particle morphology remains an ongoing challenge.

## 1.5 Methodology

### 1.5.1 Reverse micelle technique

A common challenge in surfactant synthesis is to attain proper phase contact between non-polar organic compounds and inorganic salts [Gutfelt *et al.* (1997)]. However, the authors argue that the problem is not unique to the preparation of surfactants; many examples exist in synthetic organic chemistry where reagent incompatibility limits both the rates and yield of a reaction. A common way of solving the problem of poor phase contact, Gutfelt *et al.* (1997) propose, is to carry out the reaction in a mixture of two immiscible solvents – in other words, in a microemulsion.

In nonpolar solutions, certain amphiphilic molecules form aggregates with their polar headgroups pointing to the interior, leading to their description as ‘reverse micelles’ (from the Latin word *micelle*, meaning ‘small bit’). Reverse micelles, or water-in-oil (w/o) microemulsions, are generally described as nanometre-sized water droplets dispersed in an apolar solvent with the aid of a pure or mixed surfactant monolayer, forming a thermodynamically stable and optically transparent solution. However, the dynamic nature of reverse micelles structures in which components rearrange over time and space by means of interactions or collisions, coalescing and redispersing, makes them preferable to other methods, such as sol-gel, co-precipitation and spray drying, for this type of application. This dynamic process ensures a homogeneous repartition of the reactants among the aqueous droplets or ‘water pools’, resulting in the formation of extremely monodispersed particles.

The first implementation of w/o microemulsions for the synthesis of nanoparticles which took place in 1982 concerned using nanoparticles of noble metals for catalysis. Since then, the same method has been extensively employed in catalytic reactions, ranging from room-temperature reactions, such as butane isomerisation, to high-temperature reactions, such as the catalytic combustion of methane. Recently, reverse micelles have attracted considerable attention owing to their capacity to host various hydrophilic compounds in organic solvents, as reported by Liu *et al.* (1998). Further, they have been subject to

extensive basic and applied research owing to their inherently interesting chemistry, as well as their diverse application in such fields as pharmaceuticals, chemical engineering, oil recovery, and enzyme catalysis. In particular, the use of micellar water droplets as a novel environment for nanoparticle synthesis and chemical reactions has been extensively researched. In spite of the clear advantages offered by using the reverse micelle technique as a reaction medium for reactions catalysed by catalysts and other metallic cations, few kinetic studies exist to explain the role of the microemulsion [Lopez-Quintela *et al.* (2004)]. However, w/o microemulsions are excellent solvents both for hydrophobic organic compounds and for inorganic salts [Gutfelt *et al.* (1997)]. As such, they should be regarded as alternative to two-phase systems exploiting phase transfer reagents as reaction promoters.

### 1.5.2 Advantages and disadvantages of reverse micelle technique

The major advantage of the reverse micelle technique is the simplicity of the process in which a droplet is regarded as a reactor; such a soft technique provides a good crystallinity in the absence of high temperature and pressure requirements, which favours the formation of small particles with a sufficient narrow size distribution [Curri *et al.* (2002); Marchand *et al.* (2003)]. However, the most remarkable features of the reverse micelle technique are the following: the particle is reduced directly in the microemulsion and can be used as a catalyst in suspension without further thermal treatment; a particle size with a narrow size distribution can be obtained through use of this technique; particles can be obtained at room temperature; and the support does not affect the formation of particles [Eriksson *et al.* (2004)]. The challenge to the use of the reverse micelle technique prior to its implementation as a commercial route for catalyst preparation lies in the amount of catalyst recovered during a single microemulsion, recovery and recycling of the liquid phase.

### 1.4 Research question

The key research question is whether a reproducible particle size and composition control of the mixed metal oxide, specifically of  $\alpha$ - $\text{Bi}_2\text{Mo}_3\text{O}_{12}$  can be attained; whether the desired

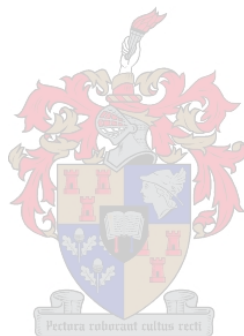
catalyst with a narrow size distribution and reproducible size control can be synthesised; and whether the technique of reverse micelle is a suitable method for achieving such a synthesis.

## 1.6 Objectives of this study

The objectives of the current research are the following:

- To do a literature study on the dynamics involved, namely the behavior of micelles at their air/water interface, as well as of a microemulsion, in relation to size control and size distribution. Since a microemulsion is a highly dynamic structure whose components rearrange themselves over time and space by means of interaction or collision, coalescence and redispersion, the study will aim to reach an understanding of the effect that such activity will have on the final nanoparticle. In addition, the literature study will involve a review of material relating to the influence of the microemulsion structure and of material relating to the factors affecting particle size and size distribution. The study, by adopting a systemic approach to learning about the system, will set out to define the operating window in which size and size distribution can be attained, allowing for the synthesis of a particle with a reproducible size control and size distribution.
- To experimentally optimise the various components and to determine the final composition of the reverse micelle technique. The complexity of the system employed requires that the parameters and conditions of the region in which the aforementioned synthesis is attainable are known in order to allow for the reproducible size control of a pure precipitate to be obtained.
- To experimentally investigate the factors affecting particle size and size distribution. The particle size and size distribution are hypothesised as being mainly dependant on the following parameters: surfactant type and concentration; temperature; nucleation and growth; stirring; alkalinity; aging; salts ratio; droplet size; co-surfactant chain length; and particle support and stabilisation.

- To experimentally synthesise the catalyst with the desirable particle size and size distribution. The resulting nanometre-sized particles are anticipated as being a potential source of study regarding their size-dependent effects on material properties, as well as a catalyst in the reactions of (amm)oxidation reactions, which would require an investigation into their internal kinetic reaction. Such a study, though not forming part of the objectives of the current research, may form the subject of ongoing research within the group.



---

# Chapter 2

## Literature Review

**Chapter layout:** In this chapter the current literature concerning the use of reverse micelles as a technique of choice in the synthesis of nanoparticles with a controllable particle size and size distribution will be discussed. As understanding the processes carried out in a reverse microemulsion system requires comprehending the microstructure of such a system, the influence of microemulsion structure in relation to particle size control will be elaborated upon. Since microemulsions form a highly dynamic system, a comprehensive study of the dynamics of reverse microemulsions in relation to particle size and size control will be broadly discussed. After the parameters that theoretically affect the particle sizes are reviewed, a general conclusion will summarise the current chapter.

*We have educated ourselves into imbecity [Malcolm Macgerridge]*

## 2 REVERSE MICROEMULSION TECHNIQUES

### 2.1.1 Definition

Microemulsions are defined as systems of water (polar), oil (apolar) and an amphiphile (surfactant, stabilising the interface between the polar and apolar solvent), sometimes also containing a fourth component, the co-surfactant.

### 2.1.2 Appearance of microemulsion

Microemulsions appear to be homogeneous solutions on the macroscopic scale, and appear to be heterogeneous on the molecular scale [Eriksson *et al.* (2004)]. Microemulsions can be formed with the expenditure of very little energy, as they can be supplemented by systemic thermal energy [Moulik and Paul (1998)]. The spontaneity of the system has been observed to homogenise itself, forming a microemulsion solution that is both isotropically and thermodynamically stable. In figure 2.1 below the structure of microemulsions at a given concentration is schematised.

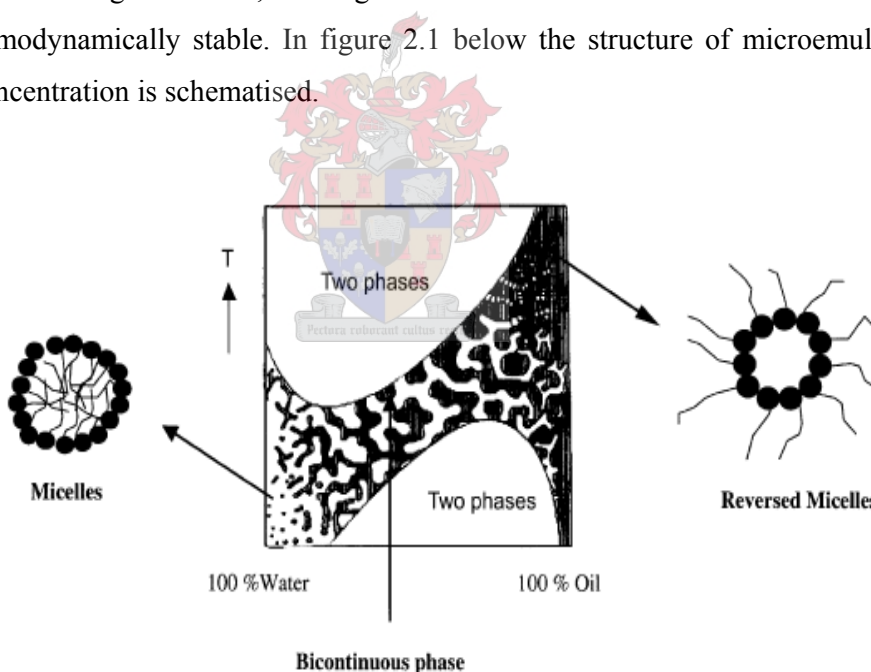


**Figure 2.1:** The appearance of a microemulsion at a given concentration of a surfactant as a function of temperature and water concentration [Eriksson *et al.* (2004)].

### 2.1.2.1 Internal structure of microemulsion

Eriksson *et al.* (2004) discussed the internal structure of a microemulsion by noting that, at a given temperature, microemulsion is determined by the ratio of its components, the structure consisting either of nanospherical monosized droplets or a bicontinuous phase. In figure 2.2 below, the internal structures of a microemulsion at a given concentration of a surfactant are schematised. At high water concentration, the internal structure of a microemulsion consists of small oil droplets in a continuous water phase (micelles). With increased oil concentration, a bicontinuous phase lacking a clearly defined shape is formed. At high oil concentration, a bicontinuous phase is transformed into a structure of small water droplets in a continuous oil phase (reverse micelles).

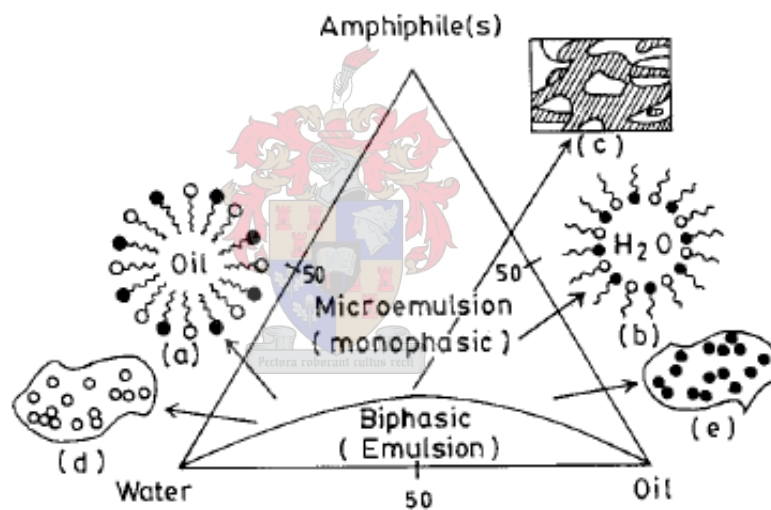


**Figure 2.2:** The comprehensive ternary phase diagram showing probable internal structure: a) oil-in-water (o/w) microemulsion; b) water-in-oil (w/o) microemulsion; c) bicontinuous dispersion; d) isolated and aggregated o/w dispersion and e) w/o dispersion [Moulik and Paul (1998)].



### 2.1.2.2 Phase behavior of microemulsion

In their early work on the equilibrium phase behavior of the microemulsion forming surfactant system, Shahidzadeh *et al.* (1999) reported that the system follows from the preferential curvature of the surfactant monolayer, namely towards either the oil or the water, and is determined by the head- and tail-group area of the surfactant molecule. If the area of the head is relatively large, micelles, which have incorporated some oil, are present in the water phase, thus forming an oil-in-water (o/w) microemulsion. If the tail-group is relatively large, featuring reverse micelles, water-in-oil (w/o) microemulsion is formed. If the two are in approximate balance, in the region of the phase where the tension is ultralow, a third, intermediate *oil/brine/surfactant* phase is formed, which can be a  $L_{\alpha}$  (lamellar) or bicontinuous phase, as illustrated in figure 2.3 below. The latter observation is supported by Lindman *et al.* (1989), who reported that, depending on the conditions, the surfactant rich dividing surface may enclose a finite volume, as in the case of micelles, or have a multiple connected ('sponge' like) topology. In the latter case, the dividing surface simultaneously separates the continuous water and oil domains, so that the structure can be referred to as bicontinuous.

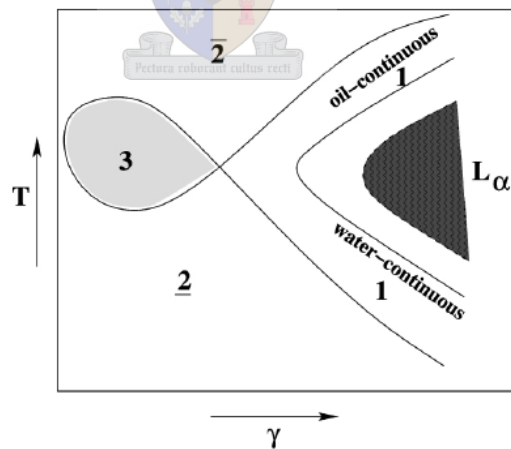


**Figure 2.3:** A schematic cut through the phase prism of a ternary mixture water-oil-CiEj-surfactant at constant ratio water to oil. In the tail of the so-called 'fish' continuous water microemulsion, spherical droplets near the emulsification failure boundary and non-spherical droplets close to the so-called 'haze point' and continuous oil microemulsion phases can be found;  $\gamma$  denotes the surfactant weight fraction [Hellweg (2002)].

### 2.1.2.3 Phase manifestation

The ternary mixture of water-amphiphile-oil or explicitly quaternary mixture of water-surfactant-co-surfactant-oil can have different phase manifestation characteristics, allowing for detailed description by the Winsor [Moulik and Paul (1998)]. Further, the concerned mixed system may essentially fall into four categories, which are indicated in figure 2.4 below:

- Dispersion of oil-in-water in contact with essentially oil (Winsor I).
- Dispersion of water-in-oil in contact with essentially water (Winsor II).
- Both oil-in-water and water-in-oil dispersion are simultaneously present in the same domain in a mixed state in a separate contact with both oil and water (Winsor III).
- A homogenous single phase of dispersion either o/w or w/o not in contact with any other phase (Winsor IV).

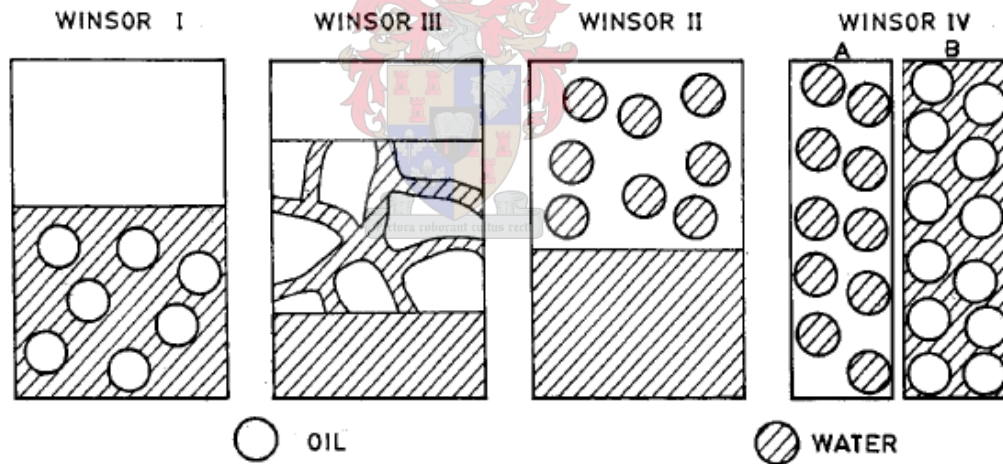


**Figure 2.4:** Different phase-forming situation for water-amphiphile-oil mixture [Moulik and Paul (1998)].

#### 2.1.2.4 Structure of micro waterpool

Water can be easily dissolved in the polar core constituted by the surfactant polar headgroups, forming the so-called 'water-pool', whose size depends on the mole ratio between the added water and the surfactant,  $W_O$  the water to surfactant ratio [Bonini *et al.* (2002)]. Further, the water pool has been proved to be a useful microreactor for the synthesis of several nanoparticle systems; the advantage of using this synthetic pathway is mainly related to the control of the size and morphology of the nanoparticles involved. The shape of the water pool in a w/o microemulsion is spherical [Panda *et al.* (2001); Santra *et al.* (2001)], with the size of the water pool greatly influencing the size of the nanoparticles formed. The water nanodroplets present in the bulk oil phase serve as a nanoreactor for the synthesis of nanoparticles of different kind of materials, whereas surfactant molecules lower the interfacial tension between the water and oil, resulting in the formation of a transparent solution [Santra *et al.* (2001)]. Thus, the size of the spherical nanoparticles can be controlled and tuned by changing the size of the water pool  $W_O$  value; in general, the higher the  $W_O$  value, the larger the particle size. In fact, Merchand *et al.* (2003) have reported that the size of the particles obtained remains in most cases directly related to the size of the water pools concerned.

Lu *et al.* (2000) discussed the structure of the water pool by noting that one of the important parts of a surfactant layer is the distribution of water and the degree to which water penetrates the surfactant layer. The importance of the water layer is made clear by considering the chemical potential of an adsorbed species, to which several factors are expected to contribute. However, three factors observed contribute to the overall effect: the roughness, the size and the surface density of the head group; the last two determine the amount of water in the intermediate region. Further, the roughness of a layer at the air/water interface, should be manifested both in the width of the surfactant distribution and in the range over which the water distribution declines from solution to vapour phase density. Although it is difficult to obtain precise information about the water distribution involved, the extent of overlap of the hydrophobic chain or any part of it with water can be determined directly, using cross-interference methods.

### 2.1.2.5 Solubilisation of water-in-oil (w/o) microemulsion

An important property of a w/o microemulsion, is its solubilisation capacity for water or oil as microdroplets dispersed during the continuous phase [Hou & Shah (1987)]. Further, the solubilisation of water in w/o microemulsions has been found to be strikingly influenced by the chemical structure of the oil and co-surfactant used. Bansal *et al.* (1980) have shown that a preferred oil-chain length exists for solubilising more water for a specific surfactant/alcohol pair than for others. Theoretically, the solubilisation capacity of water is geometrically related to the radius of droplets of microemulsions, which is thermodynamically related to the stability of w/o microemulsions.

However, the solubilisation site of a co-surfactant is clearly related to the resulting fluidity of the micellar interface [Nazario *et al.* (1996)]. In the case of alcohols (especially long-chain alcohols) an increase in the rigidity of the interface was observed for an ionic surfactant AOT, which can be achieved if the alcohol solubilises in the surfactant tail region and so pushes the surfactant head groups together, as shown in figure 2.5a below; such a solubilisation site also increases the attendant micellar curvature.

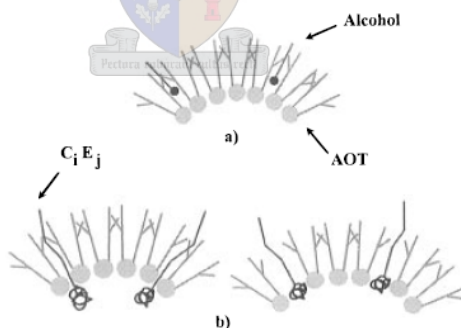


**Figure 2.5:** Schematic representation of the solubilisation site of the co-surfactants [Nazario *et al.* (1996)]

However, when the non-ionic surfactant of the form  $C_i E_j$  was used, a more fluid interface was observed, resulting in their solubilisation being such that they expand the micellar interface. The author observed that two possibilities exist for the exact solubilisation site: (i) the  $C_i E_j$  might have its polar head immersed in the water pool; or (ii) the  $C_i E_j$

might have its polar head in the surfactant head group region, as shown in figure 2.5b above. Consequently, both sites would lead to an expansion of the micellar interface, though the latter would cause a substantial increase in the interfacial area.

## 2.1.3 Formation of nanoparticles

### 2.1.3.1 Preparation of nanoparticles

The two main routes of preparation in order to obtain nanoparticles from w/o microemulsions are illustrated in figure 2.6 below [Eriksson *et al.* (2004); Li & Park (1999); Tojo *et al.* (2006)]:

- a) **Two-step microemulsion:** by mixing two microemulsions, one is containing the precursor and the other the precipitating agent.
- b) **One-step microemulsion:** by adding the precipitating agent directly to the microemulsion containing the metal precursor.

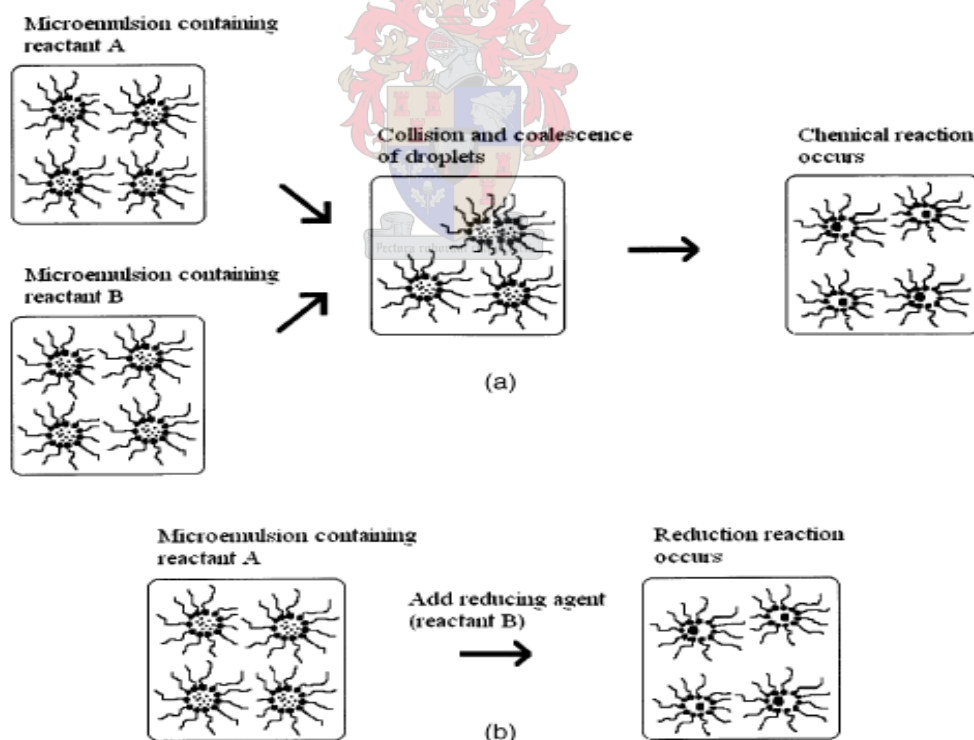


**Figure 2.6:** Modes of particle preparation from microemulsion: a) two-step microemulsion: mixing of two microemulsions; b) one-step microemulsion: direct addition of precipitating (reducing) agent to the microemulsion [Eriksson *et al.* (2004)].

Zhang and Chan (2003) propose that the final nanoparticles, as schematised in figure 2.7 below, should follow the metal composition in the precursor solution, without losing control of the particle sizes involved. In the two-step reverse microemulsion technique, the control of particle size depends on many parameters. The water/surfactant ratios, the co-surfactant/water ratios, and the concentration of aqueous phases are some of the parameters that require optimisation.

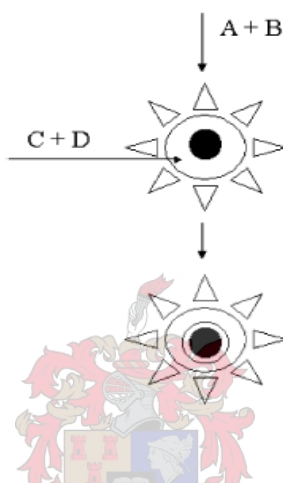


**Figure 2.7:** After the formations of nanoparticle inside the microemulsion droplets ( $A + B$  reaction), new reactants ( $C + D$ ) are introduced into the microemulsion system, producing a layer of new material. The initially produced nanoparticles act as nucleation centres for the second reaction [Lopez-Quintella (2003)].

The authors reported that the main attractive features of a two-step microemulsion reduction technique for preparing mixed metal nanoparticles are the ease and accuracy of composition control, with the reduction reaction occurring in a confined reaction zone within the microemulsions. Further, Li and Park (1999) have proposed, based on their experimental data that the particles produced by this type of process could be much smaller than the original size, in contrast to the one-step microemulsion, in which the particles produced are generally larger than the original droplet. Hence, according to Zhang and Chan (2003), the extent and uniformity of the reduction reaction can largely be controlled, since the droplets go through numerous collisions, and, as the reactants are mixed, they react to form solid particles. From such a finding it is concluded that the two-step process should yield smaller particles.

### 2.1.3.2 Particles growth

Various studies have shown that the final particles, rather than being formed inside the droplet, are only formed in the nuclei, as a result of over saturation of the solute molecule [Adair *et al.* (1998); Eriksson *et al.* (2004); Tojo *et al.* (2004)]. As microemulsions form a dynamic system, during particle formation continuous colliding of aggregates takes place. During this time, it is believed, particle growth takes place. Quintillan *et al.* (2001) have reported that particle growth can take place via reaction on existing aggregates (catalytic growth) or via ripening (growth by ripening). Growth by the latter process is expected to be faster than the former. Furthermore, Adair *et al.* (1998) have shown that, during the growth stage, particles are formed by particle growth and coagulation. Particle growth occurs as a result of the addition of solute molecules or ions to the particles concerned. While coagulation results from the combining of particles, making contact as a result of Brownian motion, as well as growth by ripening, occur as growth over smaller particles.

However, the rate of particle growth depends on the surfactant involved, which sterically prevents the nuclei from growing too fast [Eriksson *et al.* (2004)]. In such a case, the particles would grow at the same rate and consequently the particles would have a homogeneous size distribution. Though the size of the droplet would influence the size of the nuclei, the size of the final droplet would be influenced by the surrounding surfactant molecules. On the completion of growth, a suspension of small particles appears in the mixture, which is stabilised by the surfactant molecules prohibiting coalescence; the surfactant helps prevent further agglomeration of the particles concerned.

### 2.1.3.3 Mechanism of particles formation

The mechanism of particle formation can be described as occurring according to the following steps, as proposed by Debuigne *et al.* (2000) and illustrated in figure 2.8 below:

- During the *first stage*, the aqueous cores are surrounded by the surfactant.
- During the *second stage*, the organic molecule dissolved in the appropriate solvent is added drop by drop into the empty microemulsion under continuous ultrasound treatment. The solution diffuses through to the aqueous cores, which it penetrates through the interfacial film. The solvent plays a role in the transporting of organic

molecules inside the aqueous cores.

- During the *third stage*, the organic material precipitates in the aqueous cores due to its insolubility in water, resulting in the formation of nuclei.
- The *fourth stage* involves the displacement of the solvent.
- The *fifth stage* involves the exchange of organic molecules between the aqueous cores as a result of collisions between the droplets, allowing for the growth of the nuclei formed in this way.

In stages 6, 7, and 8, the already formed nanoparticles are stabilised by means of the surfactant molecules.

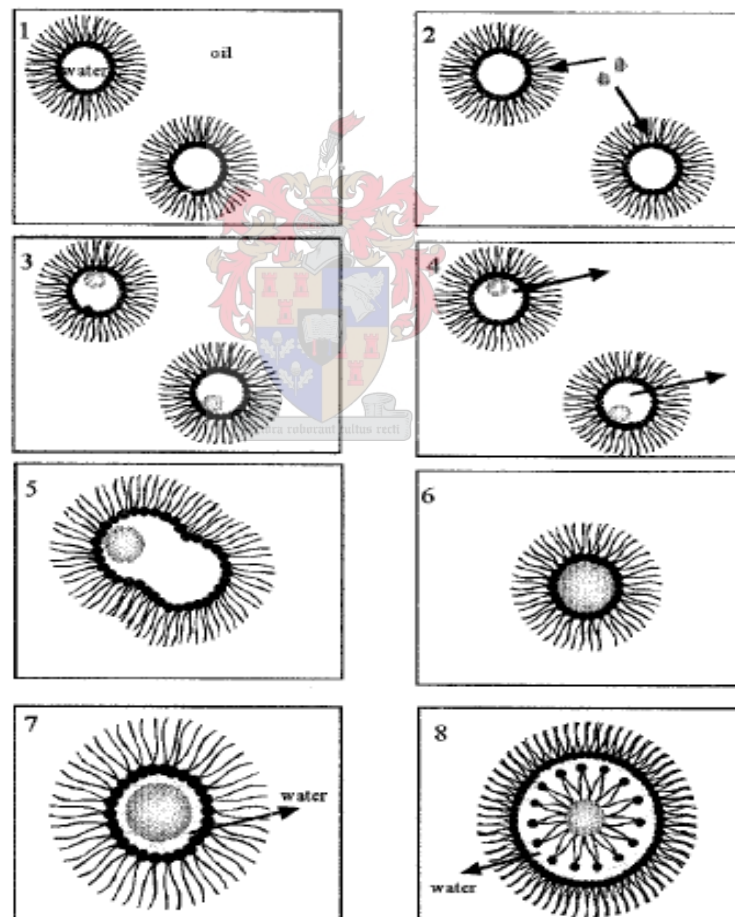


**Figure 2.8:** Hypothesis relating to the mechanism of nanoparticles formation [Debuigne et al., (2000)].



The above mechanism agrees with the observation made by Holmberg (2004), who observed that, since the starting droplets usually contain a dilute solution of a salt, and since the solid particles formed are of the same size order as the starting aqueous droplets, the final reaction mixture will consist of a relatively small number of particles, probably surrounded by water and stabilised by surfactant, and a relatively high number of ‘empty’ droplets, meaning water droplets free of salt and inorganic particles. Such water droplets will, in turn, be stabilised by the surfactant.

#### 2.1.3.4 Hypothesis of particle formation

Debuigne *et al.* (2000) have shown that three hypotheses can be proposed in order to explain the solvation and stabilisation of the final nanoparticles, being:

- The nanoparticles are in the organic phase, during which they are in direct contact with the polar heads of the surfactant. The surfactant tails are in the organic phase.
- The nanoparticles are surrounded by a layer of water. This hypothesis has been previously advanced in laboratory-based studies into silver halide nanoparticles conducted by the same authors.
- The nanoparticles are surrounded by surfactant tails, which have their polar heads toward the water phase. The water is also in contact with a second layer of surfactant polar heads.

## 2.1.4 Microemulsion dynamics

The formation of micelles in w/o microemulsion is believed to be a dynamic self-organising phenomenon in which aggregating-deaggregating processes operate in conjunction. The dynamic character of the nanoreactors is one of the most important features, which has to be taken into consideration for a comprehensive understanding of chemical reactions carried out in such media. Their flow under, and the transport of ions and molecules through them, are also of potential importance in the study of microemulsion dynamics.

### 2.1.4.1 Motion of the amphiphile chain

The motion of surfactant and co-surfactant has been studied by NMR measurements in both the three components *water-surfactant-oil* and the four components *water-surfactant-co-surfactant-oil* water in oil (w/o) microemulsion systems [Moulik and Paul (1998)]. The head group of the surfactant is believed to be the least mobile, with the motion increasing down the chain to a maximum at its end. This feature is common to both ionic and non-ionic surfactants; the terminal methyl group can freely orient in the oil phase.

However, the addition of water results in an increase in the motion of the carbon atoms, particularly those close to the head group; at a lower water content (where the water core is yet to form) the increase in mobility reaches its maximum. The motion of the surfactant in the o/w microemulsion system by NMR relaxation measurements has been inferred to be restricted by the formation of the interfacial layer between oil and water and the anchoring of the ionic head group at the interface. The behavior of the co-surfactant is inconclusive due to its fast exchange between various environments [Hansen (1973)].

The role of water in the energetics of adsorption cannot be underestimated, as, in order to adsorb to a substrate [Merchand *et al.* (2003)], an incoming surfactant may need to displace water of hydration at the solid surface. The influence of the solid on the arrangement of the adjacent water molecules will depend upon the properties of that surface, meaning that sodium cations specifically bound at the substrate tend to attract free

water molecules, which, in turn, leads to a local ordering of the water molecules at the interface.

#### 2.1.4.2 Interfacial films dynamics

Again, in both the three components and four components w/o microemulsion systems, the interfacial film between oil and water is a result of the features of surfactant and co-surfactant and plays a key role in the formation, stability and discreteness of the droplets of the microemulsion or their continuous state [Moulik and Paul (1998)]. Further, for an increasing alcohol chain length the flexibility of film has been observed to decrease; alcohols introduce more disorder in the interfacial, as their chain length increasingly differs from that of the surfactant. However, the decrease in interfacial flexibility stops at some point; if a larger amount of surfactant is added, the interfacial energy remains roughly constant and definitely does not disappear [De Gennes & Taupin (1982)]. Further, beyond a certain limiting bulk concentration, the added surfactant does not advance to the interface, but prefers to remain in one of the bulk phases in the form of micelles, as shown in figure 2.9c.

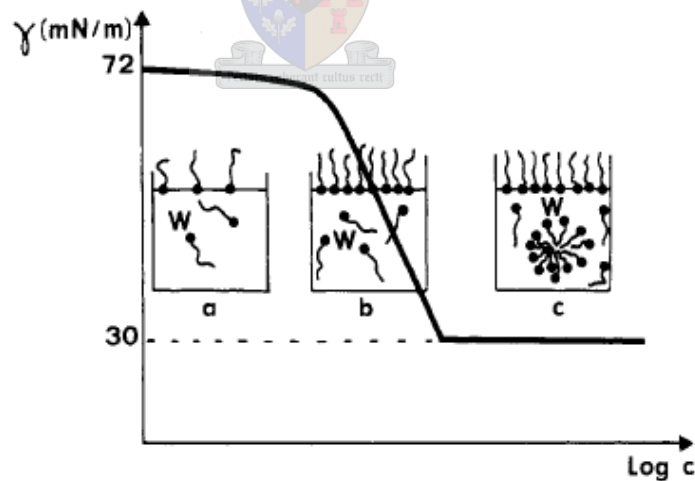


**Figure 2.9:** Interfacial behavior of amphiphiles at the air–aqueous solution interface: (a) the pressure in the dilute adsorbed film progressively decreases the surface tension  $\gamma$ ; (b) the surface tension  $\gamma$  decreases abruptly and the film becomes compact; (c) when micelles appear, the surfactant/water system is buffered;  $\gamma$  remains constant [De Gennes & Taupin (1982)].

### 2.1.4.3 Droplet fusion dynamics

Due to their small size, the droplets are subject to Brownian motion [Holmberg (2004); Lopez-Quintella (2003); Merchand *et al.* (2003); Nazario *et al.* (1996); Tojo *et al.* (2006)]. With the continuous collision of the droplets, dimmers and other aggregates form, which, after a short lifespan, rapidly disintegrate into droplets of the original size. As a result of the continuous coalescence and decoalescence process, the content of the water pools of the two w/o microemulsions becomes evenly distributed over the entire droplet population, with reaction occurring in the droplets.

In addition, the surfactants adsorbed on the particle surface can inhibit the excess aggregation of particles when the particle size approaches that of the water pool [Chen & Wu (2000)]. Consequently, the particles present in such a medium are generally very fine and uniform. The fairly rapid redistribution of components among droplets in microemulsion due to the two distinct types of processes [Cason *et al.* (2001); Moulik and Paul (1998); Wu & Lai (2004)] which are illustrated in figure 2.10 below.

- **Fusion and fission:** Droplets collide, temporarily merge (during fusion) into a larger droplet and then break (during fission) into smaller droplets. This dynamic process leads to reaction by way of mass exchange and transfer.
- **Fragmentation and coagulation:** Droplets break, losing fragments that subsequently associate or coagulate with other droplets. These dynamic processes also contribute to the chemical reaction and mass distribution involved.

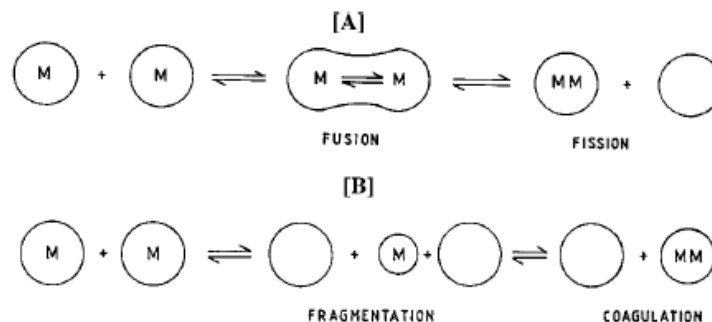


**Figure 2.10:** A) Collision, fusion and fission with mass transfer; and B) Fragmentation followed by coagulation causing mass transfer [Moulik and Paul (1998)].

#### 2.1.4.4 Exchange of components between existing environments

The process of exchange of components between the existing environments comprises the following steps [Cason *et al.* (2001); Moulik and Paul (1998); Pileni (1997)]:

- the exchange of water between the bound and free state;
- the exchange of counterions between the ionic head groups of the surfactant and core water;
- the exchange of co-surfactant among the interfacial film, the continuous phase and the dispersal phase (if soluble in the phase); and
- the exchange of surfactant between the interfacial and the aqueous phase.

The process is illustrated in figure 2.11 below.

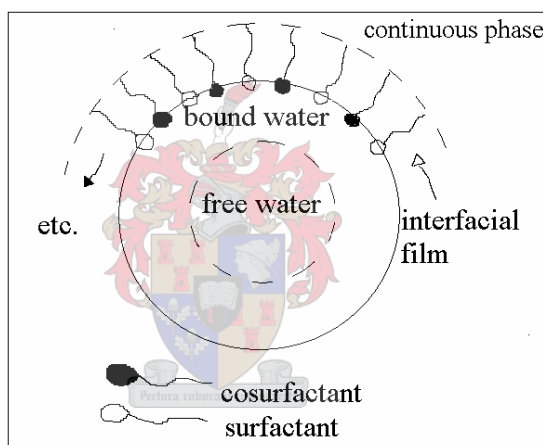


**Figure 2.11:** Schematic illustration of the dynamic behavior of the exchange of components in reverse micelle for spherical droplet [Hansen 1974].

The dynamic behavior of water exchange between the free and bound forms suggests the dynamic nature of the counterion association–dissociation in both micelle and microemulsion. Moreover, since the surfactant counterion is available in every reverse micelle, nuclei can form directly inside the reverse micelles, while accommodating the added salt. Such a result reduces the effect that the opening of the surfactant layer has on the rate of nucleation and, hence, on particle size.

#### 2.1.4.6 Viscosity of microemulsion

Among the fundamental physicochemical studies of colloidal dispersion, Moulik and Paul (1998) have reported that measurement of viscosity can provide first-hand information on the internal consistency of colloidal dispersion, as well as add to the corpus of knowledge available on the overall geometry of the particles of the disperse phase. Since this transport property is broad based, a comprehensive discussion in relation to other physical studies needs to be entered into.

Further, the Windsor I and II (as depicted in figure 2.4) o/w and w/o microemulsion systems have low viscosity. The Newtonian fluids, the Windsor III or the bicontinuous formulation may frequently exhibit non-Newtonian flow behavior and plasticity, with their flow under low and high shears showing distinct and specific features. The microemulsion in this regard conforms to the complex nature of the rheology of the non-Newtonian system. The complexity of rheological behavior depends on the system and experimental conditions involved, in which both Newtonian- and non-Newtonian behavior may arise.

#### 2.1.4.7 Self diffusion of microemulsion

For a continuous phase solvent at high-volume fraction the diffusion coefficient often nears that of the pure liquid. The dominating diffusion process is clearly a form of molecular diffusion in a medium similar to pure liquid [Jonstromer *et al.* (1995)]. However, the argument of Jonstromer *et al.* (1995) regarding a solvent showing a strongly reduced mobility over macroscopic distances is less clear. For a solvent confined to closed aggregates, one expects the dominating diffusion process to be the diffusion of the aggregate. Moreover, structural transitions within a microemulsion phase occur gradually, with the diffusion coefficients providing a smooth variance as the structure changes. In some cases, where the microstructure is neither that of a typical particle nor that of a typical bicontinuous type, the system concerned behaves rather as though finite aggregates and continuous diffusion paths were to coexist in the same solvent. In such transition regions, the diffusion process is less clear, complicating interpretations of the diffusion coefficients.

## 2.1.5 Factors affecting the particle size

### 2.1.5.1 Composition control of reverse micelle technique

#### a) Role of a surfactant

Unlike adsorption at the air/water interface, amphiphile molecules can order themselves in the bulk of a solution, as has been experimentally observed by Islam and Kato (2002). In this process, the amphiphile molecules form a micelle core as a result of the cooperative association of the hydrophobic alkyl chains, while the hydrophilic head groups extend from the core into the aqueous medium. As with the surface properties, the bulk properties of an amphiphile also depend on the length of the alkyl chain; the size and charge of the head group; the temperature; and the nature of the solvent medium. Collectively, these phenomena govern the bulk properties, such as the size of a micelle, the critical micelle concentration (cmc), and the degree of association of an amphiphile. Micellisation is an important phenomenon, involving the dependence of a number of interfacial phenomena, such as detergency and solubilisation, and on the existence of micelles in solution [Henon & Meunier (1993)].

The extent of surfactant molecule adsorption onto the surface of the nanoparticles varies according to the chemical structure of the surfactant molecules involved. The size of the micelle core is described by the molar ratio of the two surfactant molecules in solution and is given in terms of the water to surfactant ratio,  $W_o$ , as described in the previous sections of this thesis:

$$W_o = \frac{[\text{water}]}{[\text{surfactant}]} \quad (2.1)$$

Cason *et al.* (2001) have shown that the final particle size in AOT/alkane micelles is independent of  $W_o$ , although particle growth is a function of  $W_o$  and the bulk solvent type. An alternate view is postulated: sizes are largely controlled by the stabilisation of the particles and the surfactant acting as the stabilising ligand, as proposed by Shah *et al.* (2002). A similar argument has also been proposed by Kitchens *et al.* (2003), with their experimental results supporting the assumption that the surfactant has a twofold influence: one on particle growth and one on the stabilising process. Santra *et al.* (2001) support such

an argument, observing that the nanoreactor water pool is spherical in shape, with surfactant molecules surrounding the nanodroplet wall. The walls act as cages for the growing particles, thereby reducing the average size of the particles formed during the collision and aggregation process.

In a subsequent paper, Cason *et al.* (2001) further proposed that the surfactant initially provides the initiation site, the micelle core, for the reduction of the metal, followed by particle growth through intermicellar exchange. Towards the end of particle growth, the surfactant acts as a stabilising ligand, with weak interaction between the metal particles and the surfactant head group. They conclude by noting that growth rate is inversely related to particle size. Hence, increased interaction between the solvent and the surfactant tails results in a more stable micelle system and an enhanced ability to stabilise larger particles while reducing the intermicellar exchange.

In contrast, non-ionic surfactants consist of a polyoxyethylene (POE) moiety, with a terminal hydroxyl group as a polar part and a long hydrocarbon chain as a tail part [Santra *et al.* (2001)]. The terminal hydroxyl group would therefore interact by means of a weak hydrogen bonding force with the oxygen atoms present on the particle surface. In such a case, the tail part would then face away from the particle surface. Further, the preferential surfactant adsorption restricts the sideways interconnection of the particles, allowing further systematic aggregation. During this process, the hydrophobic tails of the surfactants remain parallel, interacting with each other to stabilise the system until acicular particles form.

Santra *et al.* (2001), on the basis of their study of the use of non-ionic surfactants, observe that the formation of particles is first accompanied by a very fast precipitation reaction and aggregation process. As discussed in section 2.1.4, the water nanodroplets (nanoreactors) containing reagents undergo rapid coalescence that allows for mixing, precipitation reaction, and aggregation processes for the synthesis of nanoparticles. The authors concluded by noting that non-ionic surfactants affect both particle size and the aggregation process.



The hydrophile-lipophile of the non-ionic surfactant is largely influenced by the ensuing temperature due to the conformation of the hydrophilic POE chain [Glatter *et al.* (2000); Kunieda *et al.* (1996); Teorne *et al.* (2001)]. Hence, while non-ionic surfactants tend to form aqueous micelle at lower temperature, at higher temperature forming reverse micelles. At the transition temperature, known as the HLB (hydrophobic-lipophilic balance) temperature, bicontinuous microemulsions (or surfactant phases) coexist with an excess water and oil phase. Above the HLB temperature, a water-in-oil type highly concentrated emulsion forms, as a non-ionic surfactant is lipophilic in any given water-in-oil (w/o) system.

### b) Role of co-surfactant

The composition of the four-component microemulsion is completely defined by three parameters: the surfactant molar concentration; the molar ratio between the water and the surfactant ( $W_0$ ); and the molar ratio between the alcohol and the surfactant ( $P_0$ ). The alcohol has two effects on the interfacial properties of the w/o microemulsion, which can be described as microstructural and dynamic issues, as illustrated in figure 2.12 below.

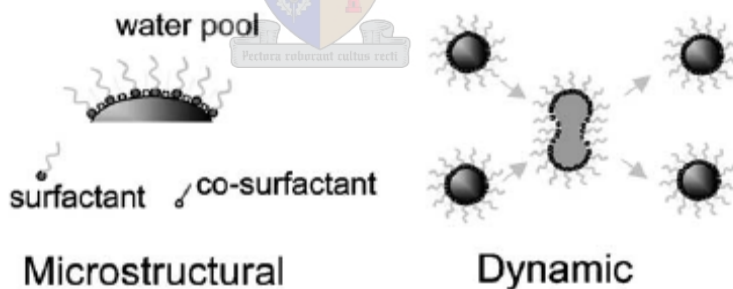


**Figure 2.12:** Schematic representation of the co-surfactant effect in the quaternary w/o microemulsion [Curri *et al.* (2002)].

Curri *et al.* (2002) have described both interfacial properties in detail: from a microstructural standpoint, the alcohol modifies the surface-packing parameters by adsorbing to the interfacial film and thus influencing the radius of curvature of the microemulsion droplet.

Such an effect is of particular relevance to the system under study: the CTAB cannot form reverse micelles in *n*-hexane without the assistance of pentanol, due to its unfavourable packing parameter. Furthermore, a dynamic role is also played by the presence of alcohol, since a droplet formed in such conditions does not show the same interface rigidity as that observed in ternary w/o microemulsions, where the mere presence of the surfactant makes the interfacial film more compact. Furthermore, the addition of co-surfactants to ternary, stable, w/o microemulsion systems decreases interface organisation by affecting the compactness and temporal stability of the film. Surfactants, as such, continuously migrate between the interface and the bulk organic phase.

An early study, conducted by Giustini *et al.* (1996), of the complex four-component system, CTAB/*n*-pentanol/*n*-hexane/water, showed it to have a relatively simple microstructure, with its stability being found to be determined by the radius of the curvature of the interfacial film,  $R^0$ , involved. However, at low-water content the droplet radius is notably smaller than  $R^0$ . When the droplet radius grows larger than  $R^0$ , i.e., due to increasing the water to surfactant molar ratio,  $W_0$ , the microemulsion phase separates into a Winsor II system. Furthermore, the water present then has a fixed solubility within the organic bulk. The surfactant, in the meantime, resides at the interface, forming a rigid mixed film of known composition with the co-surfactant. As a consequence, the dimension of the droplets follows a simple geometrical model.

Curri *et al.* (2002) subsequently observed that, when alcohols are used as co-surfactants, the interface stability is inversely proportional to the length of the alcohol alkyl chain. Though the nature of the exact dependence varies from system to system, pentanol usually ranks as a strong interface destabiliser. In such a physically ‘frustrated’ configuration, the droplets tend increasingly to interact with the external environment, with a resultant heightening of their exchange dynamics. Samples of different size and size distribution have been prepared under varying preparation conditions, modulating  $P_0$  and  $W_0$ . The dependence of the particle radius on the alcohol content can easily be related to the acknowledged role of the co-surfactant as an agent capable of increasing the interface dynamic of the droplets concerned.

### c) Size of water of droplet

The size of the particles depends on the size of the droplets present within the w/o microemulsion, with the droplet size being influenced by the water-to-surfactant ratio  $W_0$  [Eriksson *et al.* (2004)]. Lopez-Quintela (2004) has shown that the particle size can be increased in line with a growth in droplet size. The author observed that, in principle, a linear relationship could be expected. However, one has to consider that, in many cases, due to the association of flexibility with droplet size, these two effects are superimposed, with a much larger particle size being observed [Eriksson *et al.* (2004); Ghosh and Moulik (1998); Panda *et al.* (2001)], suggesting that the effect could be less noticeable when working with more rigid surfactant films.

Pileni (1998) has experimentally shown that the shape and size distribution of nanoparticles depends critically on the colloidal structure within which the synthesis is performed. Such a finding is well demonstrated by the formation of a homogeneous reverse micelle solution when the water content is reduced, with the shape of the water droplet then changing from that of a sphere to that of a cylinder. Further, the investigation conducted by Kunieda *et al.* (1996) found that the water droplet size can be influenced by the development of instability in the gel-emulsion arising due to the temperature differences.

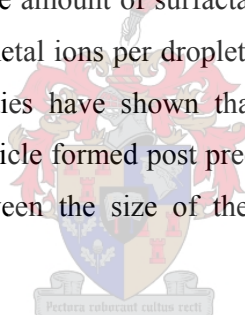
In contrast, Modes *et al.* (1989) reported that droplet size can increase in the presence of salt, as an effect of increased film flexibility, due to a direct interaction between the surfactant and the particles in the form of surface adsorption. According to Esquena *et al.* (1997), the mean size of the droplet in the microemulsion does not always represent an upper limit to the size of the semiconductor particles formed, as the experimental data evidence the formation of particles larger than the original water droplet. Lopez-Quintela (2003) discovered that the increase in particle size can be achieved by the addition of surfactant film flexibility. Increase in the latter can be achieved by a variety of means, including increasing the amount of co-surfactant present; approaching the microemulsion instability phase boundaries; changing the droplet size; and changing the chain length of the oil or the co-surfactant.

#### d) Effect of alkane chain length

Shahidzadeh *et al.* (1999) reported that, at constant salt concentration, varying the alkane chain length leads to changes in the area of the tailgroup. For short chains, the preferential curvature of the surfactant monolayer will be towards the oil, while the addition of oil leads to the formation of a water-in-oil microemulsion. Increasing the chain length leads to a balance between head- and tailgroup with, in this second region of the phase diagram, a third phase being formed, coexistent with the water- and oil-rich phases and containing most of the surfactant. Upon increasing the chain length still further, the preferential curvature is towards the water, and an oil-in-water microemulsion is formed.

#### 2.1.5.2 The effect of surfactant concentration

Lusiecki *et al.* (1993) observed that, when the amount of water and oil is kept constant at fixed values, an increase of the amount of surfactant will increase the number of droplets, meaning that the number of metal ions per droplet will decrease, with a resultant decrease in particle size. Several studies have shown that the size of the droplet significantly impacts on the size of the particle formed post precipitation of the precursor. However, no direct correlation exists between the size of the droplet and the size of the particles obtained.



Various studies have reported that a microemulsion is a dynamic system, as previously indicated in section 2.1.4. Such dynamism means that, during the process of particle formation, a constant collision of aggregates takes place. Consequently, the formation of particles proceeds in two steps: first, nucleation occurs inside each droplet; then, the aggregates proceed to form the final particles. The size of the droplet influences the size of the resultant nuclei; however, the size of the final particles is controlled by the surrounding surfactant molecules.

#### 2.1.5.3 Effect of temperature

As can be seen from figure 2.1 in section 2.1.2, the system is extremely sensitive with respect to temperature, due to the physical and chemical properties of its constituents

[Eriksson *et al.* (2004)]. Raising the temperature will destroy the oil droplet, while the water droplet will be destroyed by a decrease in temperature. This observation accords with the observations made by Panda *et al.* (2001), who observed that the dependence of size on temperature was also reversible. Though the increase in droplet size results from aggregation, the aggregates are weakly associated entities, which undergo dissociation with decreasing temperature. With increased thermal energy, the microdroplets are activated to assemble together and to grow in size, either by means of fusion or by means of agglomeration; hence, with the lowering of temperature, as in percolation, the activation barrier leads to deaggregation or fission. Such a phenomenon merits further exploration.

Teorne *et al.* (2001) reported that temperature has a significant effect on the supramolecular organisation of surface-active species in aqueous solution. In non-ionic surfactants, compatibility with water depends on the extent of hydration of the hydrophilic portion of the molecules, which is sensitive to changes in temperature, as observed by Eriksson *et al.* (2004). Further, the hydrophobic and hydrophilic moieties were shown to have a distinct effect on the thermal stability of the weak bonds involved in self-assembly. Increasing the length of the hydrophilic POE chain of the surfactants appeared to increase the thermal stability of their pre-micellar aggregates. However, complete thermal stability of aggregates required somewhat higher concentrations than was the case with smaller surfactants. In addition, as parameters such as the critical micelle concentration (cmc) and the cloud point were found to be affected by hydration, they were recognised as being temperature dependent.

Glatter *et al.* (2000) made an interesting observation in their studies on different non-ionic surfactants using Small Angle Neutron Scattering (SANS) when approaching the critical temperature,  $T_c$ . Their investigations revealed that a non-ionic surfactant system shows the trend of a sphere-to-rod transition with increasing temperature, with such a trend showing negligible, if any, increase with concentration. Further, approaching  $T_c$ , the strong increase of the scattering intensity observed in a forward direction for all samples can be explained as the onset of attractive interactions, independent of the actual size or shape of the micelles concerned. Such a finding is clear evidence of micellar growth and attractive interaction.

In contrast, Teorne *et al.* (2001) note that pre-micellar aggregates formed at low surfactant concentrations are loosely associated and likely to be disrupted by thermal agitation. Above the cmc, thermal stability is expected to increase, while further heating is known to lead to additional (supramicellar) aggregation in some cases. The latter process, known as *clouding*, occurs most among POE surfactants. Clouding involves dehydration of the hydrophilic POE chain, leading to the formation of aggregates large enough to scatter visible light.

Another interesting phenomenon to be considered is directly related to percolation, which involves increasing the temperature with constant reagent concentrations. Nazario *et al.* (1996) reported that percolation, rather than generally being considered a distinct phenomenon, is regarded as a transition from a discrete droplet phase to a bicontinuous phase. Further, during percolation the droplets are usually deemed to come in contact with one another, with ions being transferred by some kind of ‘hopping’ mechanism and/or channels being formed, through which micellar contents can be exchanged. In addition, as percolation depends on the clustering of micelles [Alexandridis *et al.* (1995)] anything that might promote or reduce clustering will obviously affect the percolation process. This phenomenon is illustrated in figure 2.13 below.

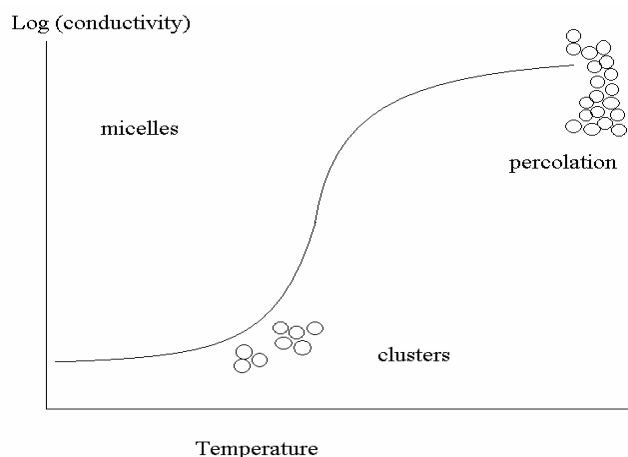


**Figure 2.13:** Schematic diagram of percolation in water-in-oil microemulsion system [redrawn from Alexandridis *et al.* (1995)].

In addition, Jada *et al.* (1989) have reported that the number of such clusters increases very rapidly above the percolation threshold, which corresponds to the formation of the first infinite cluster of droplets. Such an increase gives rise to the changes observed in properties, in particular to the increase of electrical conductivity.

#### 2.1.5.4 The effect of nucleation and growth

Nucleation is generally referred to as the process by which atoms (or ions) that are free in solution come together to produce a thermodynamically stable cluster. Further, according to Tojo *et al.* (2006), the cluster must exceed a specific size (that of the critical nucleus) determined by the prevailing competition between the aggregate curvature (Laplace pressure) and the free energy favouring the growth of the new phase. Once the critical size of the critical nucleus is exceeded, the cluster becomes a supercritical nucleus, capable of further growth. If the nucleus is smaller than the critical size, spontaneous dissolution can occur or the cluster will dissolve, rather than grow.

Shevchenko *et al.* (2003) have reported that the synthesis of nanoparticles involves two consecutive stages: formation of nuclei larger than the critical (during the nucleation stage), and growth of these nuclei (during the growth stage). The latter can occur by way of the following mechanisms: (i) growth consuming molecular precursors from the surrounding solution; (ii) Ostwald ripening or coarsening, in which larger particles grow at the expense of dissolving smaller ones; and (iii) fusion of several particles (in a process of oriented attachment).

However, in a subsequent study, Shevchenko *et al.* (2003) observed the extreme complexity of investigating the macroscopic mechanism of the former, due to the difficulty originating in the basics of the nucleation phenomenon: the bottleneck for the nucleation process is the formation of critical nuclei, which are the most unstable species, with the highest chemical potential in the reaction mixture. As a result, the critical nuclei are present at a concentration that is so low that it prevents their structural characteristics being probed by means of any currently available methods. Moreover, it has been found that the phase that nuclei require need not be that which is thermodynamically stable.

Furthermore, the total number of consumed monomers (as well as the total volume of formed particles) is constant. In such a case, the balance between the rate of nucleation and growth should affect the final particle size, as illustrated in figure 2.14 below. While fast nucleation provides high particle concentration, yielding smaller particles, slow nucleation provides low concentration of seeds, consuming the same amount of monomer and resulting in large particles. Thus, a control over the nucleation rate allows tuning of the final nanocrystal size in the absence of Ostwald ripening.

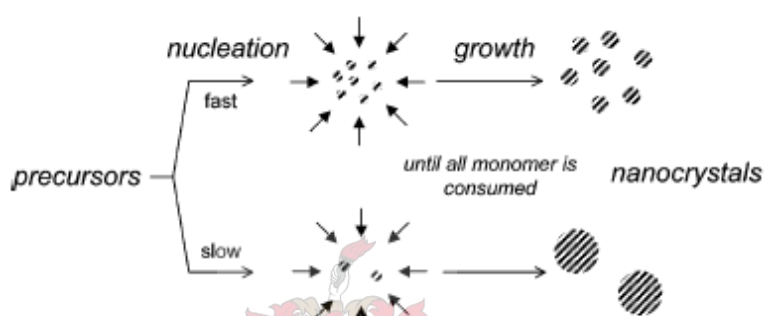


**Figure 2.14:** Schematic representation of nanoparticles synthesis in the absence of the Ostwald ripening stage [Shevchenko *et al.* (2003)].

Amongst various methods reported for controlling the size of nanoparticles, the most notable is that of seeding growth. Jana *et al.* (2001) have reported that in the seeding growth method, small metal particles, after initial preparation, are used as seeds (nucleation centres) for the preparation of larger size particles, as illustrated in figure 2.14 above. In their study of seeding growth for size control of gold nanoparticles, the authors experimentally determined that particle size could easily be manipulated by varying the ratio of seed to metal salt. They also found a step-by-step particle enlargement to be more effective than a one-step seeding method in avoiding any secondary nucleation. In addition, such a method can be used for larger scale synthesis of gold nanoparticles.

Their findings are consistent with those of Chen and Wu (2000), who found that, in the synthesis of nickel nanoparticles by the reduction of nickel chloride with hydrazine in the cationic microemulsion, the atoms formed during the latter period were used mainly for



colliding with the nuclei already formed, rather than for the formation of the new nuclei as such, with a resultant formation of larger particles. Therefore, the average diameter of the nanoparticles can be seen to be determined by the number of nuclei formed at the beginning of the reduction. However, the difficulty in finding a suitable growth condition that inhibits additional nucleation during the growth stage limits the application of such methods.

#### 2.1.5.5 Effect of support

Due to their widespread application, nanoparticles formed via reverse microemulsion need to be deposited on some kind of support. The most common procedure of the variety of ways in which this can be done is by way of adding a solvent, such as tetrahydrofuran (THF), that dissolves the surfactant and is miscible with both oil and water [Eriksson *et al.* (2004); Holmberg (2004)]. According to these authors, THF will compete with the surfactant molecules adsorbed onto the particles; displace them in such a way as to result in an unstable suspension. If the support material is added at the same time as is the solvent, the particles will adhere to the support. However, Holmberg (2004) suggests that the support material be added first, with the solvent being subsequently poured into the mixture. The ready-made catalyst, being namely the support onto which the noble metal particles are deposited can then be filtered off, with the surfactant subsequently being removed by way of rinsing with more solvent.

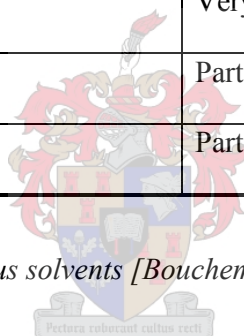
Eriksson *et al.* (2004) proposed that a proper mixing of the solution together with the support material will increase the possibility of obtaining a homogeneous distribution of the particles on the support. Such a proposal agrees with the observation made by Holmberg (2004) that the rate at which THF is added is critical: too fast a rate of addition will lead to extensive particle agglomeration. Further, under optimised conditions, a relatively even distribution of nanoparticles across the support surface can be obtained, although some agglomeration into larger particles will inevitably occur.

Eriksson *et al.* (2004) conclude that, based on their own experience, such a task is difficult, with its success largely depending on the properties of the support. However, Bouchemal

*et al.* (2004) observed that the principal property for the solvent used in spontaneous emulsification is the quasi-total miscibility, with the continuous phase as shown in table 2.1 below. Though acetone, in light of this point alone, seems to be the most appropriate solvent, its high flammability levels could limit its potential for industrial use.

<b>SOLVENT</b>	<b>WATER MISCIBILITY</b>
Acetone	Miscible
Ethanol	Miscible
Tetrahydrofuran	Very soluble
Methyl ethyl ketone	Very soluble
Methyl acetate	Very soluble
Ethyl acetate	Partially miscible
Isopropyl acetate	Partially miscible

**Table 2.1:** Miscibility of various solvents [Bouchemal *et al.* (2004)]



#### 2.1.5.6 Effect of Oswald ripening.

One of the main problems with w/o microemulsion is Oswald ripening [Izquierdo *et al.* (2002); Kalbanov (1994); Quintillan *et al.* (2001); Tojo (1997)], which results from the difference in solubility between small and larger droplets (for details of the mechanism, see Appendix C4). Theoretically, Oswald ripening should lead to condensation of all droplets into a single drop, meaning phase separation. However, such separation does not occur in practice, since the rate of growth decreases with an increase in droplet size. Several methods may be applied in order to reduce the effect of Oswald ripening, including the addition of a second disperse phase component, which is insoluble in the continuous phase, meaning the squalene and modification of an interfacial film at the oil water interface. The latter method can be controlled by way of varying the nature and concentration of the surfactant involved.

### 2.1.6 Methods (and mechanism) of emulsification and the role of surfactant

The emulsion step is of major importance in the classical interfacial polycondensation process, as it determines the droplet size distribution and, hence, particle size [Bouchemal *et al.* (2004)]. Three different mechanisms may account for the mechanism of emulsification [Shahidzadeh *et al.* (1999)]:

1. **Interfacial turbulence:** Such turbulence occurs when local interfacial tension depression tears droplets of oil away from the oil-water interface, dispersing the oil during the aqueous phase.
2. **Diffusion and stranding:** When one of the majority phases of three component systems diffuses into a second phase, carrying and dispensing occurs in the third phase, with insolubility in the second phase.
3. **Zero or negative interfacial tension:** Such tension occurs when the interfacial is locally negative, resulting in the area of the interface tending to increase spontaneously.

### 2.1.7 Monte Carlo Simulation

Various studies on the use of the Monte Carlo Simulation to study the control of size and size distribution have been reported. The studies have observed, by way of a multitude of experiments that no definite conclusion can be reached regarding the control of particle size and size distribution. The study carried out by Tojo *et al.* (1997) made use of simulation to study reactions that are controlled by interdroplet exchange involving droplet-droplet collision. Their simulation model took into consideration several conditions: that (i) reagents are transferred from the droplet with more to the droplet with fewer reagents; that (ii) Ostwald ripening is enforced; and that (iii) the reaction between droplets X and Y does not carry product P, or, if it does, the reaction is either autocatalysed or non-autocatalysed by P; and that (iv) there is a maximum permitted particle size, with 'empty' droplets being removed from the simulation.

Another study [Quintillan *et al.* (2001)] took into account the number of units that could be

transferred during a collision, by means of introducing a factor  $k$  that greatly influenced the rate of growth. When the growth was mainly due to autocatalysis, it was found reasonable to assume that an increase of  $k$  led to an increase in final particle size, as shown in figure 2.15. In contrast, growth by ripening was found not to depend on the presence of  $k$ , because ripening only involves the interchange of aggregates. The simulations of the authors revealed that nanoparticle size does not depend on  $k$  when the concentration excess is high enough, when ripening is responsible for such behavior. In addition, for each surfactant there exists a determined value of  $k$  that leads to the smallest particle size.

Consistency between experimental and simulation results, using different synthesis conditions, shows the validity of the simulation model used [Quintillan *et al.* (2001); Tojo *et al.* (1997)]. Such consistencies the authors concerned relate to observations that microemulsion droplets control particle size in a lower size range, that particle size increases with growing surfactant film flexibility and reagent concentration, and that, in order to obtain the smallest particles possible, both film flexibility and droplet size should be low.

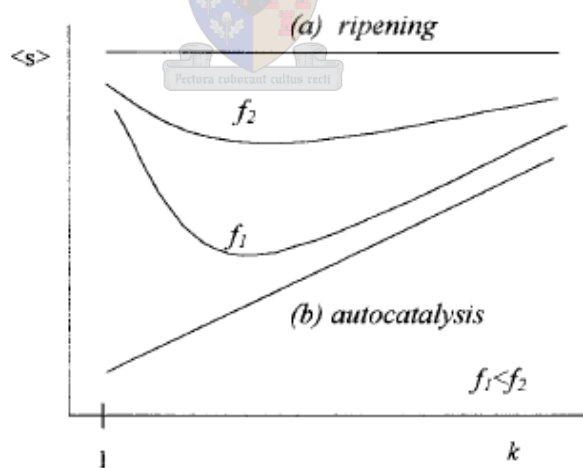


**Figure 2.16:** Plot of the average particle size ( $\langle s \rangle$ ) in relation to the reactant exchange parameter ( $k$ ). Curve (a) represents behavior in a purely ripening process and (b) that in a pure autocatalytic process. Curves  $f_1$  and  $f_2$  show the previsible behavior for two different film flexibilities:  $f_1 < f_2$  [Quintilla *et al.* (2000)].

However, the simulation model used does not take into consideration that microemulsions are dynamic systems whose components rearrange themselves over time and space by means of redispersal and coalescence. As noted earlier in section 2.1.3, due to Brownian motion, such droplets collide and interchange reactants at a constant rate. Such a rate determines the elasticity of the surfactant film flexibility involved, which also influences the reactant interchange among the nanodroplets themselves. The interdroplet exchange of particles growing inside the droplet is inhibited by the inversion of the film curvature in the fused dimmer which, in turn, depends on the flexibility of the film. Therefore, in order to gain an understanding of reactions carried out in w/o microemulsion, the dynamic nature of the system must be fully assessed.

## 2.2 HYPOTHESIS

Based on a review of the most relevant current literature, it is hypothesised that:

- When the amount of water and oil is kept constant at fixed values, an increase of the amount of surfactant will increase the number of droplets formed, meaning that the number of metal ions per droplet will decrease, with a resultant decrease in particle size.
- The size of a droplet will influence the size of the nuclei; however, the size of the final particles will be controlled by that of the surrounding surfactant molecules.
- A decrease in particle size can be achieved by surfactant film flexibility. The increase in the flexibility of the film can be achieved by increasing the amount of the co-surfactant; approaching the microemulsion instability phase boundaries; changing the droplet size; changing the chain length of the oil or the co-surfactant; etc.
- Size is largely controlled by the stabilisation of the particles concerned and by the surfactant acting as the stabilising ligand.
- As a general rule, a fast nucleation process will result in the production of small particles.
- No direct correlation exists between the size of the particles and the size of the droplets, meaning that droplet size does not influence particle size.
- Reverse micelle provides a suitable technique for the synthesis of pure  $\alpha$ - $\text{Bi}_2\text{Mo}_3\text{O}_{12}$ .

---

# Chapter 3

# Experimental

This chapter contains a description of the experimental technique used in this study. The data regarding chemicals used can be found in appendix B (see table B1).

There are no mistakes, only lessons; growth is a process of trial and error, experimentation. The 'failed' experiments are as much a part of the process as the experiments that ultimately 'works' [Cherie Carter-Scott].

### 3.1 REVERSE MICELLES FORMATION

#### 3.1.1 Titration analysis

The objective of the experiments undertaken for this study was to study the stability of micelles for various surfactants. The study involves visual inspection of changes in a mixture with various aqueous solutions. Initially, oil/surfactant mixtures with 5, 10, 15, 20, 25 and 30 per cent mass surfactant were prepared by adding surfactant to a constant amount of oil, such as, in making a 10 wt. % mixture, 1 g surfactant was added to 9 g oil. The aqueous solution was then dripped by means of a burette into an initially clear mixture of an oil surfactant. The samples were kept at a constant temperature of 25 °C by means of a water bath.

#### Components of the mixture

**Surfactant:** The surfactants used consisted of nonionic dodecyl-poly (ethylene oxide-23) ether (C12E6; Brij 35) and the ionic surfactant Cetyltrimethylammoniumbromide ( $C_{16}H_{33}(CH_3)_3-N^+Br^-$ , CTAB). The latter surfactant was used together with a co-surfactant, pentanol, with a mixture of 12.5/87.5 wt. %.

**Oil:** The two oils that were used were a short chain, *n*-hexane, and a long chain, *n*-decane.

**Aqueous solution:** The aqueous solutions that were added to a mixture of oil-surfactant ratios consisted of distilled water; acidified distilled water; molybdate salt; aged molybdate salt; bismuth salt and aged bismuth salt solution.

#### Preparation of aqueous solution

Distilled water was used as received, without further purification. Acidified distilled water was prepared by adding concentrated nitric acid to distilled water, until a pH of 1.5 was obtained. The bismuth and molybdenum salt solutions were prepared as follows: the molar concentration of 0.05 mol/l bismuth solution was prepared by dissolving 0.3396g of bismuth nitrate in concentrated nitric acid, to which was slowly added 15 ml of distilled water, the final pH of the solution being maintained at 0.8. The molar concentration of 0.07 mol/l molybdate salt was prepared by dissolving 1.2997g of ammonium molybdenum hydride in 15 ml of distilled water, which was then acidified to a pH of 2.5 by means of the addition of concentrated nitric acid. The two salt solutions were also aged for a week to see whether their properties would change.

### **Determination of a stable region stable region**

The micelles were formed by dripping the aqueous solution with a burette into the prepared oil surfactant maintained at a constant temperature of 25 °C, with the stirring rate being kept constant throughout the addition of the aqueous solution. The boundary between the stable and unstable region was determined by visually observing the changes in the appearance of the mixture. While the micelles remained stable, the mixture remained clear, a state which could be distinguished from the cloudy microemulsion which formed when larger quantities of the aqueous solution were added to the mixture.

### **3.1.2 Malvern Zetasizer 1000 HAS analysis**

#### **Preparation of micelles**

The micelles were prepared as described in 3.1 in the case of the titration analysis, with the only difference being that samples with 10 and 25 vol. % mixture of *n*-decane/surfactant were used. The white precipitate that formed directly after the mixing of a surfactant and oil was left to settle, with only the clear liquid being removed and triply filtered, using a 0.4 μm filter. A range (5, 10, 15 and 20 vol. % to a brij35/decane mixture and 2.5, 5, 7.5% and 10 vol. % to a CTAB/decane mixture) of aqueous solution (prepared following a similar procedure to those described in 3.1) was then added to the oil/surfactant mixture. The mixture was stirred for 3 minutes in a sonic bath rather than with conventional stirrers. Since the samples to be analysed by means of the Zetasizer had to be free of dust particles, care was taken to avoid vaporisation and to keep the containers tightly sealed at all times in order to keep the mixture dust-free and unaltered in composition throughout. The micelles were analysed by means of the Zetasizer, following the procedure described in section 3.4.1.



### 3.2 SYNTHESIS OF $\alpha$ -BISMUTH MOLYBDATE NANOPARTICLE

The following experiments were performed in order to investigate the effect of various factors on particle size and size distribution. The factors under investigation as regards their interaction were salinity (or salt concentration); nucleation and growth; temperature; aging and support of the catalyst particle; the bismuth-molybdenum ratio; and stirring (at different rates). The experimental runs are summarised in tables 3.1 and 3.2.

#### 3.2.1 Preparation of Decane-Brij35 mixture

Two mixtures of brij35-decane were prepared by adding 33 g of brij35 to 300 g of decane, resulting in a 10 wt. % mixture, and by adding 83 g of brij35 to 250 g decane, resulting in a 25 wt. % mixture. Both mixtures were separated into sub-mixtures of 20 g each, resulting in sixteen different mixtures.

#### 3.2.2 Preparation of salt solution

**Molybdate salt solution:** The preparation of 0.64 M molybdate salt solution was achieved by dissolving 4.520 g of ammonium molybdenum hydride in distilled water to make a 40 ml solution. The molar concentration of 0.32 M molybdate salt was obtained by diluting 20 ml of the 0.64 M with 20 ml distilled water. A molar concentration of 0.16 M was again obtained by diluting 20 ml of the 0.32 M with 20 ml distilled water. The same procedure was used to obtain a molar concentration of 0.8532 M, 0.4266 M and 0.2133 M, starting with 6.253 g of ammonium molybdate hydride.

**Bismuth salt solution:** A similar method was followed to obtain the molar concentration of 0.2133 M, 0.1067 M and 0.0533 M by dissolving 4.138 g in 2 ml concentrated nitric acid, and adding distilled water to make a 40 ml mixture, with the pH controlled at 1.5. The exception in the case of the preparation of bismuth solution was that the water that replaced the removed salt solution contained 1 ml of nitric acid per mixture of 20 ml.

### 3.2.3 Investigation into various factors

#### 3.2.3.1 Investigation into the effect of salt concentration

Six different runs were performed in order to determine the effect of the salt concentration on the size and size distribution of the catalyst particle formed. The first three runs were performed by varying the salt solution, with the surfactant concentration maintained at 10 vol. %, while the surfactant concentration was maintained at 25 vol. % for the other three runs. The salt solutions were prepared in the same way as were those described in part 3.2.2. The bismuth and molybdate salt solution were added separately to the oil/surfactant mixture. The mixture containing the molybdate salt was added over a period of 20 minutes to the mixture containing the bismuth salt. The addition was subjected to constant stirring at a temperature of 25 °C. The catalyst particles formed were separated from the remaining liquid by means of centrifuge and suspended in ethanol for analysis by means of TEM, as described in section 3.4.2.

#### 3.2.3.2 Investigation into the effect of nucleation and growth

Four experimental runs were performed to investigate the effect of nucleation and growth on the catalyst particle. These experimental runs were similar to those in 3.2.3.1, with the exception being that the mixing time of the two reverse micelles, one containing the precursor and the other the reducing agent, were varied in order to study the nucleation and growth of the particle concerned. The duration of mixing of the reverse micelle was 20, 60 and 120 minutes in turn. The fourth run was a free run performed at a surfactant concentration of 10 vol. %.

#### 3.2.3.3 Investigation into the effect of aging

Three runs were performed in order to investigate the effect of aging on the mixture of two reverse micelles. These experimental runs were similar to those conducted in 3.2.3.2, with the exception being that the mixture containing the two micelles was left to stand for 24 hours.

#### 3.2.3.4 Investigation into the effect of temperature

Four experimental runs were performed to investigate the effect of varying temperatures on the catalyst particle involved. These experimental runs were similar to those described in 3.2.3.1, with the exception that the first two runs were nucleated for 60 minutes, with the temperature being kept constant at 30 °C and 35 °C respectively. The third run was nucleated for 20 minutes, while the temperature was kept at 35 °C. A free run, performed at 50 °C, was performed to investigate whether the effect of temperature was raised far enough.

#### 3.2.3.5 Investigation into the effect of stirring

Four runs were performed to investigate the effect of stirring and how vigorous the stirring should be on the catalyst particle. Though the experimental runs were similar to those described in 3.2.3.1, the mixture were nucleated for 20 minutes while the temperature of the mixture was kept at 35 °C for all runs. The stirring rate was increased one and a half, two and three times in turn.

#### 3.2.3.6 Investigation into the effect of salt ratio

Two runs were performed to investigate the effect of the salt ratio on the catalyst particle. These experimental runs were conducted along similar lines to those described in 3.2.3.5, with the exception being that the salt solution were added in such a way that a saturated aqueous phase was achieved with a bismuth molybdate ratio of ½. One run was performed at 10 vol. % surfactant, while the other run was performed at 25 vol. % surfactant.

#### 3.2.3.7 Investigation into the effect of support and solvent used

Three experimental runs were performed to investigate the effect of support, as well as the effect of the solvent used to suspend the catalyst. The experimental runs were conducted along similar lines to those described in 3.2.3.5, with the exception being that the catalyst was supported by means of the addition of silica carbide and washed with tetrahydrofuran (THF). The first run was washed with THF only, while the second run was both washed with THF and supported with silica. The micelles of the third run were supported with silica only.

### 3.3 SYNTHESIS OF A PURE $\alpha$ - $\text{Bi}_2\text{Mo}_3\text{O}_{12}$

The following experiment was performed as proposed by Keulks *et al.* (1974), being set up as illustrated in figure 3.1 below.

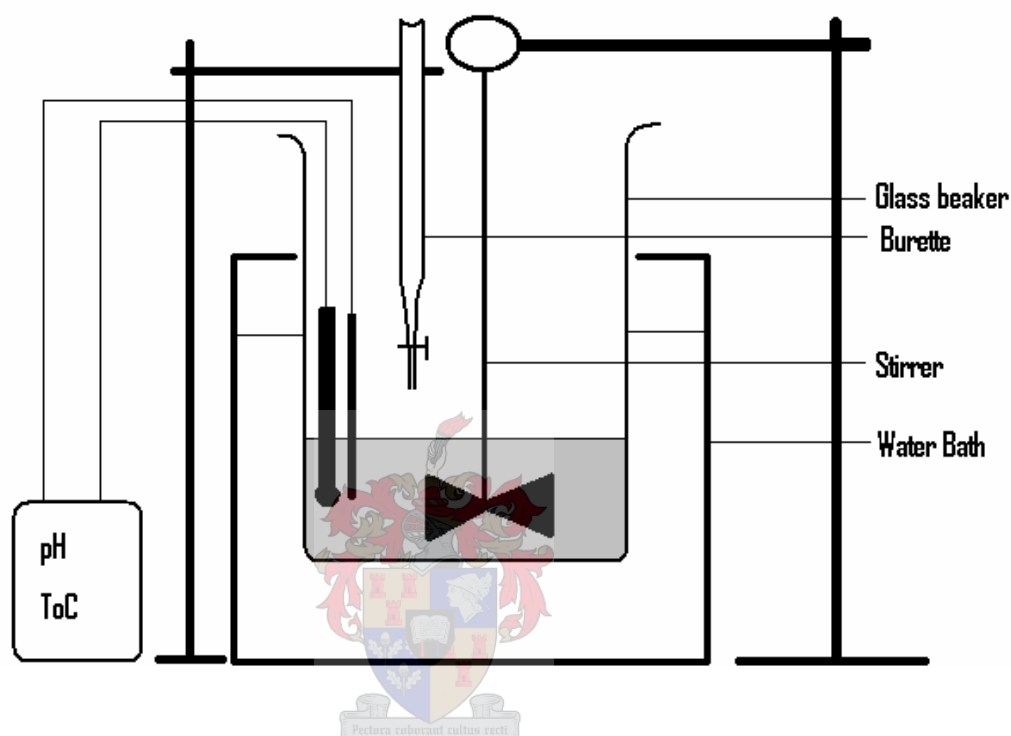


**Figure 3.1:** Set-up for the synthesis of a pure  $\alpha$ - $\text{Bi}_2\text{Mo}_3\text{O}_{12}$

#### 3.3.1 Preparation of the salt solution

The preparation of the salt solution by coprecipitation technique requires that the bismuth and molybdate atoms be present in a ratio of 2 to 3 respectively, in order to obtain the pure alpha phase. Thus both salts were prepared as in the titration analysis, ensuring that the final bismuth molybdate ratio was maintained at 0.67.

#### Acidification of the bismuth salt solution

The preparation of bismuth salt solution was done by acidifying the bismuth salt (28.989g of  $\text{Bi}(\text{NO}_3)_3 \cdot 5\text{H}_2\text{O}$ ) with enough acid (up to 30 ml) to dissolve the bismuth, regardless of the pH of the bismuth salt solution produced. The acid solution was then further diluted with distilled water (1170 ml) in a large glass beaker.

### **Acidification of the molybdate salt solution**

Coprecipitation required that synthesis should take place at a very low pH, hence the pH of the ammonium paramolybdate was lowered by means of acidifying the molybdate solution, which was prepared by adding 15.912 g of  $\text{NH}_4\text{Mo}_7\text{O}_{24}\cdot 4\text{H}_2\text{O}$  to 200 ml distilled water until a pH of 1.5 was reached. Concentrated nitric acid was slowly added to the molybdate salt solution under vigorous stirring, with the pH being monitored by means of a pH probe until it stabilised at 1.5. Once a white precipitate had formed at a pH of about 2.8, the acid solution was allowed to stand for a period of about one hour after the dissolution of the salt solution.

### **3.3.2 Mixing the acid salt solutions**

The bismuth nitrate solution was slowly added to the acidified molybdate salt solution at the rate of 10 ml per minute for a total addition time of 4 hours, while the temperature of the mixture was kept at 35 °C by immersion in a water bath. While adding the acidified bismuth nitrate solution to the ammonium paramolybdate solution, the mixture was maintained at a constant pH of 1.5 by back titrating with an aqueous ammonium hydroxide solution. The mixture was subjected to constant electric stirring during the addition of the bismuth and ammonium hydroxide. On completion of the addition of the bismuth nitrate solution, the precipitate was allowed to stand in the mother liquor for a period of four hours, after which it was filtered and dried at 120 °C for two hours, and then placed in a crucible for calcination.

### **3.3.3 Calcination programme**

The calcination programme was set as follows:

- 25 °C – 120 °C for 3 hours
- 120 °C – 200 °C for 2 hour
- 200 °C – 450 °C for 4 hours
- 450 °C for 12 hours.

A small amount of crystal was then analysed using X-Ray diffraction, as described in section 3.4.4.

### 3.4 ANALYTICAL TECHNIQUE

#### 3.4.1 Analysis by means of the Malvern Zetasizer

##### Calibration

Before the analysis was performed, the Zetasizer had to be calibrated for a specific oil/surfactant (decane/brij35 and decane/CTAB) viscosity. The standard latex particle was usually used to calibrate the Zetasizer. The glass cuvette was rinsed and filled with 3 mL oil/surfactant mixture and a drop of filtered distilled water. The result was then agitated for 3 minutes in a sonic bath, after which a small amount of standard latex particle was added to the mixture. After the mixture was agitated in a sonic bath for another 3 minutes, the exterior of the cuvette was thoroughly dried, before the cuvette was placed in an analyzer for a period of 30 minutes for each oil/surfactant mixture.

##### Analysis by means of the Zetasizer

After the calibration was performed on the Zetasizer, the glass cuvette was rinsed and filled with 3 ml oil/surfactant mixture, which was agitated for 3 minutes, using a sonic bath as earlier described. The cuvette exterior was then thoroughly dried before the cuvette was placed in the analyzer. The droplet size was determined by means of dynamic light scattering (DLS) using a Malvern 1000 HSA instrument at 25 °C, at an angle of 90°. Size measurements were taken at intervals of ca 33 seconds for a total of 30 minutes. The data that was obtained by way of this procedure was then imported to statistica and plotted as a function of time vs. particle size diameter.

#### 3.4.2 Analyzing on Transmission Electron Microscopy (TEM)

##### Centrifuge

The solution resulting from the mixing of the two reverse micelles was washed with acetone in order to break the reverse micelles. After the clear solution above the precipitates was poured off, the precipitates were placed in a centrifuge for ca 10 minutes. The clear solution above the precipitates were then again poured off, with the precipitates being washed with acetone for a second time, whereupon they were placed in a centrifuge for another 10 minutes. The clear solution above the precipitates were then poured off and suspended in ethanol until examined using a Transmission Electron Microscope (TEM).

### Analysis by way of TEM

A suspended catalyst particle was diluted by adding 500  $\mu\text{l}$  of ethanol to a drop of suspension mixture. A drop of the particle-containing diluted solution was then placed on a small aerated carbon grid, where it was allowed to dry for 24 hours. After drying, it was placed on the TEM and observed on-screen, whereupon the catalyst particles appeared darker, while the surroundings appeared brighter.

### 3.4.3 Analysis by way of SEM


The sample for viewing, after being mounted on a small stub, was coated with gold; the stub was then placed and secured during the SEM stage. The sample chamber was then vacuumed and the energy of the electron beam was selected at 7 kV, with spot size of 192 and a beam current of 80  $\mu\text{A}$ , together with a working distance of 7 mm. The beam was then switched on to enable the image of the sample to be viewed on-screen.

### 3.4.4 Analysis by way of the XRD

After being placed on a copper coin, the sample was mounted on a sample holder, consisting of an amorphous polymer. The catalyst particle was then sprinkled onto glass that was fixed onto the sample holder by means of prestick, with solid samples being attached by means of prestick directly to the sample-holder. The analysis was performed for a few hours per sample, depending on the counting statistics and the length of time required per sample or per step. After the data was obtained and converted into ASCII format, it was exported to Excel, where it was plotted as a function of Intensity vs.  $2\theta$ . The peak positions were then matched with the PDF-data base reference powder files, with the existing phases being identified by means of their peaks, with the database forming the main feature of the particle powder analysis.

# Chapter 4

## Results and Discussion



*Chapter layout:* The results of all the experiments performed are presented in this chapter, with the data from the results being presented in appendix D.

Admitting that you do not have all the answers is a sign of strength not of weakness [Anon.]



## 4.1 OPTIMIZATION OF THE REVERSE MICELLE

As discussed in the literature review, the nanoparticles formed depend on the composition of the reverse micelle. Further, the stability of the reverse micelles, which depends on the composition involved, affects the size and morphology of the particle formed. Hence, the first two parts of this section (the Titration and Zetasizer analysis) will explain how the composition of the reverse micelle affects the attendant stability, and will also suggest the final composition that should be used in the synthesis of nanoparticles.

### 4.1.1 TITRATION ANALYSIS

#### 4.1.1.1 Stability in a mixture of Brij 35 and hexane

Experimental results obtained are illustrated graphically. Figures 4.1.1.1 to 4.1.1.4 show the stability of micelles when different aqueous solutions were added to a brij 35-hexane mixture. The first region (R1) corresponds to a clear phase; the second region (R2) corresponds to a hazy phase; the third (R3) region corresponds to a murky phase; and the fourth and last region (not shown) corresponds to a milky phase for all stability diagrams. Figures 7.1.1.1 and 7.1.1.2 are found in appendix A1A. A compilation of the experimental data can be found in appendix D1 (see table D1A).

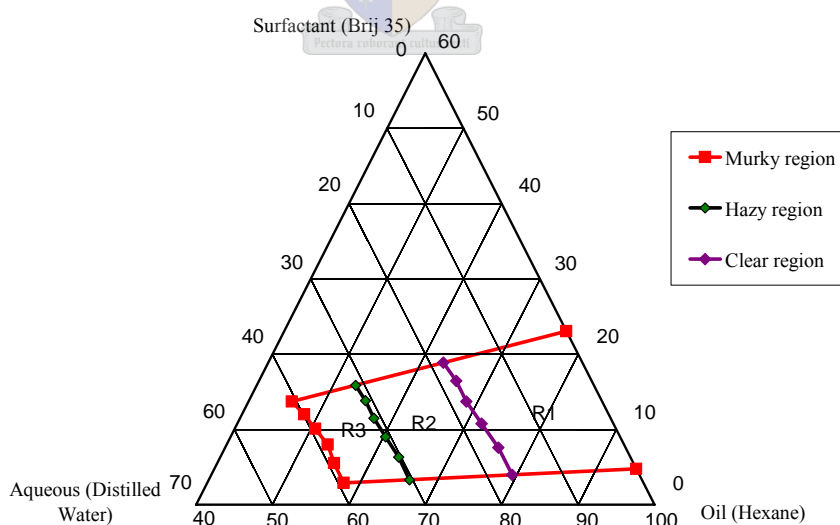


**Figure 4.1.1.1:** The stability region of micelles subject to the addition of distilled water to a mixture of hexane and Brij 35. The stability region shown corresponds to that of a clear, hazy, murky and milky solution corresponding to R1, R2 and R3 (with R4 not shown).

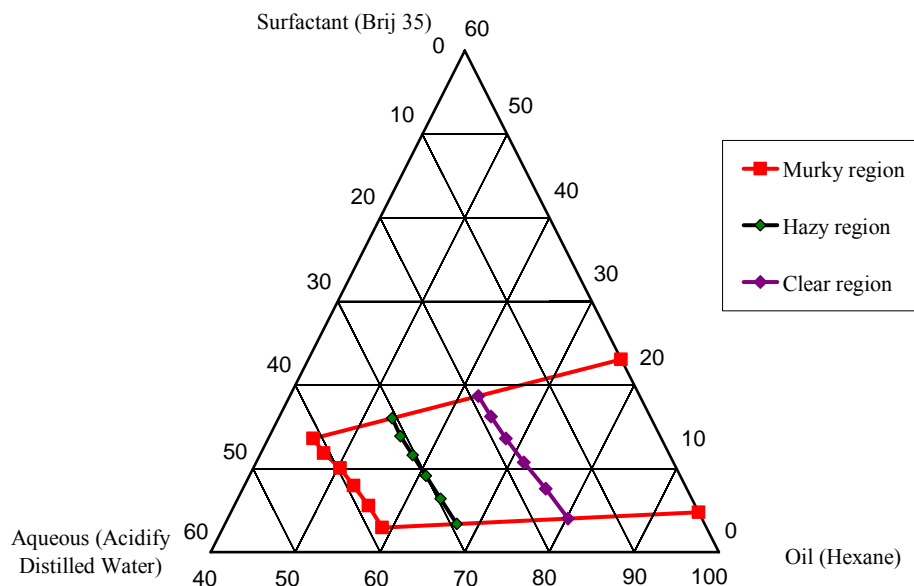


**Figure 4.1.1.2:** The stability region of micelles subject to the addition of acidified distilled water to a mixture of hexane and Brij 35. The stability region shown corresponds to that of a clear, hazy and murky solution (with that of a milky solution not shown).

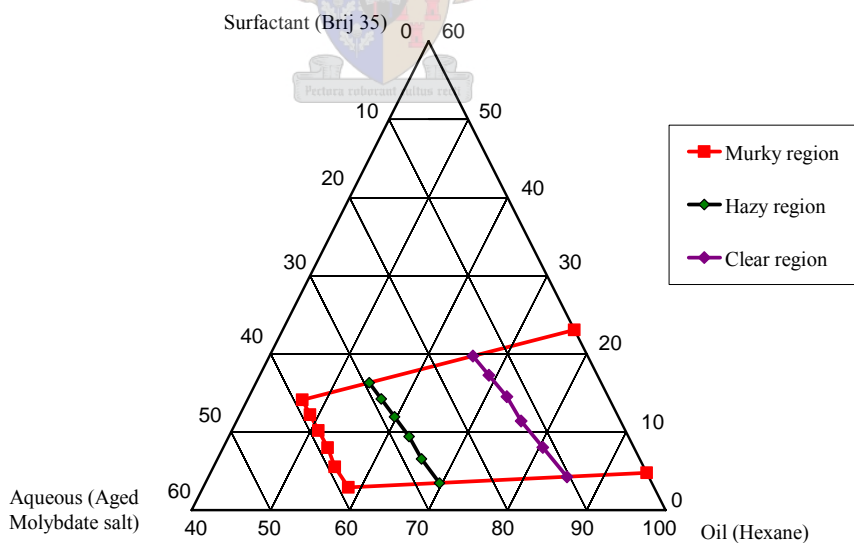


**Figure 4.1.1.3:** The stability region of micelles subject to the addition of aged molybdate salt to a mixture of hexane and Brij 35. The stability region shown corresponds to that of a clear, hazy and murky solution (with that of a milky solution not being shown).

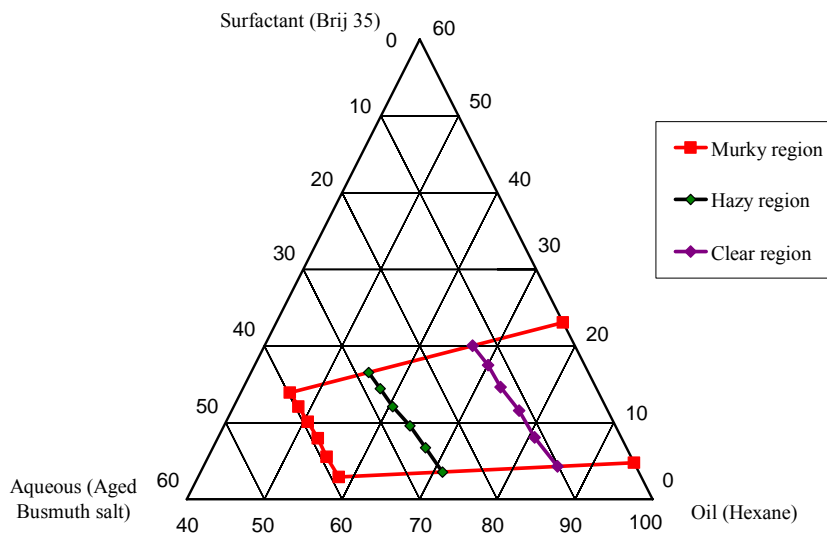


**Figure 4.1.1.4:** The stability region of micelles subject to the addition of aged bismuth salt to a mixture of hexane and Brij 35. The stability region shown corresponds to that of a clear, hazy and murky solution (with that of a milky solution not shown).

#### Visual observation for stability in a mixture of brij 35 and hexane

- **Formation of micelle**

Generally, the formation of micelles proceeded very slowly, as different aqueous solutions were added to an oil-surfactant mixture. On first addition of the aqueous solution, the clear mixture became hazy, with increased addition of the aqueous solution the mixture became murky and then milky in appearance, appearing to be semi-globular, though not viscous. The milky phase represented the final transition undergone by the mixture, since no change was observed in the appearance of the mixture with still further addition of the aqueous solution. The transition from clear to hazy solution represented the instability point of the micelles, while the presence of a milky solution showed an emulsion free of micelles.

- **The effect of temperature on the stability and the formation of micelle**

When the temperature of the mixture was changed slightly, say from 25 to 30 °C, without changing any other condition of the mixture, such as the stirring rate, generally no change was observed in the appearance of the mixture, except when the milky phase was about to

be reached. At this point it was difficult to distinguish between the murky and the milky phase just prior to the formation of the latter. Such a trend was observed for all addition of aqueous solutions.

- **The effect of stirring on the stability and formation of micelles**

When the micelles were stirred slowly while the aqueous solution was being added, it became quite difficult to stir the mixture, especially when the milky phase was reached. Such difficulty in stirring was due to the increasing globulisation of the mixture and viscosity change, after the solution became milky. However, when the mixture was stirred extremely vigorously from the start of the addition of the aqueous solution, there was no need to increase the stirring rate, even as the solution became milky. Hence, the latter method was followed for the addition of all aqueous solutions. In following this method, when the stirring was increased while the temperature of the mixture was kept constant, no change was observed in the appearance of the mixture. Hence, the conclusion can be drawn that the change in the stirring rate had little or no effect on the formation and stability of the micelles. However, in order to overcome the difficulty in stirring when the micelles became globular, the stirring rate had to be kept vigorous from the beginning.

- **Concentration of the surfactant**

The stability of the micelles increased very slightly with the increasing concentration of the surfactant, meaning that larger quantities of the aqueous solution were needed for the mixture to become unstable for higher surfactant concentration. Such a finding held true for the addition of all aqueous solutions. Hence, the larger the quantity (volume) of the surfactants added to a mixture, the greater will be the stability of the micelles formed.

- **Change in pH**

Changes in the pH of the aqueous solution were observed to have little, if any, effect on the stability of the micelles formed. This was especially true when the distilled water was acidified in order to test for a change in the pH levels present (see Figure 4.1.1.2). Similar results to those obtained for distilled water were obtained, with a statically insignificant difference in the stability of the micelles formed.

- **Relative solubility of the two salts**

The relative solubility of the two salts present was probably due to the fact that the bismuth salt was obtained as a solid, which did not readily dissolve in the acid. By contrast, the molybdate salt dissolved readily in distilled water, since this salt was obtained as a fine powder.

- **Aging of salts**

The aging of molybdate salt was observed to have little or no effect on the stability and the formation of micelles, although a slight increase in its stability was observed at a lower salt concentration. However, the aging of the bismuth salt was observed to have a significant effect on the stability and formation of the micelles. Such a finding was due to the greater concentration of the aged salts, which served to improve the stability of the micelles formed.

### **Discussion of the results regarding stability in a mixture of brij 35 and hexane**

The general trend observed for the above comparisons (see Figures 4.1.1.1 to 4.1.1.4) was that micelles proved to be stable at an aqueous content of less than 20 vol. % for all aqueous solutions added. The importance of such a finding is that a small (or large) amount of water content at the interface may significantly affect the behavior of the interface and, consequently, the stability of the micelles. The stability of the micelles in the reverse micelle phase is believed not only to depend on the composition of the solution, but also, more specifically, on the quantity of aqueous solutions added. The observed general trend when comparing the above figures is that the amount of core water in the reverse micelles affects the fluidity of the interface and, therefore, the probability that a collision will lead to coalescence, as observed by Cason *et al.* (2001). Pileni (1997) has shown that at low water content the micelle interface becomes hydrated, inducing a strong interaction between the water molecules and the surfactant polar head group, with the water becoming 'bound' to the surfactant head group, with which it creates a tight interface.

Further, one can expect that, as the water content is increased, the bound water near the head group of the surfactant becomes free within the micelle core, thereby increasing the

size of a micelle or droplet and spreading the surface area of the surfactant head groups, as shown by Cason *et al.* (2001). Such an action should serve to create more fluid at the interface, increasing the number of successful collisions and resulting in coalescence of the droplet, thereby reducing the stability of the micelles. In addition, the high water and surfactant content can assist in explaining the observed transition in the formation of micelles. Under such high water and surfactant content conditions, the L2 phase contracts to a smaller  $W_O$  (the water- to-surfactant ratio). A point is reached when no surfactant becomes available for the building up of new micelles, which leads to a phase separation, as was experimentally observed by both Curri *et al.*, (2000) and this study.

Further, one can observe from the trend revealed in Figures 4.1.1.1 to 4.1.1.4 that the area of the stability region stays roughly constant with an increase in the surfactant concentration. Such constancy is to be expected, since a decrease in the interfacial area has to stop at some point as more surfactant is added to the system. This observation agrees with that made by De Gennes and Taupin (1982), who observed that if a large amount of surfactant is added, the interfacial energy stays roughly constant, rather than decreasing. These two researchers attributed such behavior to the fact that, beyond a certain limiting bulk concentration, the added surfactant does not go to the interface, but prefers to stay in one of the bulk phases in the form of micelles. Such a finding was also experimentally shown by Islam and Kato (2000). When the system has reached a state of zero or negative interfacial tension, in this way the formation of micelles is hindered by the earlier formation of micelles. Surfactant plays a key role in preparing suspensions of the right particle size, which, when stored, will be stable for an extended length of time.

In contrast to such a finding, the above figures show that, although the region of stability stays more or less constant, a slight decrease in stability occurs in the presence of a decreased surfactant concentration. Such a decrease is important since, as will be shown later in section 4.2, a large amount of surfactant is needed for the formation of micelles and a large cluster of stable nuclei. Such an observation can be attributed to the fact that, at higher surfactant concentrations, more surfactant molecules are present to surround the water droplet formed; hence, the interface appears flexible. This observation agrees with

that made by Lopez-Quintella (2003), who has experimentally shown that the flexibility of film can be achieved by increasing the amount of co-surfactant approaching the microemulsion phase boundary; a co-surfactant plays a similar role to that of a surfactant, which is to stabilise the interface. The similarity in role is important because, as will be shown in section 4.1.2, the rate of particle growth is controlled by the presence of surfactant, which, according to Eriksson *et al.* (2004), prevents the nuclei from growing too fast. However, a fast nucleation has been postulated as likely to lead to the formation of small particles. Hence, the minimum concentration of surfactant must be used to speed up the growth of the nucleus.

Film flexibility not only depends on the concentration of surfactant, but also on the molecular chain length of the alkane of oil used. A flexible interface has been observed when oil with a longer alkane chain length, such as C12E5, is used. Shahidzadeh *et al.* (1999) used different oil chain lengths to study the effect of their difference in length on the stability of the micelles formed. Their experimental results have shown that when a short chain length is used, which, in this case, is octane; the interface of the droplet becomes highly unstable, forming long tongues of oil within the surfactant solution. When compared to a situation of equilibrium, in which most of the surfactant was found to be present in the oil rather than in the water phase, they inferred that the instability identified was Marangoni driven. They therefore assumed that the surfactant must prefer to adsorb at the oil-water interface rather than in the bulk, or 'wrong', phase; compared to a situation of equilibrium, the surfactant will penetrate into the oil phase, leading to a strong surface tension gradient: the Marangoni effect. Hence, to increase stability over that observed for hexane in this study, the density gradient in the surfactant interface must be overcome, which can be achieved by increasing the oil chain length or the hydrophilic Polyoxyethylene (POE) chain of the surfactant. However, for the system under study, the nonionic brij 35 (C12E6) has a fairly substantial polyoxyethylen (POE) part, which is extremely hydrophilic and, therefore, strongly hydrated. Hence, the less pronounced instability observed must be controlled by other factors, such as oil-chain length.

The observed effect of temperature on the micelles can be explained by considering the

diffusion processes at work in reverse micelles, which, at low temperatures, are expected to diffuse at the same rate as at higher particle concentration. The studies of Leaver and Olsson (1994) into the viscosity of nonionic surfactant C12E5 systems near the emulsification failure boundary have shown that both above and below the emulsification failure boundary the micelles diffuse at the same rate, indicating that the size of the micelles remains constant, due to the gradual nature of the phase separation with excess oil. With a rising of temperature, the self-diffusion coefficient was found to increase dramatically – the surfactant and oil then diffuse together as micelles, with their diffusion constant no longer being equal, as the oil diffuses significantly faster than does the surfactant. The difference in the diffusion processes should bring about structural changes at the interface, resulting in the behavior observed in regard to micelle stabilisation.

Further, temperature has a significant effect on a reverse micelle system formed with non-ionic surfactant systems. The hydrophile-lipophile property of nonionic POE surfactant has been observed by Kunieda *et al.* (1996) to change from hydrophilic to lipophilic when the temperature is raised. Further, the behavior of the curvature towards the water also changes from convex to concave. Hence, one can expect that, with increase in temperature, an inversion in phase from oil in water (o/w) to water in oil (w/o) occurs, due to a decrease in the solubility of the water content. Such a finding is significant, because any phase change should then dramatically affect the behavior of the interface. Phase changes of nonionic surfactants have been extensively studied by Kunieda *et al.* (1996), who used the phase inversion temperature (PIT) method. Their experimental results have shown that self-organizing structures change from micelles to reverse micelles via the vesicles. Due to the water trapped in the vesicles, and their being larger than micelles, there was a decrease in electroconductivity. Further, when the temperature was slowly raised, the water droplet size in the resulting micelles was found to be large. However, fine droplets were observed under conditions of rapid change in temperature. Such a finding agrees with the observation made by Liu *et al.* (1998), who added a nonionic surfactant to a reverse micelle system of *AOT/water/n-heptane*. Their experimental results showed that the more nonionic surfactants are added and/or the larger their Ethyleneoxide (EO) chains, the larger the droplet.



#### 4.1.1.2 Stability in a mixture of CTAB in pentanol and hexane

Figures 4.1.2.1 to 4.1.2.4 below show the stability of micelles, as obtained under experimental conditions when various aqueous solutions were added to a CTAB-hexane mixture. The first region (R1) corresponds to a clear phase; the second region (R2) corresponds to the hazy phase; the third (R3) region corresponds to the murky; and the fourth and final region corresponds to the milky phase (which is not shown) for all the stability diagrams. Figures 7.1.2.1 and 7.1.2.2 are found in appendix A1B. A compilation of the experimental data can be found in appendix D1 (table D1B).

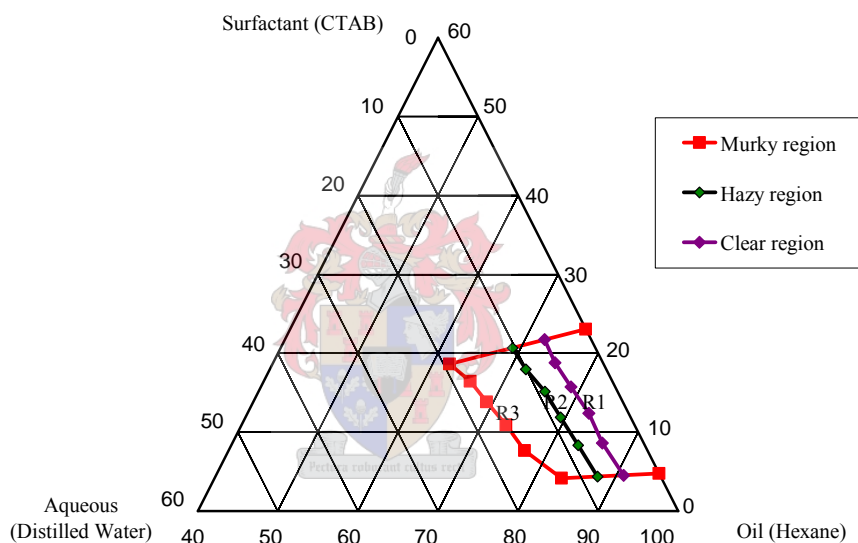


**Figure 4.1.2.1:** The stability region of micelles subject to the addition of distilled water to a mixture of hexane and CTAB, the latter was dissolved in pentanol. The stability region shown corresponds to that of a clear, hazy and murky solution corresponding to R1, R2 and R3 (with that of a milky solution (corresponding to R4) not shown).

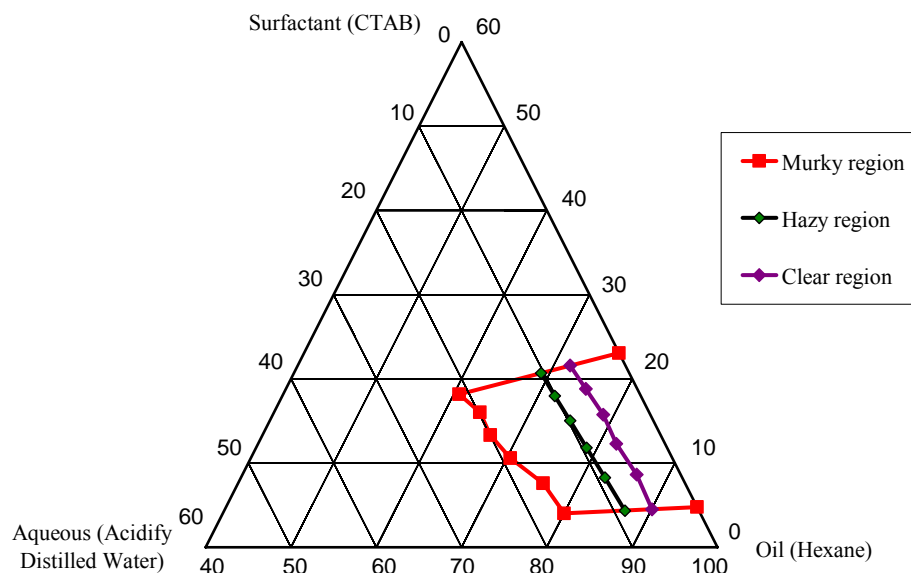


**Figure 4.1.2.2:** The stability region of micelles subject to the addition of acidified distilled water to a mixture of hexane and CTAB, the latter was dissolved in pentanol. The stability region shown corresponds to that of a clear, hazy and murky solution (with that of a milky solution not shown).

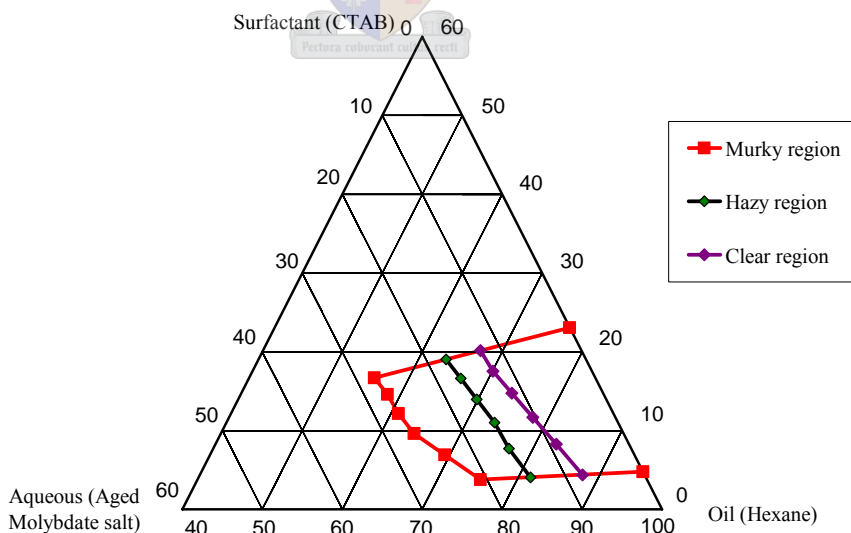


**Figure 4.1.2.3:** The stability region of micelles subject to the addition of aged molybdate salt to a mixture of hexane and CTAB, the latter was dissolved in pentanol. The stability region shown corresponds to that of a clear, hazy and murky solution (with that of a milky solution not shown).

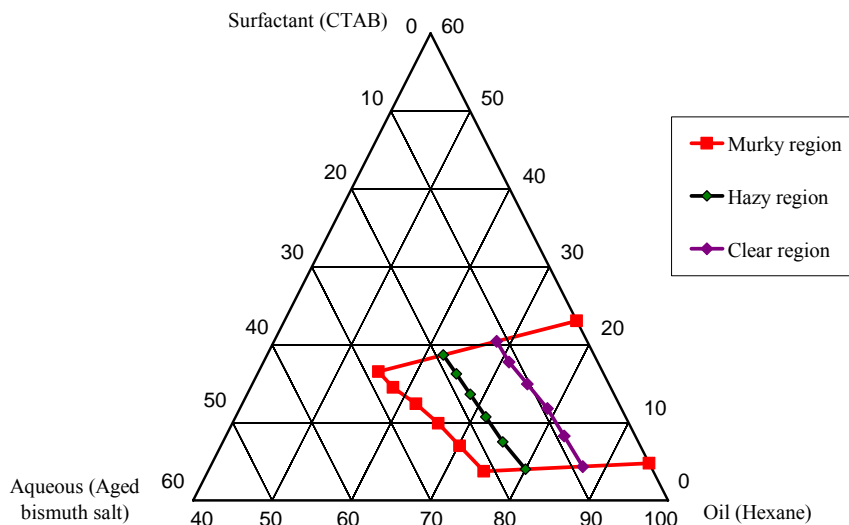


**Figure 4.1.2.4:** The stability region of micelles subject to the addition of aged bismuth salt to a mixture of hexane and CTAB, the latter was dissolved in pentanol. The stability region shown corresponds to that of a clear, hazy and murky solution (with that of a milky solution not shown).

Overall, the observations made are consistent with those made when brij 35 was used as a surfactant, apart from the following:

- **Dissolution of CTAB**

Due to the low solubility of the surfactant CTAB in hexane, it was dissolved in pentanol, which then gave a better solubility in hexane, although the mixture remained slightly cloudy, indicating its resistance to solubilising with oil.

- **Formation of micelles**

An unusual trend in the formation of micelles was observed, especially after the mixture turned milky. When the latter occurred, it formed a solid-like precipitate, which separated from the micelle and became difficult to stir. However, since this phase represented the last transition, with no observable change in the appearance of the micelle, such precipitation could not have significantly affected the measured stability of the micelles present. In addition, since the micelles were stirred vigorously from the start, as has already been described in section 4.1.1.1, there was no need to increase the stirring rate of the micelles.

- **Concentration of the surfactant**

The stability of the micelles increased slightly with an increase in the concentration of the surfactant, meaning that it took larger amounts of the aqueous solutions for the mixture to become unstable for higher surfactant concentrations. Such a finding held true for all additions of aqueous solutions. Hence, a larger amount of the surfactant (specifically CTAB) can be observed to increase the stability of the micelles present.

- **Change in pH**

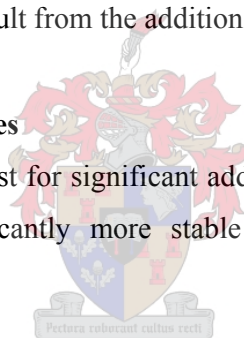
A change in pH had little or no significant effect on the stability of the micelles, especially when distilled water was acidified to test for any changes in the stability of the micelles.

- **Aging of salt**

No effect was observed to result from the addition of bismuth salt.

- **Stability of the micelles**

The surfactant (CTAB), at least for significant additions of the aqueous content, produced micelles which were significantly more stable at high, rather than low, surfactant concentration.

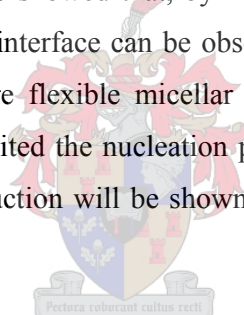


### **Discussion of results for stability in a mixture of CTAB and hexane**

The general trends observed for the above comparisons (as shown in Figures 4.1.3.1 to 4.1.3.4) are consistent with those observed when brij 35 was used as a surfactant. The area of the stability region stays roughly constant with increasing surfactant concentration, though a slight increase is observed at higher surfactant concentration. Further, the micelles are generally stable at an aqueous content of less than 10 vol. %, with their stability being far less pronounced than that obtained when brij 35 was used as a surfactant. Such fluctuation in stability is to be expected, since the addition of a co-surfactant into the system introduces further complexities at the interface, such as the way in which surfactant partitions itself at the micellar interface. Ionic surfactant adsorption is so sensitive to the interactions of counter- and co-ions with the charged groups of the surface that subsequent discussion will be based on how such sensitivity affects the way in which surfactants

partition themselves at the interface. The co-surfactant is introduced due to the low solubility of CTAB in hexane, which, due to its unfavorable packing, prevents it from forming micelles in oil without the assistance of pentanol. However, its interaction with the surfactant gives rise to the phenomenon of percolation. Further, as revealed in the above Figures, the micelles were found to be significantly more stable at higher than at lower surfactant concentration. Such a finding agrees with the observation made by Lopez-Quintela (2004), who showed that CTAB has the remarkable solubilisation capacity of a high concentration aqueous salt solution.

The addition of alcohol is expected to give rise to lower organisation at the micelle interface. Hence, the chain length of the alcohol can also be expected to have a supramolecular effect on organising occurring at the interface. Such an effect was studied by Esquena *et al.* (1997), who showed that, by introducing a longer alcohol chain to the reverse micelle, a more rigid interface can be observed, resulting in a lower intermicellar exchange. In addition, a more flexible micellar interface allowed a faster diffusion of material, which, in turn, inhibited the nucleation process and thus reduced the number of existing particles. Such a reduction will be shown in section 4.1.2 as being crucial to the formation of a stable nucleus.



Further, if the surfactant and co-surfactant are chosen such that their tail lengths are the same, the strength of interaction between the two surfactants will closely approximate the absence of percolation. However, if the difference in tail length is increased, the strength of the ensuing interaction will also increase, with percolation being expected to occur at smaller droplet radius. However, if the droplet radius is increased, the overlap volume is, likewise, expected to increase, with the potential interaction of the surfactant and co-surfactant also increasing. Eventually, in such a case, percolation will occur, as has been experimentally observed by Hamilton *et al.* (1990). However, the phenomenon of percolation is highly dependant on the occurrence of particle aggregation.

The composition of the four-component system described in the figures above is defined by the molar ratio between the alcohol and the surfactant concerned ( $P_0$ ), as well as by the

water-to-surfactant concentration ( $W_0$ ). Hence, a change in water content will have a direct effect on the  $P_0$ , with a decrease in water content being observed to increase the alcohol content at the interface, or decrease of  $P_0$  at a constant weight ratio of a surfactant and water. This decrease causes the dilution of micelle interface, resulting in a more labile interface, hence the observed lower stability in the observed general comparisons when compared to that observed in the ternary system. Such a postulation has been advanced by Chen and Wu (2000), who studied a four-component system with a composition of CTAB and *n*-hexanol. Their experimental results showed that a greater mobility of the interface favoured the rearrangement of the reverse micelle droplets, leading to a formation of larger droplets. Furthermore, the reverse micelles formed in this way were recognised as being dynamic, with the particle formed being larger than that of the micelle droplet.

On the other hand, increase of the water content increases the flexibility of the interface. Maidment *et al.* (1997), in their study of the loading of pentanol into a reverse micelle system, clearly showed that the addition of pentanol decreases the minimum amount of water needed to stabilise the reverse micelles. They observed that, as the water content was increased, the pentanol partitioned out of the interface into the oil and water domains, which was contrary to the behavior expected of the co-surfactant, which was that it should partition at the micelle interface, while, at a high alcohol level, the high water side contracts to a smaller  $W_0$ .

In the general trend observed in the comparisons made in the above figures, using ionic surfactants was found to result in more complicated adsorption at the interface, due to the charge present on the head group, when compared to that of the nonionic surfactant. In the above figures, especially in the acidification of distilled water noted in Figure 4.1.2.2, the observed effect of the acid is clear, since the ionic surfactant will adsorb with a charged head group. Hence, a change in the pH solution will have a limited effect on several factors in the surfactant substrate system, as experimentally observed by Merchand *et al.* (2003). The factors affected in this way include the level of dissociation of surfactant groups, the degree of counterion binding of micelles, and the overall ionic strength.

### 5.1.1.3 Stability in a mixture of brij 35 and decane

Figures 4.13 to 4.16 below graphically illustrate the experimental results obtained, showing the stability of micelles when different aqueous solutions were added to a Brij 35-decane mixture. The first region (R1) corresponds to a clear phase; the second region (R2) corresponds to a hazy phase; the third (R3) region corresponds to a murky phase; and the fourth and final region corresponds to milky phase (which is not shown) for all the stability diagrams. Figures 4.14 and 4.18 appear in appendix A1C, while a compilation of the experimental data can be found in appendix D1 (table D1C).

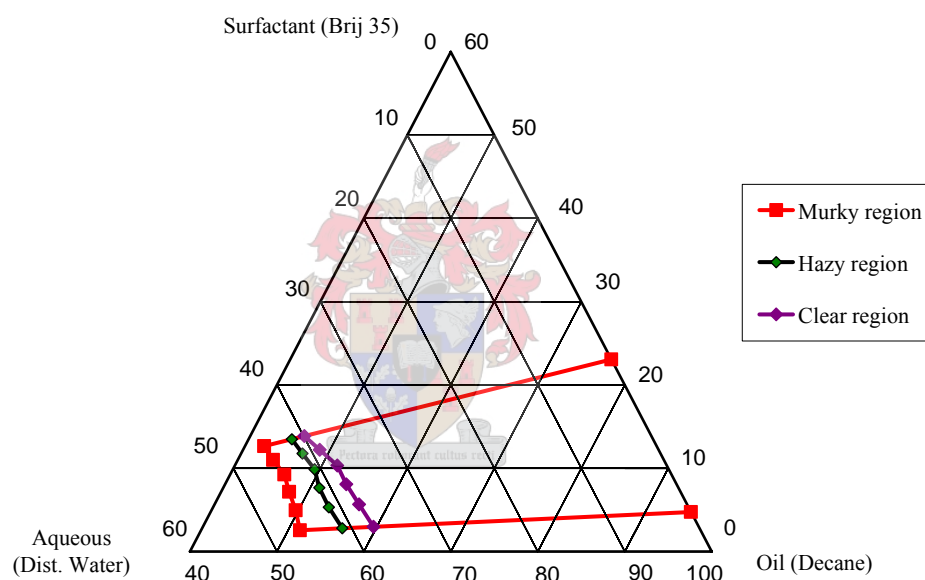


**Figure 4.1.3.1:** The stability region of micelles subject to the addition of distilled water to a mixture of decane and Brij 35. The stability region shown corresponds to that of a clear, hazy and murky solution corresponding to R1, R2 and R3 (with that of a milky solution not shown).

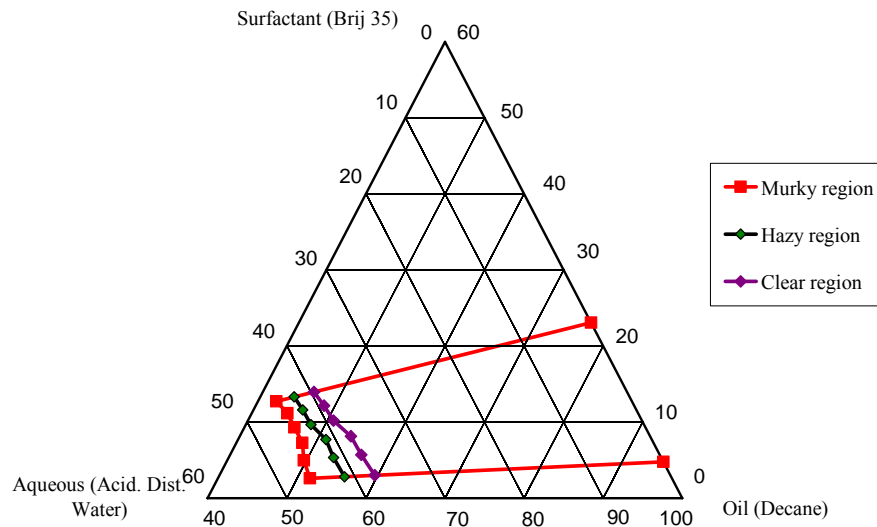


**Figure 4.1.3.2:** The stability region of micelles subject to the addition of acidified distilled water to a mixture of decane and Brij 35. The stability region shown corresponds to that of a clear, hazy and murky solution (with that of a milky solution not shown).

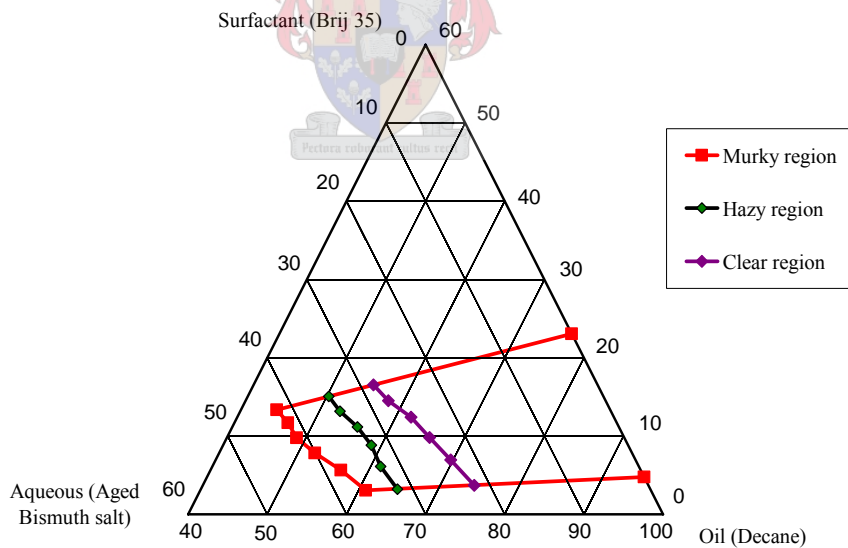


**Figure 4.1.3.3:** The stability region of micelles subject to the addition of aged bismuth salt to a mixture of decane and Brij 35. The stability region shown corresponds to that of a clear, hazy and murky solution (with that of a milky solution not shown).



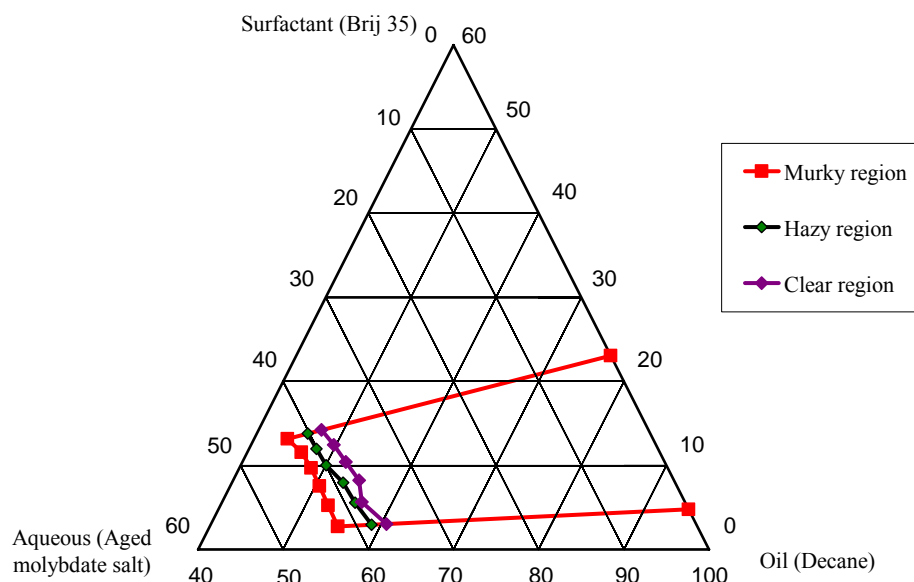


**Figure 4.1.3.4:** The stability region of micelles subject to the addition of aged molybdate salt to a mixture of decane and Brij 35. The stability region shown corresponds to that of a clear, hazy and murky solution (with that of a milky solution not shown).

The overall observations are consistent with those made when hexane was used as oil, apart from the following:

- **Stability of micelle**

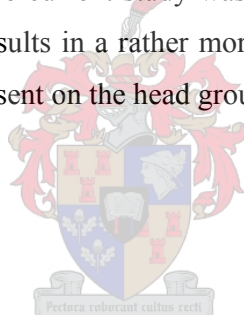
The long-chain oil produced more stable micelles than did the short chain oil. The stability of the bismuth solution was lower than that of the molybdate solution, but still higher than when hexane was used as oil.

### Discussion of results for stability in a mixture of brij 35 and decane

The general trends observed for the above comparisons (as shown in Figures 4.13 to 4.16) were consistent with those observed when hexane was used as an oil, as described in section 4.1.1.1, except that there was far greater stability. Such a finding is in line with the discussion in section 4.1.1.1, since the longer length of the alkane chain of the oil used leads to an increase in the rigidity of the interface. In their study in which they used different alcohol chain lengths, Shahidzadeh *et al.* (1999) observed that the three-phase region formed by decane lacks the

Marangoni effect, so that the surfactant does not penetrate into the oil phase, where it experiences a strong surface tension. Such non-penetration is important, as the surfactant must adsorb at the micelle interface and not in the bulk phase.

However, the results obtained by Cason *et al.* (2001) contradict the above observation. Using an ionic surfactant AOT, they related their observation of the decrease in the flexibility of the micelle interface with an increased alkane chain length to a differing degree of oil penetration into the surfactant chain region. They attributed this dependence to the bulky nature of the oil used, which did not allow it to solvate the surfactant tails as readily, whereas the less bulky oil was able to pack into the micelle tail and to solvate the surfactant tails effectively. The two systems, therefore, are expected to behave differently, since the oil used is different, the oil used in Cason *et al.*'s work being highly branched, whereas the decane used in the current study was linear. Secondly, as previously shown, the use of ionic surfactants results in a rather more complicated adsorption at the micelle interface due to the charge present on the head group.



#### 4.1.1.4 Stability in a mixture of CTAB in pentanol and decane

Figures 4.1.4.1 to 4.1.4.4 below graphically illustrate the experimental results obtained, showing the stability of micelles when different aqueous solutions were added to a constant CTAB-decane mixture. The first region (R1) corresponds to a clear phase; the second region (R2) corresponds to a hazy phase; the third (R3) region corresponds to a murky phase; and the fourth and final region corresponds to a milky phase (which is not shown) for all the stability diagrams. Figures 7.1.4.1 and 7.4.1.2 appear in appendix A1D, while a compilation of the experimental data can be found in appendix D1 (see table D1D).

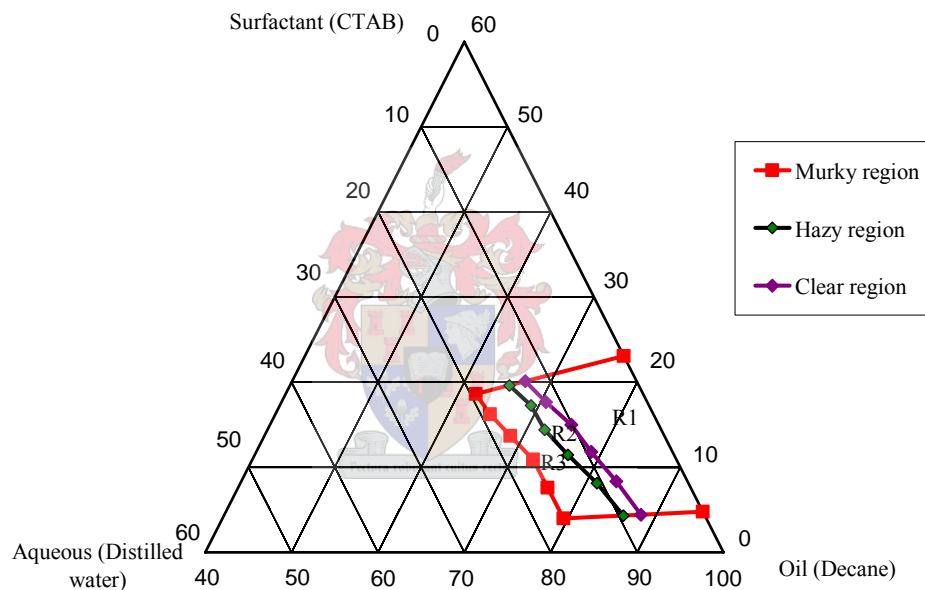


**Figure 4.1.4.1:** The stability region of micelles subject to the addition of distilled water to a mixture of decane and CTAB, the latter was dissolved in pentanol. The stability region shown corresponds to that of a clear, hazy and murky solution corresponding to R1, R2 and R3 (with that of a milky solution not shown).

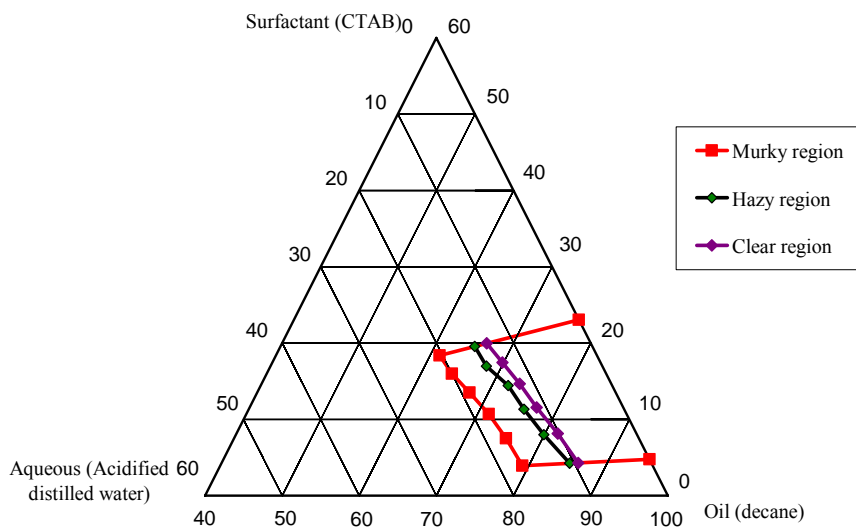


**Figure 4.1.4.2:** The stability region of micelles subject to the addition of acidified distilled water to a mixture of decane and CTAB, the latter was dissolved in pentanol. The stability region shown corresponds to that of a clear, hazy and murky solution (with that of a milky solution not shown).

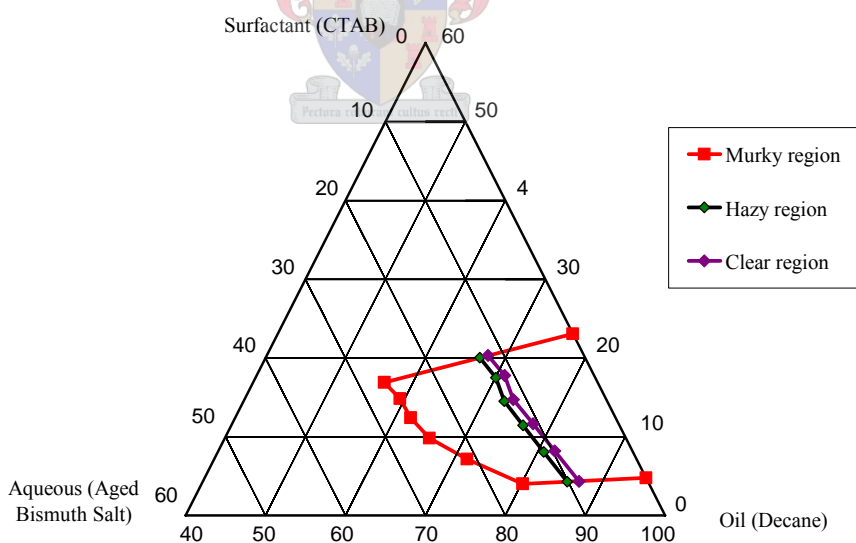


**Figure 4.1.4.3:** The stability region of micelles subject to the addition of aged bismuth salt to a mixture of oil (decane) and surfactant (CTAB), the latter was dissolved in pentanol. The stability region shown corresponds to that of a clear, hazy and murky solution (with that of a milky solution not shown); the hazy and murky regions are shown to overlap.

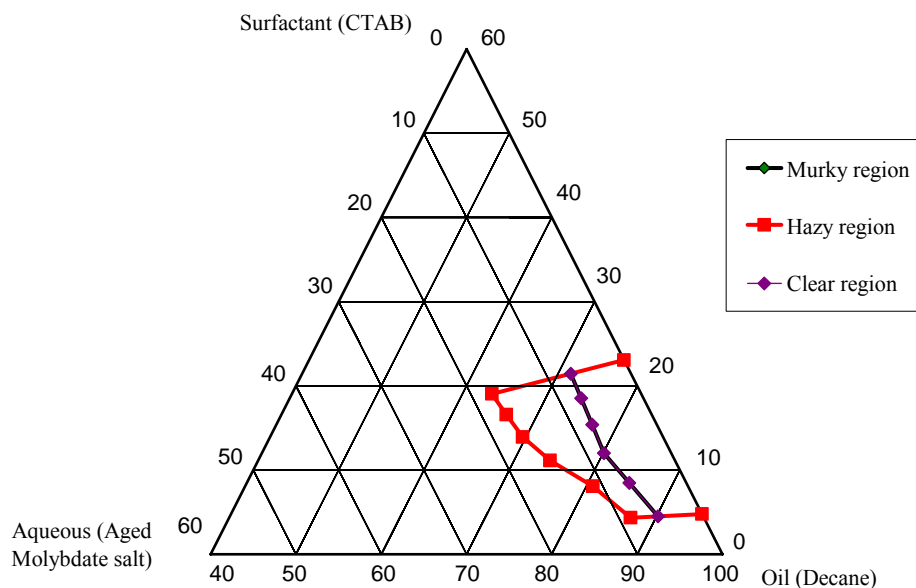


**Figure 4.1.4.4:** The stability region of micelles subject to the addition of aged molybdate salt to a mixture of decane and CTAB, the latter was dissolved in pentanol. The stability region shown corresponds to that of a clear, hazy and murky solution (with that of a milky solution not shown).

Overall, the observations are consistent with those made when hexane was used as oil, apart from the following:

- **Overlap in the results**

The hazy region was observed to experience overlap for the addition of molybdate (as can be seen in Figures 7.1.4.1 and 7.1.4.2 in appendix A1D) and aged molybdate salt. Such an overlap was due to the rapidity of the transition (from clear to hazy, to murky). As the instability region was reached, it became more difficult to distinguish between the transitions concerned.

- **Stability of micelle**

As with brij 35, the long-chain oil was found to produce significantly more stable micelles than did the short-chain oil.

- **Abnormality in the high salinity results**

The abnormality in the results observed especially at high surfactant concentration (20, 25

and 30 vol. %) was not observed when hexane was used as oil. The observed abnormality arose due to the growing viscosity of the mixture, the separation of the mixture into two phases, with white precipitates attaching to the surface of the system container, making stirring of the mixture quite difficult. However, since such a development represented a final transition, it could not have had a significant effect on the measured stability of the mixture concerned.

#### **Discussion of results for stability in a mixture of brij 35 and decane**

The general trends observed for the above comparisons (as shown in Figures 4.1.4.1 to 4.1.4.4) are consistent with those noted when hexane was used as oil, with the exception of the addition of distilled and acidified distilled water. The stability appeared higher than at lower surfactant concentration for the addition of the aged salts. In contrast, for the addition of both the distilled and the acidified distilled water, the stability was similar at both low and high surfactant concentration. Such a finding was unexpected, since various studies, including the current one, have so far shown that the surfactant CTAB has a high solubilisation capacity at high salinities. However, given the explanation by Cason *et al.* (2001), of the behavior of the micelle interface for ionic surfactant when an alkane chain length is increased, the explanation for such an observation is clear: due to the bulky nature of the oil concerned, it cannot solvate the surfactant tail. However, the reason why such an observation is not consistent with the addition of different aqueous solutions is still unclear.

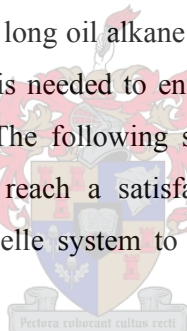
The addition of salt is expected to result in a decrease in the head group of the surfactant and thus to decrease the radius of the droplet, as experimentally observed by Hamilton *et al.* (1990). However, the correlation between the stability of the micelle interface and the droplet radius cannot be inferred, since the droplet size depends on many factors that impact on the composition of the reverse micelle systems. Though the observed overlap in the results is not easily explained, it can be argued that, at a high aqueous content, the micelle interface is expected to become more flexible. The first two transitions can therefore be expected to appear in similar regions, and the last transition, which represents high water content, can also be expected to be significantly wider than the two regions themselves.

#### 4.1.1.5 Other observations

The surfactant (brij 35) was observed during experimentation to be highly hydrophilic. When left in an open atmosphere, bubbles were observed forming on top of the surfactant solution, though such a formation could not be observed on use of the other surfactant (CTAB). When left in an open atmosphere, no bubbles were observed on top of the surfactant solution. Therefore, in order to minimise the contact of brij 35 with the atmosphere a dried syringe was used to draw the required amount of the surfactant.

#### 4.1.1.6 Final composition

From both visual observation and the above discussion, the conclusion can be drawn that the combination of ternary system with the longer oil chain length, decane, results in a far more stable micelle, while the quaternary system shows a higher stability at high surfactant concentration for both short and long oil alkane chain. Therefore, a more reliable analysis, such as the Malvern Zetasizer, is needed to enable a decisive conclusion to be drawn in regard to the final surfactant. The following subchapter will therefore discuss such an analysis in detail in order to reach a satisfactory conclusion in regard to the final composition of the reverse micelle system to be employed in the synthesis of catalyst particles.



## 4.1.2 Malvern Zetisizer analysis

Though titration analysis is a reliable method, the use of such an analysis does not allow a final conclusion to be drawn as regards which final composition should be used, since such a method does not give the exact particle size of the micelles formed. The Malvern Zetisizer analysis was therefore performed so that a reliable conclusion could be drawn regarding the exact composition of the reverse micelles concerned. The sizes measured are therefore relative, as no calibration was possible. The analysis was done for only 10 and 25 vol. % surfactant concentration from 5 vol. to 20 vol. % of the aqueous solution over a time period of 1 800 seconds for each experiment.

### 4.1.2.1 Stability in a mixture of Brij 35 and decane

Experimental results obtained using the Malvern Zetisizer is shown in Figures 4.2.1.1 to 4.2.1.6 below. The figures show the stability of micelles measured over a time period of 1800 seconds, during which different aqueous solutions were added to a constant Brij 35-decane mixture. A compilation of the experimental data can be found in tables D2.1 to D2.6 in appendix D2.

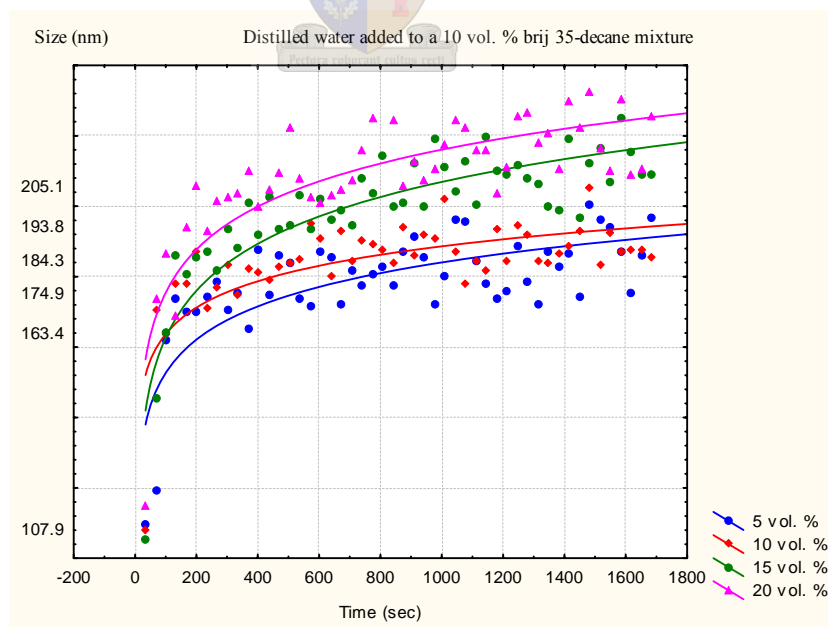


**Fig 4.2.1.1:** The stability of micelles for the addition of distilled water to a 10 vol. % brij35-decane.



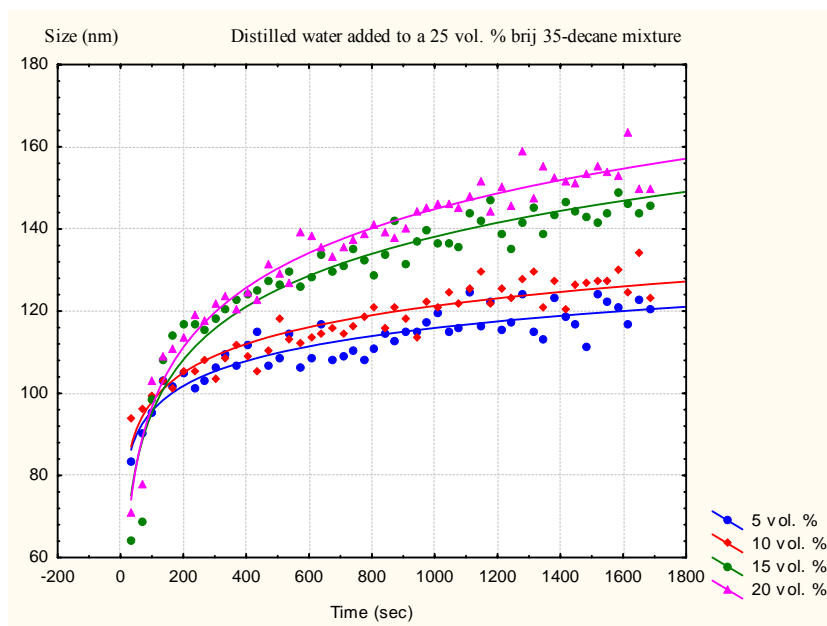


**Fig 4.2.1.2:** The stability of micelles for the addition of distilled water to a 25 vol. % brij35-decane.

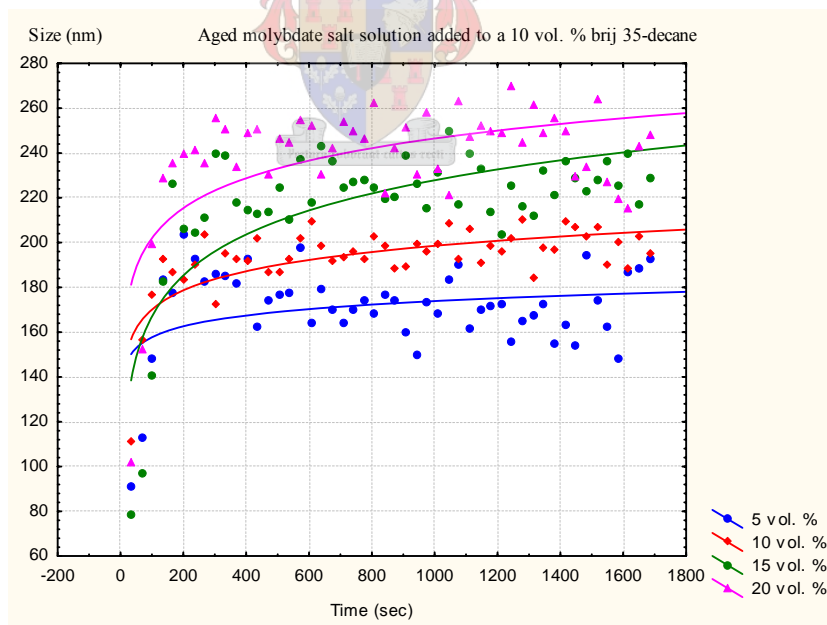


**Fig 4.2.1.3:** The stability of micelles for the addition of an aged molybdate salt solution to a 10 vol. % brij35-decane.

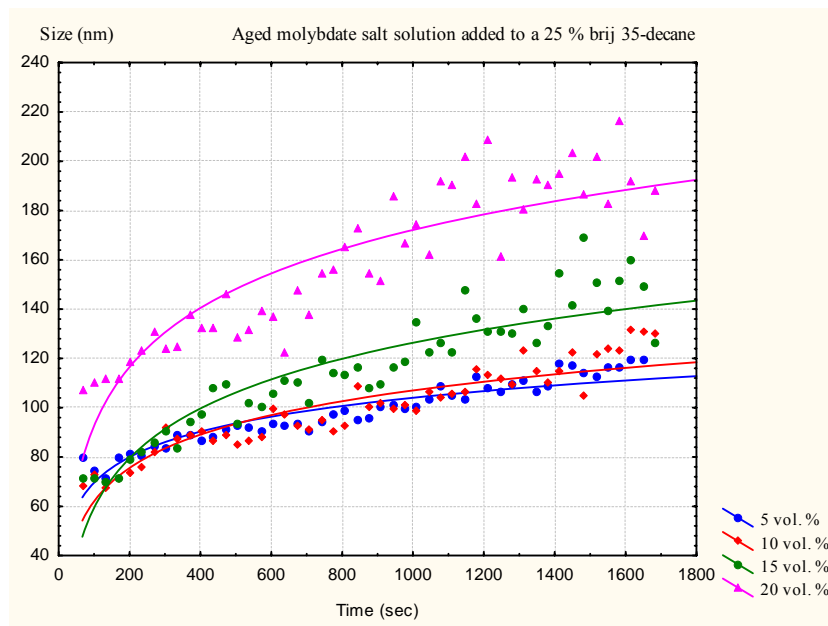


**Fig 4.2.1.4:** The stability of micelles for the addition of an aged molybdate salt solution to a 25 vol. % brij35-decane.

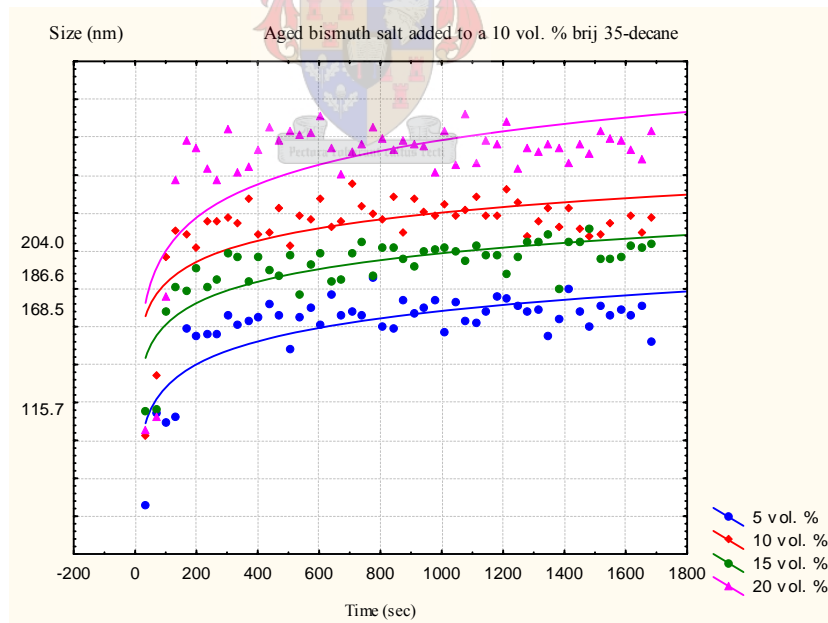


**Fig 4.2.1.5:** The stability of micelle for the addition of an aged bismuth salt solution to a 10 vol. % brij35-decane.

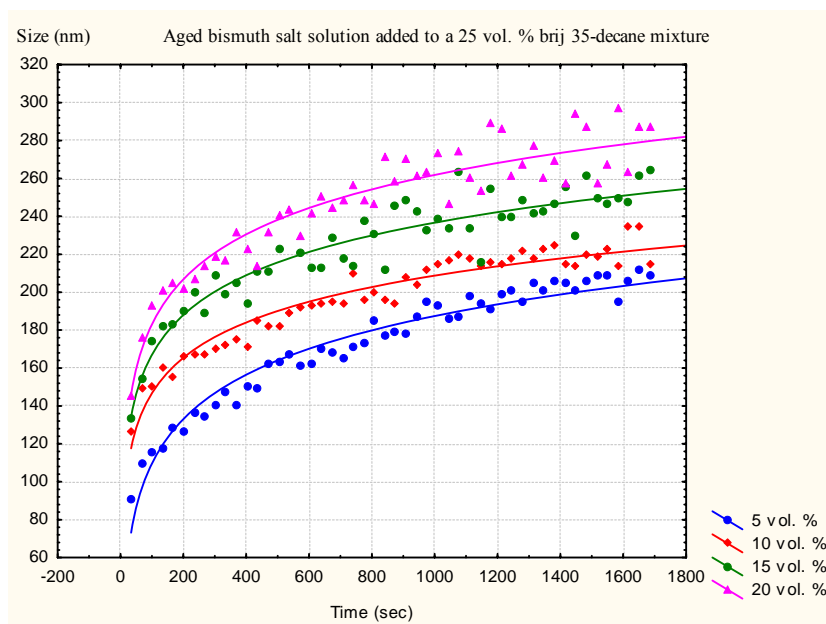
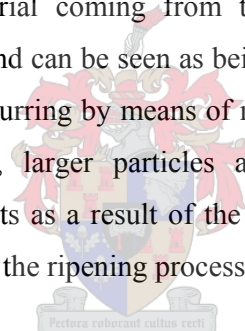


**Fig 4.2.1.6:** The stability of micelles for the addition of an aged bismuth salt solution to a 25 vol. % brij35-decane.

All solutions were observed to grow purely autocatalytically for an initial 200 seconds, after which the growth rate was restricted solely to Oswald ripening. The initial catalytic process is more significant for low, than for high, surfactant concentrations. However, after the initial 200 seconds, the ripening process is more significant at low, than at high, surfactant concentrations. Taking into consideration that catalytic growth involves the interchange of aggregates, the observation can be made that at first there is no particle interchange, or, if any does take place, such interchange leads to the development of a particle larger than the original. The increased ripening growth observed for a low surfactant concentration after the initial 200 seconds is consistent with the observations made during titration analysis, during which micelles were observed to be less stable for lower surfactant concentrations, with increasing stabilisation occurring with the addition of more surfactant. Though initial catalytic growth for the higher concentration surfactant is significantly less, even after 1 800 seconds such growth did not flatten out in comparison to lower surfactant concentration.

The finding that initial growth is purely catalytic after the initial 200 seconds, with subsequent growth only occurring due to Oswald ripening, is consistent with the observations made by Quintillan *et al.* (2001). In their simulations they assumed that for interdroplet exchange to occur, the reactant should be redistributed in accordance with a crude concentration gradient principle, regardless of the presence or absence of a product if both colliding droplets were to carry the same reactant. The gradient principle states that *reactant must be transferred from the droplet with more reactant to the droplet with less reactant*. By introducing factor  $k$ , the number of units transferred, Quintillan *et al.* (2001) were able to state how much droplet interchange had, in fact, taken place. Further, when the growth rate was purely catalytic, they were able to assume that an increase in  $k$  led to an increase in final particle size, since growth by ripening does not include interdroplet exchange. In contrast, growth by ripening assumes that larger particles will grow by condensation from the material coming from the more solubilised smaller particles. Accordingly, the observed trend can be seen as being due, initially, to all particles being of similar sizes, with growth occurring by means of material transfer. With the occurrence of greater material interchange, larger particles are formed. Larger droplets can then coagulate with smaller droplets as a result of the breaking up of the larger droplets, in a process of fission, resulting in the ripening process.



The above discussion shows that the rate of ripening does not depend on the concentration of the micelles, which is consistent with the experimental observations made by Kalbanov *et al.* (1994). In their studies using nonionic surfactant SDS with undecane, they showed that varying the concentration of the surfactant did not affect the rate of Oswald ripening, despite the system showing a considerable increase in its solubilisation capacity. They explained this behavior by arguing that (i) the surfactant micelle cannot absorb the oil directly from the emulsion droplet, necessitating a stage of molecular diffusion through the medium; and that (ii) micelles are not in local equilibrium with the molecular solution, presumably because the rate of oil monomer exchange between the aqueous solution and the micelle interior is quite low. They concluded by noting that such an observation could not be of a general nature, and that studies with other surfactants were necessary. This discussion will be advanced still further in section 4.1.2.2, when the stability diagrams of

ionic surfactant CTAB is discussed. The above observation is contrary to that made by Izquierdo *et al.* (2002), who experimentally observed that the ripening rate increases with an increase in surfactant concentration for a C12E4 surfactant. The argument presented by such authors centres on the fact that (i) the droplet size will decrease with an increase in the surfactant concentration, in confirmation of earlier observations; and the fact that (ii) the number of micelles increases as the surfactant increases. This argument is contrary to the findings of the current study, in which ripening was observed to occur independently of the number of micelles formed, resulting in the observed contradiction.

The previous discussion presupposes that the intermicellar exchange processes are governed by dimmers or aggregates formed by contact between two micelles and by the exchange of processes between two water pool droplets, as experimentally shown by Pileni (1997). Further, the first factor is reported to be related to the attractive interaction between droplets, involving the probabilities of collision of two micelles, whilst the latter factor is associated with interface flexibility, being related to the dynamic properties of the *water-surfactant-oil* interface, as shown by Moulik and Paul (1998). Such a finding is consistent with the observations made by Quintillan *et al.* (2001). Hence, the observed trend above, the intermicellar exchange, can be concluded as being tuned by controlling either of the two factors.

The previous figures show that, in the absence of Ostwald ripening, tuning the particle size would be rather difficult to do, consistent with the observations made by Schevchenko *et al.* (2003), who argued that, in the absence of Ostwald ripening, particles can grow only until all molecular precursor are consumed, and the total amount of consumed monomer (as well as the total volume of formed particles) is constant. Hence, the authors note that, in this case, the balance between the rate of nucleation and growth should affect the final particle size. Further, a fast nucleation is observed to provide high particle concentration, with small particle size, and a slow nucleation to provide a low concentration of seed, consuming the same amount of monomer and resulting in larger particles. They conclude by observing that control over the nucleation rate allows the tuning of final nanoparticle size in the absence of Ostwald ripening.

The above figures show that the size of the micelles increased in line with an increase in aqueous content. Such a finding is consistent with the observations made during titration analysis, which are discussed in section 4.1.1. Increasing the water content leads to an increase of water within the micelle core, spreading the surface area of the surfactant head group, thereby increasing the size of the resultant micelles. At low water content, it can be argued that most water is bound to the head group of the surfactant molecule, and the hydrolysis rate is expected to be slow, as was shown by Adair *et al.* (1998).

Further, the ratio of water to surfactant concentration,  $W_0$ , plays an important role in determining the interaction of the water pool with the surfactant or bulk water. Earlier work has shown that at low  $W_0$  most water pool will strongly interact with a surfactant, thereby creating a tight interface. At high  $W_0$ , the water pool behaves as bulk water, strongly interacting with a surfactant or co-surfactant. Hence, in the above figures one can observe that the size of the nanodroplet increases as the water pool increases and visa versa. By varying the amount of water content, change in the size of the droplet formed is possible.

Such an observation has already been advanced in the studies of Curri *et al.* (2000), who observed that, for a certain chosen ternary system, the water content dictates the diameter of the water core. As a result, the control over nanoparticle diameter could be expected to be achieved by merely varying the water content. However, the final size of the particle formed cannot be controlled solely by such variation, so that it is likely that it will have a controlling influence over the growth rate of the particles concerned. Such a finding was also proven by Bonini *et al.* (2002) and Cason *et al.* (2001), who showed that particles of the same size can be obtained regardless of the water content.

#### 4.1.2.2 Stability in a mixture of CTAB in pentanol and decane

Experimental results obtained using a Malvern Zetisizer analysis is illustrated in figures 4.2.2.1 to 4.2.2.6 below. These figures show the stability of micelles, measured over a time period of 1 800 seconds, when different concentration aqueous solutions were added to a constant concentration CTAB-decane mixture. The stability of micelles for higher salt solutions (0.75 vol. and 10 vol. %) are not included, since the sizes measured fell outside the range of Zetisizer analysis. A compilation of the experimental data can be found in appendix D2 (see tables D2.7 to D2.12).

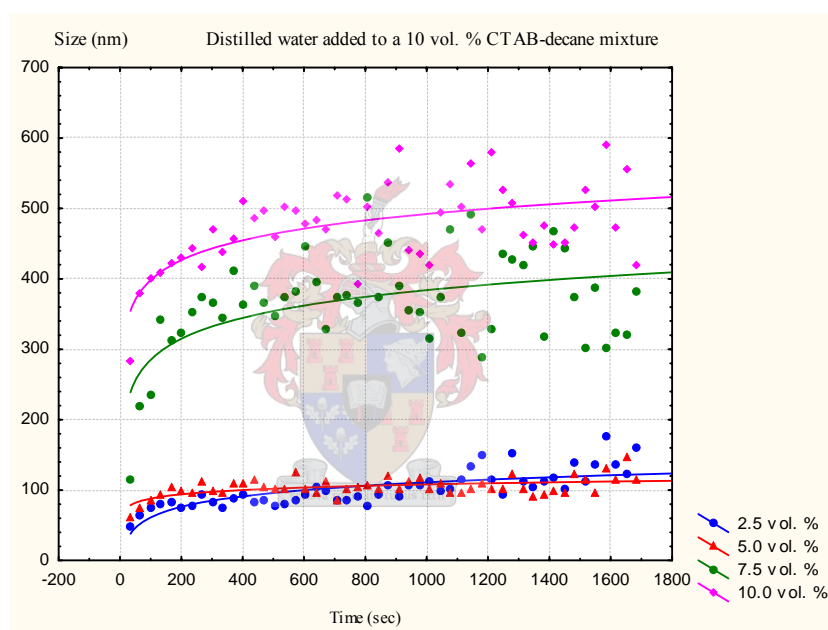


**Fig 4.2.2.1:** The stability of micelles for the addition of distilled water solution to a 10 vol. % CTAB-pentanol-decane.

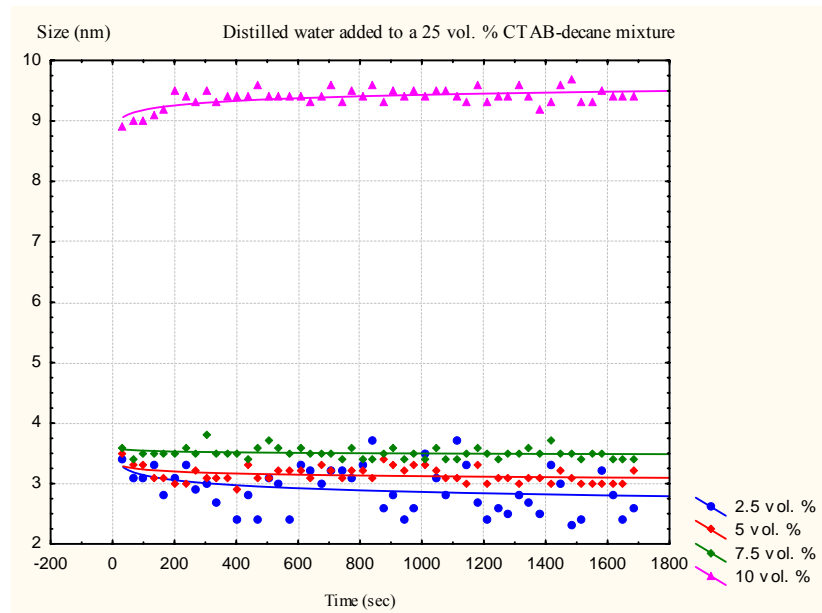


**Fig 4.2.2.2:** The stability of micelles for the addition of distilled water to a 25 vol. % CTAB-pentanol-decane.

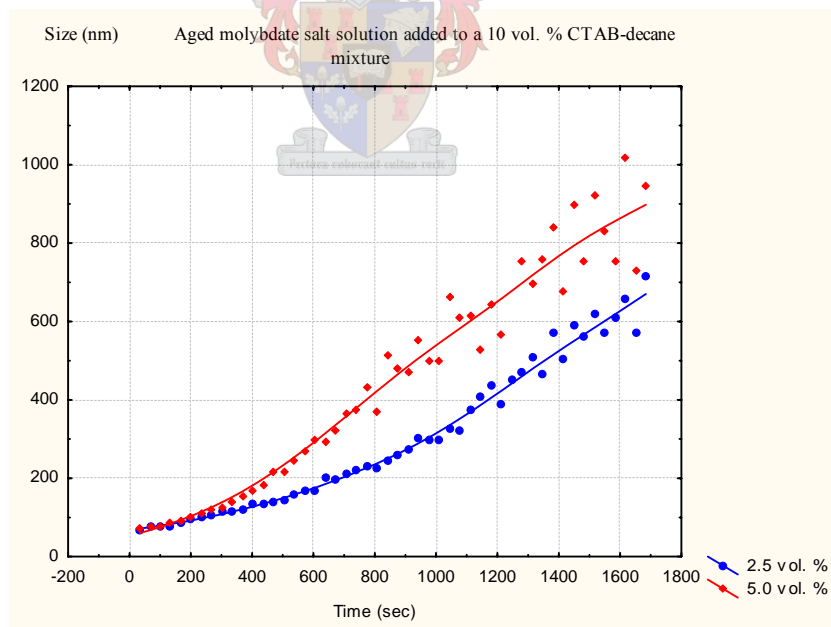


**Fig 4.2.2.3:** The stability of micelles for the addition of an aged molybdate salt range solution to a 10 vol. % CTAB-pentanol-decane.



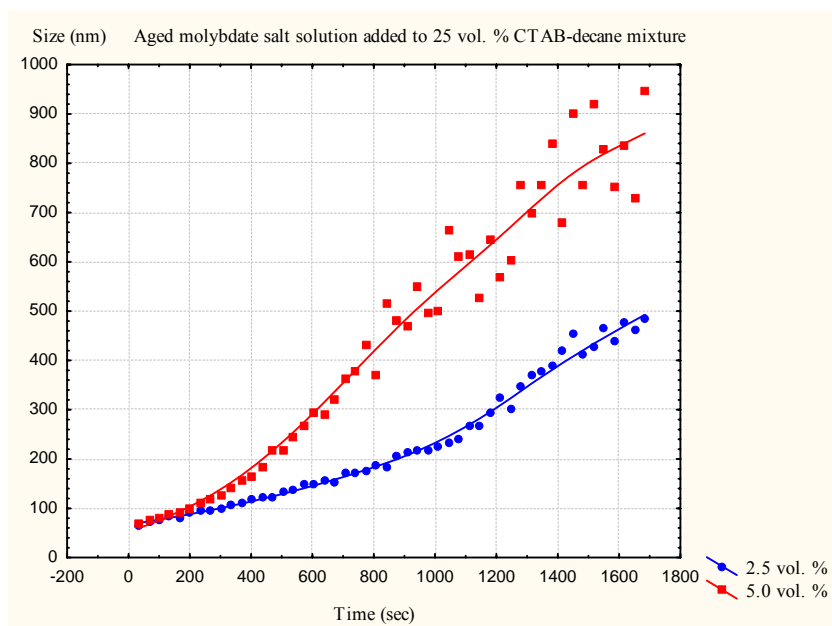


**Fig 4.2.2.4:** The stability of micelles for the addition of aged molybdate salt solution to a 25 vol. % CTAB-pentanol-decane.

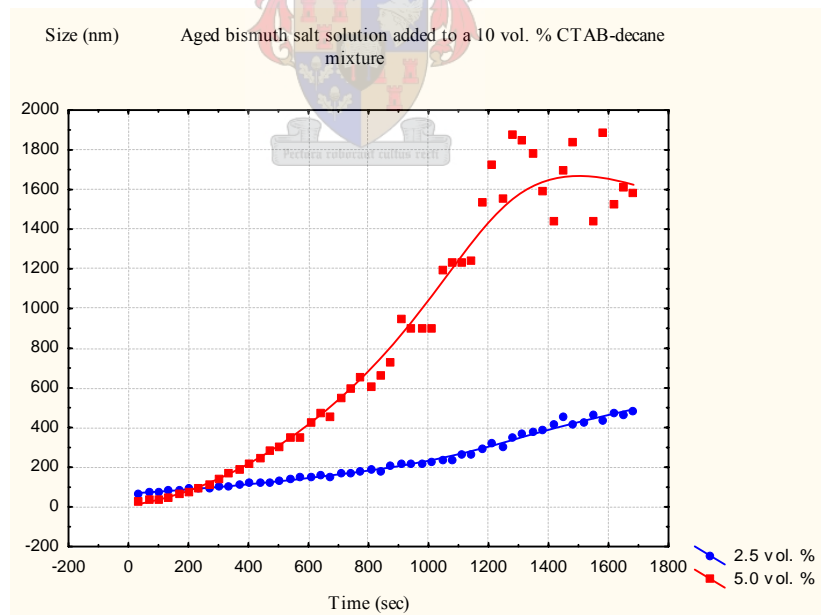


**Fig 4.3.2.5:** The stability of micelles for the addition of an aged bismuth salt solution to a 10 vol. % CTAB-pentanol-decane.

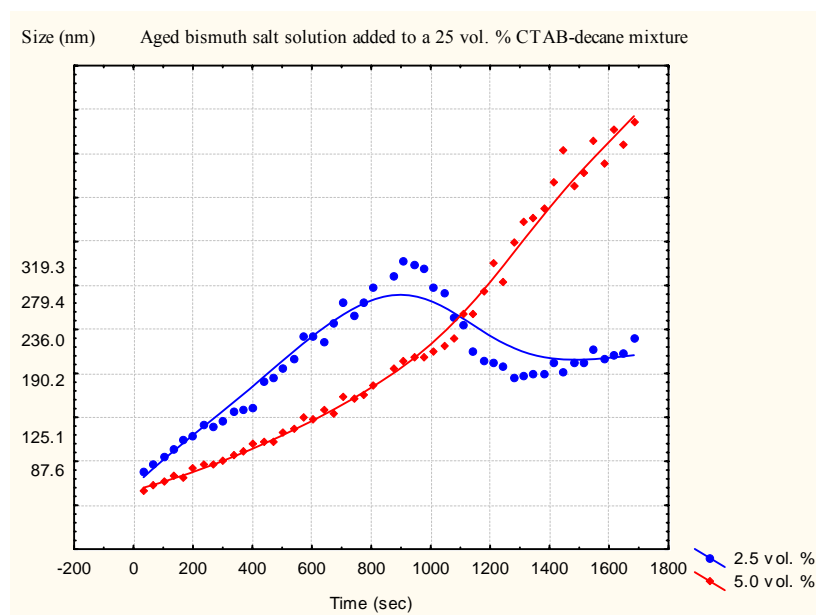


**Fig 4.2.2.6:** *The stability of micelles for the addition of an aged bismuth salt solution to a 25 vol. % CTAB-pentanol-decane.*

The general trend observed for Figures 4.2.2.1 to Figure 4.2.2.6 is that, for the addition of distilled water at low surfactant (see Figure 4.2.2.1) concentration for the addition of lower aqueous content (2.5 vol. and 5.0 vol. %), the growth of particles is due purely to ripening, with sizes averaging at around 100 nm. Whereas, for the addition of higher concentration solution aqueous, initial growth is purely catalytic, becoming ripening after an initial 200 seconds, consistent with the observation made when brij 35 was used as a surfactant, as described in section 4.1.2.1. At high surfactant concentration, particle growth occurs purely as a result of ripening, with larger size micelles present in the higher aqueous content. For the addition of molybdate salts, growth is purely catalytic, though suggesting initial ripening growth, while, for the addition of bismuth salts, visible behavior is shown. As earlier indicated, the interfacial layer plays a crucial role in the stability of the micelles, and the addition of a co-surfactant has been shown to affect the micelle interface dramatically. Hence, the observed trend revealed in the above figures is unsurprising, though the behavior observed on the addition of distilled water at higher aqueous content is unexpected.

The behavior observed in the general trend in the quaternary CTAB system can be attributed mainly to the presence of a co-surfactant in the interfacial film. The results obtained are not contrary to those obtained by Curri *et al.* (2002), who attribute such behavior to the alkyl tail of the pentanol, which increases the interfacial curvature by increasing the surfactant packing parameter, thus favoring the formation of smaller particles with low water content, suggesting a microstructural effect. Further, the exchange of reactance between water pools should be considered the reason for size polydispersity.

In the observed general trend in the above figures one can observe that alcohol plays a crucial role in determining particle radius, since it acts as an agent in increasing the interface dynamics of the droplet, suggesting a dynamic effect. The nanodroplet formed under such conditions as the quaternary systems does not show the same interface rigidity observed in ternary systems. Further, the addition of alcohol suggests a strong interaction between the co-surfactant tail and the surface of the particle. The observed behavior for the addition of water illustrates the remarkable solubility of water in the organic phase, as experimentally evidenced by Giustini *et al.* (1996), whereas the addition of salts results in an increase in droplet size in agreement with the observations made by Curri *et al.* (2000), and as observed in the above figures. In addition, the use of an ionic surfactant can be invoked by noting that its addition results in a rather more complex micellar interface.

#### 4.1.2.3 Final composition

Discussion of the above results shows that the ternary system, consisting of brij 35 as a surfactant and decane as oil at low water content and at a high surfactant concentration, results in stable micelles. The quaternary system, consisting of CTAB, results in extremely large particle sizes for the addition of salts, even at low aqueous concentration. However, stable micelles were obtained at extremely low amounts of water content, though the attendant growth consists purely of ripening. Hence, the ternary system consisting of brij 35 can be used for the synthesis of catalyst particles. The subsequent subchapter discusses various factors that affect the preferred composition for the synthesis of  $\alpha$ -bismuth molybdate nanoparticle in detail.

## 4.2 SYNTHESIS OF $\alpha$ -BISMUTH MOLYBDATE NANOPARTICLE

### 4.2.1 Effect of salt concentration on catalyst particle

The results obtained from the experimental runs performed to investigate the effect of salt concentration on the particle size are presented in Figures 4.3.1.1 and 4.3.1.2. Further figures for all experimental runs are presented in appendix A2A. A compilation of experimental data can be found in appendix D3 (see table D3.1).

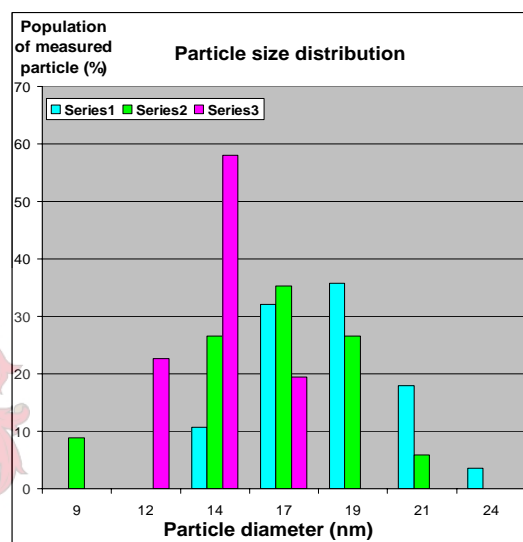
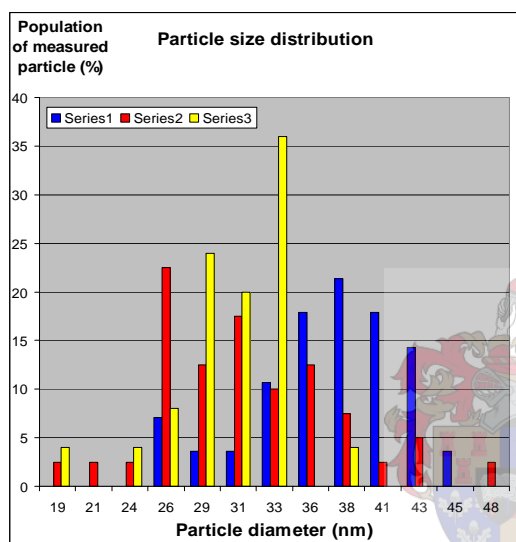


**Figure 4.3.1.1:** Particle size distribution for investigation into the effect of salt concentration for 10 vol. % surfactant. Series 1, 2 and 3 correspond to 0.64 mol/l molybdate and 0.2133 mol/l bismuth; 0.32 mol/l molybdate and 0.1067 mol/l bismuth; and 0.16 mol/l molybdate and 0.0533 mol/l bismuth salts respectively.

**Figure 4.3.1.2:** Particle size distribution for investigation into the effect of salt concentration for 25 vol. % surfactant. Series 1, 2 and 3 correspond to 0.64 mol/l molybdate and 0.2133 mol/l bismuth; 0.32 mol/l molybdate and 0.1067 mol/l bismuth; and 0.16 mol/l molybdate and 0.0533 mol/l bismuth salts respectively.

The figures show that, as the reactant concentration increases, the particle size increases for both low 10 vol. % and higher 25 vol. % surfactant concentrations, with a narrow size distribution being obtained at low reactant concentration. A decrease in surfactant concentration results in an increase in particle size, with particle agglomeration being observed for all salt surfactant concentration. Further, the particle shape is observed to be spherical for all reactant concentrations.

The summary for specific experimental runs is presented in table 4.1 below. The experimental runs were performed at a temperature of 25 °C.

**Table 4.1:** Summary for experimental runs for catalyst synthesis for investigation into the effect of salt concentration.

Series	vol. % Brij35	T	[Mo]	[Bi]	Particle size range	Average particle size distribution
		°C	(mol/L)	(mol/L)	(nm)	(nm)
1	10	25	0.64	0.2133	26–48	38
2	10	25	0.32	0.1067	19–43	33
3	10	25	0.16	0.0533	24–33	31
1	25	25	0.64	0.2133	14–24	19
2	25	25	0.32	0.1067	14–21	18
3	25	25	0.16	0.0533	12–17	14

### Discussion on the effect of salt concentration

The observation that, by increasing the reactant concentration, particle size increases can be expected is shown by Lopez-Quintella (2003). Two reasons that can possibly account for the effect of the reactant concentration on particle size are illustrated by Chen and Wu (2000), who studied the reduction of chloride using hydrazine. Their study was able to show that, at low hydrazine concentration, the reactant concentration was so low that it led to a formation of fewer nuclei at the very start of the reduction. The number of atoms formed at the outset of the reduction remained constant, due to a high ion concentration. However, as the concentration of hydrazine increased, the enhanced reduction rate favoured the formation of more nuclei. Consequently, the atoms formed during the latter period were used for the growth of particles, resulting in the formation of larger particles. Such an observation is in agreement with that obtained by Holmberg (2004) that, due to the dilute nature of the salt solution, the solid particles formed are of the same sized order as the starting aqueous droplets, resulting in the narrow particle size distribution observed at a lower reactant concentration than that shown in the above figures.

The observed increase in particle size as the surfactant concentration is increased is not contrary to findings, having previously been reported. Further, such an observation is consistent with those made during the Malvern Zetasizer analysis described in section 4.1.2. At a higher surfactant concentration (25 vol. %), the particle sizes were found to exceed those at lower surfactant concentration (10 vol. %). Lopez-Quintela (2003) has shown that an increase in particle size can be achieved by means of increasing the surfactant film flexibility. A flexible film allows for the exchange of particles, while a highly flexible film allows for the exchange of even larger particles. By increasing the surfactant concentration in the system, more surfactant becomes available for surrounding the droplet, allowing the film to become flexible. At low surfactant concentration, the water present can be assumed to exist as a bulk phase, with the interface becoming highly flexible, resulting in the larger particles observed. A correlation between the exchange of materials and the final particles obtained has been advanced by Lisiecki (2004), who has shown that the growth of copper seeds so produced is directly related to the exchange of water pools between two micelles occurring during the exchange of processes.

The observed agglomeration of particles for all salt concentrations and both surfactant concentrations is easily explained by way of the two hypotheses developed by Debuigne *et al.* (2000). The first hypothesis states that the coalescence controlled the diffusion, consisting of the combination of several particles to form a new dendric structure, which forms by way of kinetic control. The second hypothesis states that Ostwald ripening is slower than coalescence, with the solid phase dissolving in the liquid phase and the molecule migrating towards the larger particle under conditions of thermodynamic control. However, the mechanism controlling such aggregation is not known.

## 4.2.2 Effect of nucleation and growth

Results obtained from the experimental runs performed to investigate the effect of nucleation and growth on the particle sizes are presented in Figures 4.3.3.1 and 4.3.3.2. Further related figures are presented in appendix A2B and A2C. A compilation of experimental data can be found in appendix D3 (see table D3.2).

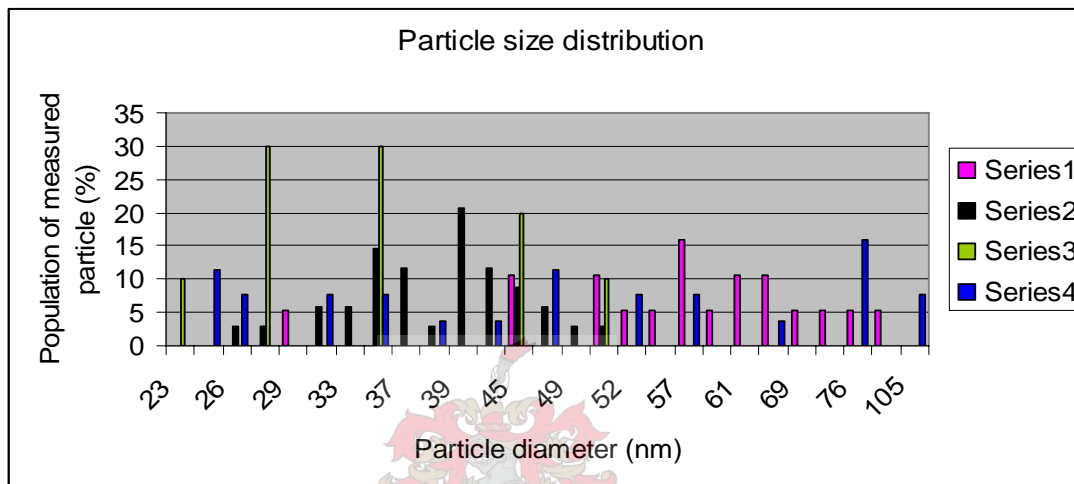


**Figure 4.3.3.1:** Particle size distribution for the investigation into the effect of nucleation and growth. Series 1, 2 and 3 correspond to the catalyst particles that were nucleated for 120, 60 and 20 minutes respectively at 25 vol. % surfactant. Series 4 corresponds to the catalyst particles that were nucleated for 120 minutes at 10 vol. % surfactant.

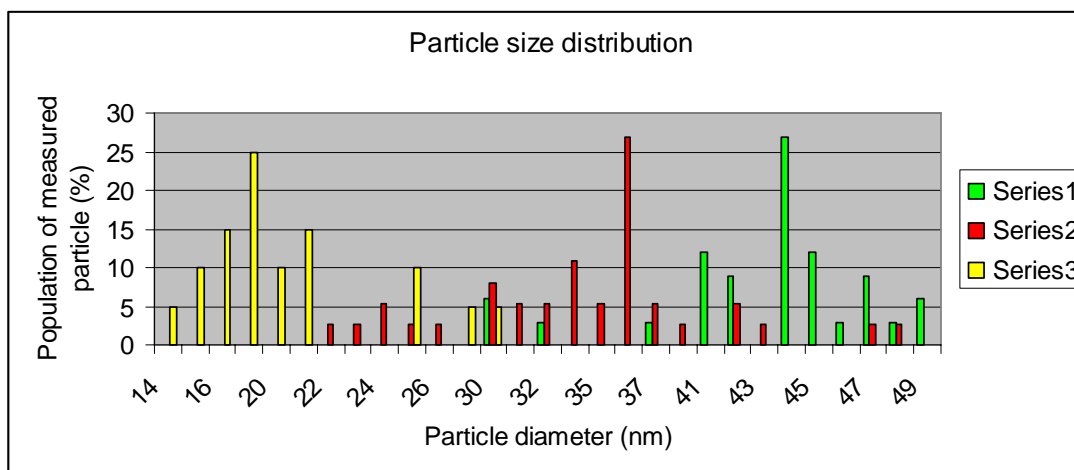


**Figure 4.3.3.2:** Particle size distribution for the investigation into the effect of nucleation and growth, with the reverse micelles being aged for 24 hours prior to nucleation. Series 1, 2 and 3 correspond to the catalyst particles that were nucleated for 120, 60 and 20 minutes respectively.

The above figures show that when micelles are nucleated for a longer period (120 minutes) they result in larger particles with an uneven, wider particle size distribution. When the reverse micelles were aged for 24 hours before being nucleated, the particles were smaller, depending on the nucleation period concerned. The summary of the data obtained from the specific experimental runs, which were performed at 25 °C, is presented in table 4.2 below.

**Table 4.2:** Summary of data obtained from experimental runs for catalyst synthesis for investigation into the effect of nucleation and growth.

Series	vol. % Brij35	T	Bismuth	Molybdate	Nucleation	Aging	Particle size range	Average particle size
		(°C)	(mol/L)	(mol/L)	(min)	(hrs)	(nm)	(nm)
1	25	25	0.2133	0.64	120	24	30–49	44
2	25	25	0.1067	0.32	60	24	22–48	36
3	25	25	0.0533	0.16	20	24	14–31	19
1	25	25	0.2133	0.64	120	0	45–81	57
2	25	25	0.1067	0.32	60	0	26–51	39
3	25	25	0.0533	0.16	20	0	23–56	28
4	10	25	0.0533	0.16	120	0	24–105	47

### Discussion on the effect of nucleation and growth

The observed effect of nucleation and growth on particle size, where larger particles were obtained for slow nucleation, has been previously reported by Schevchenko *et al.* (2003) and Eriksson *et al.* (2004). Boutonnet (1982) was able to show that, when hydrazine is used as a reducing agent for a transitional metal salt, fast nucleation resulted in smaller particles and the reduction process occurred very rapidly. The explanation for the observed smaller particles as a result of fast nucleation has been explored by Schevchenko *et al.* (2003). In their study regarding the synthesis of CoPt<sub>3</sub>, they were able to show that slow nucleation provides a low concentration of aggregates, exchanging the same amount of material and resulting in larger particles than would otherwise have been obtained. Such a finding was to be expected since, before nucleation can occur, several particles must



collide. Hence, there is a smaller probability of particles colliding for a low concentration of aggregates, while the probability of collision will be greater for a higher concentration of aggregates.

Various studies have shown that a minimum cluster of micelles is required to form a stable nucleus, and that a collision between several atoms must occur for nuclei to form. This observation has been advanced by Chen and Wu (2000), in their study of the reduction of nickel chloride with hydrazine. Once the nuclei were formed, they were able to show that the growth process would be superior to the nucleation, since the probability of collision between atoms was much lower than that of collision between one atom and the already formed nuclei. Hence, all nuclei were found to form almost simultaneously and to grow at the same rate, with the number of nuclei formed at the beginning of the reduction determining the number and size of the resulting particles. In addition, they observed essentially monodispersed nanoparticles, consistent with the observations recorded above in which, for a slow nucleation, a wider particle size distribution was observed, whereas, for a fast nucleation, a narrow particle size distribution was observed.

While the above explanation suggests that particle size depends upon the number of aggregates in the reverse micelle system, this is only partly true, because the exchange of material depends on the success of each collision. The exchange of material depends largely on the interfacial film, as has previously been shown, with a flexible film allowing the exchange of material, while a highly flexible film allows the exchange of larger material. Such an explanation can help to account for the behavior observed, where, for a slow nucleation, when the surfactant is reduced to 10 vol. % an observed increase in particle size (to 47 nm) and a wider particle size distribution (24nm–105 nm) was observed. The above explanation does not contradict other studies that have shown that, because the surfactant surrounds the nanodroplet wall, an increase in surfactant concentration will result in a larger surface area for the interfacial film, thus creating a rigid wall. Such walls then act as cages for the growing nanoparticle, thereby reducing the average particle size during collision. Eriksson *et al.* (2004) were able to show that the presence of surfactant prevents the nuclei from growing overly fast. The observed non-

uniform distribution of particles is easily explained by noting that, for a slow nucleation, in principle nucleation can be expected to occur as a function of time. In fact, Lopez-Quintela (2003) has shown that, due to diffusion, new nuclei are formed in this way. Hence, already existing and newly emerging particles will both grow at different rates, causing the observed non-uniform particle size distribution for longer periods of nucleation.

### 4.2.3 Effect of temperature

The results obtained from the experimental runs performed at temperatures of 30 °C and 35 °C in order to investigate the effect of temperature on the particle sizes are presented in Figure 5.3.2.1. The free run recorded in Figure 5.3.2.2 was performed at a raised temperature of 50 °C. Further figures are presented in appendix A2D while a compilation of experimental data can be found in appendix D3 (table D3.3).

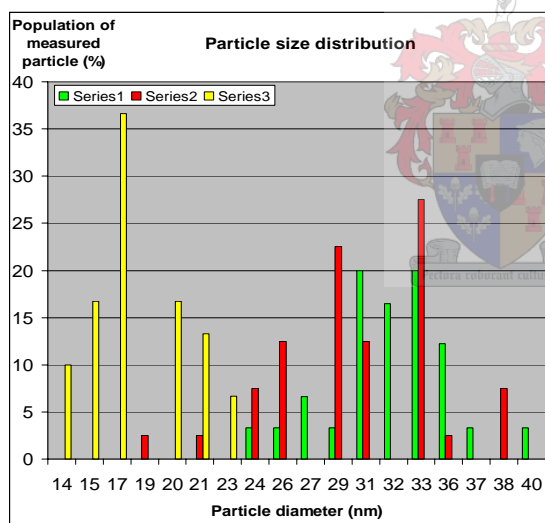


**Figure 4.3.5.1** Particle size distribution for the investigation into the effect of temperature. Series 1 and 2 were performed at temperature of 30 and 35 °C and nucleated for 60 minutes. Series 3 was performed at 35 °C and nucleated for 20 minutes.

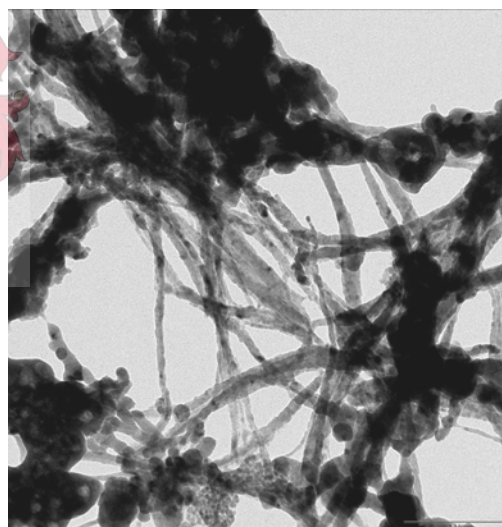


**Figure 4.3.5.2 (Free run):** TEM photograph of the catalyst prepared at a temperature of 50 °C.

The above figures show that when the temperature was raised to 30 °C and 35 °C while the reverse micelles were nucleated for a period of 60 minutes (as in series 1 and 2, respectively), a slight decrease in particle size occurred when compared with the particle sizes described in section 4.2.2, which resulted from the temperature being kept at 25 °C. The particle sizes decreased from 36 nm to 33 nm for a 5 °C and 36 nm to 29 nm for a 10 °C increment. When the reverse micelles were nucleated for a short period (20 minutes), the particle sizes decreased from 19 nm to 17 nm for a 10 °C increment. The summary of the specific experimental runs is presented in table 4.3 below. When the temperature was raised still further, to 50 °C (as recorded in Figure 4.42), the particle morphology changed from that of spheres to that of nanorods.

**Table 4.3:** Summary of experimental runs for catalyst synthesis for investigation into the effect of temperature

Series	vol. % Brij35	Bismuth	Molybdate	T	Nucleation	Particle size range	Average particle size
		mol/L	mol/L	°C	min	(nm)	(nm)
1	25	0.2133	0.64	30	60	21–40	33
2	25	0.1067	0.32	35	60	19–38	29
3	25	0.0533	0.16	35	20	14–23	17

### Discussion on the effect of temperature

The decrease in particle size at a raised temperature can be understood in relation to the effect that temperature has on particle size in terms of particle aggregation, which, in turn, is related to the concentration of the surfactant. At high surfactant concentrations, more particles can be expected to form than at a lower surfactant concentration. Such an observation has been advanced by Panda *et al.* (2001), who have shown that, by increasing the thermal energy of the system, the microdroplets are activated to assemble together and to grow in size, either by fusion or by agglomeration. Further, Toerne *et al.* (2001) have shown that the complete thermal stability of aggregates requires a somewhat higher surfactant concentration, because at a low surfactant concentration aggregates are loosely

associated and likely to be disrupted. With the effect of temperature being thought of as a reversible phenomenon, one would expect that particle sizes could be tuned by changing the temperature of the system, which, however, is not the case. Shevchenko *et al.* (2003) were able to demonstrate that nucleation rates rise faster with increasing temperature than do growth rates, meaning that nucleation is more sensitive to temperature than growth rate, with the result that temperature can be used to adjust the balance between nucleation and growth rates. Section 4.2.2 has shown that fast nucleation results in smaller particles, so that, by increasing the temperature, nucleation is expected to speed up, resulting in smaller particles, as observed in Figures 7.3.5.2 to 7.3.5.3 in appendix A2D. In fact, Schevchenko *et al.* (2003) was able to show that at a higher temperature more nuclei are formed, with the resulting particles of CoPt<sub>3</sub> being smaller.

The observation that when the temperature was raised high enough, phase changes from spheres to nanorods occurred was not unexpected. The observed phenomenon was previously reported by Toerne *et al.* (2001), who showed that above the critical micelle concentration (cmc), thermal stability is expected to increase, while further heating is known to lead to additional (supramicellar) aggregates. The observed transition is also in agreement with that found by Glatter *et al.* (2000), who showed experimentally that a sphere-to-rod-like transition was observed for a nonionic C12E6 surfactant system. Further, the critical temperature was observed to be 48 °C, slightly below the 50°C applied to the particles concerned here, as recorded in Figure 4.3.5.2.

#### 4.2.4 Effect of stirring

The results obtained from the experimental runs performed to investigate the effect of stirring on the particle sizes are presented in Figures 4.3.6.1 and 4.3.6.2. Further figures are presented in appendix A2E. A compilation of experimental data can be found in appendix D3 (see table D3.4).

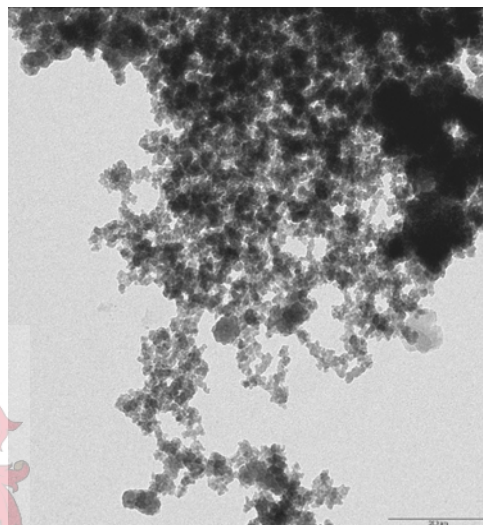
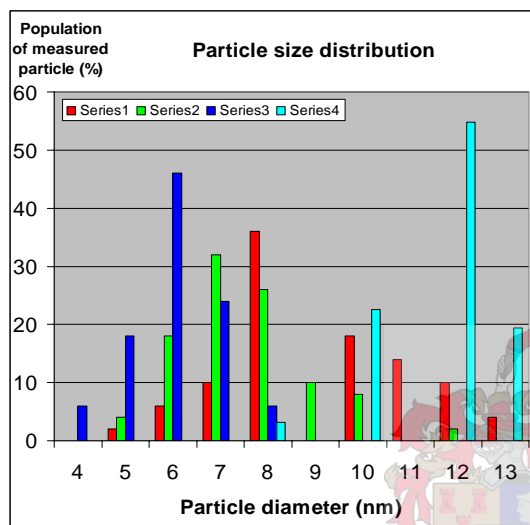


**Figure 4.3.6.1:** Particle size distribution for the investigation into the effect of stirring. Series 1, 2, and 3 correspond to the reverse micelles which were stirred at 1.5, 2.0 and 3.0 times the normal stirring speed respectively. Series 4 was performed at 10 vol. % surfactant concentration.

**Figure 4.3.6.2 (Series 3):** TEM photograph of the catalyst particles. The reverse micelles were stirred at 3.0 times the normal speed and nucleated for 20 minutes for 25 vol. % surfactant concentration. The temperature of the mixture was kept at 35 °C.

The above figures show that when the reverse micelles were stirred at twice the normal speed (series 2 in Figure 4.3.6.1) the particle sizes were found to be smaller, with a narrow particle distribution when compared with the size of particles recorded in section 4.3.6.2. When the stirring rate was raised to three times the normal stirring rate (series 3 in Figure 4.3.6.1) the particle size was reduced even further, with the average particle size distribution being narrower. Changing the concentration of the surfactant increased the particle sizes, as seen in section 4.2.1. The summary of the specific experimental runs is presented in table 4.4 below.

**Table 4.4:** Summary of experimental runs for catalyst synthesis during the investigation into the effect of stirring.

Series	vol. % Brij35	Bi.	Mo.	Stirring rate	Temp.	Nuclea tion	Particle size range	Ave. particle size
		mol/L	mol/L		°C	min	(nm)	(nm)
1	25	0.2133	0.64	1.5	35	20	5–13	8
2	25	0.1067	0.32	2.0	35	20	5–12	7
3	25	0.0533	0.16	3.0	35	20	4–8	6
4	10	0.0533	0.16	3.0	35	20	8–12	12

### Discussion on the effect of stirring

As can be observed in the above figures, the stirring rate has a significant effect on catalyst particle size. The catalyst particle of the static batch can be expected to be significantly larger than that of the stirred batch. In the former system, one can expect mass transfer to be the controlling factor, while, in the latter system; the reaction rate can be expected to be kinetically-controlled. In the study conducted by Sajjadi and Jahanzad (2006) comparing a highly diffusion-controlled polymerization reaction to a kinetically-controlled one, they showed that, under diffusion-controlled conditions, the overall rate of monomer transport, as well as the rate of particle growth, declined, resulting in prolonged nucleation. Further, the same authors noted that, under kinetically-controlled conditions, all monomers produced the same number of particles, whereas under diffusion-controlled conditions different numbers of particles were produced. This latter observation suggests that, at a low stirring speed, the particles so formed will have a non-uniform particle size distribution. Such a finding would be consistent with the above observation, according to which, the catalyst particles were seen to have a broader non-uniform average particle size distribution (series 2, Figure 4.3.6.1) at lower stirring speed. In contrast, at a higher stirring rate the inverse was found to be true, with a narrow average particle size distribution being observed. Further, since a diffusion-controlled condition resulted in prolonged nucleation, one can also expect that the resulting particle sizes will be larger, as was shown in section

4.2.2, where a fast nucleation resulted in the development of smaller particles. Hence, the decline in particle size reflected in Figure 4.3.6.1 agrees with this observation.

The observed decrease in particle size with an increasing temperature for higher stirred catalyst particles can be related to an increased viscosity of the reverse micelles at a higher temperature. The study conducted by Leaver and Olsson (1994) into the dependence of the surfactant concentration on viscosity along the emulsification failure boundary showed that viscosity increased with an increase in temperature. Such an effect they attributed to the attractive interaction of aggregates, in agreement with the observation made by Glatter *et al.* (2000). The authors were able to show that approaching the critical temperature  $T_c$  (found to be about 48 °C for C12E6), an attractive interaction, independent of actual shape or size, was observed, indicating micellar growth and attractive interaction. However, Jonstromer (1995) disagrees with such a finding, observing that attractive interaction is independent of the sizes of the micelles. Experimental observation suggests that the micellar diffusion coefficient for any given concentration depends on both size and interaction, effects which can be difficult to separate from each other.

The observed behavior for the sonication was rather unexpected, since Ghule *et al.* (2004) had shown that sonication for a certain period (6 hours in their case) of time resulted in the formation of nanorods with well-defined structure. Such a finding is supported by Debuigne *et al.* (2000), who have shown that an organic substance is better dispersed in a microemulsion when using ultrasound. Further, a greater number of nuclei are formed in contact with the aqueous core, with the sizes of the nanoparticle being smaller than in the case of the use of a normal stirrer. However, the particle size distribution was observed to be less narrow that was the case where ultrasound was used.

### 4.2.5 Effect of salt ratio

The results obtained from the experimental runs performed to investigate the effect of salt ratio on the particle sizes are presented in Figures 4.3.7.1 and Figure 4.3.7.2. A compilation of the experimental data can be found in appendix D3 (see table D3.4).

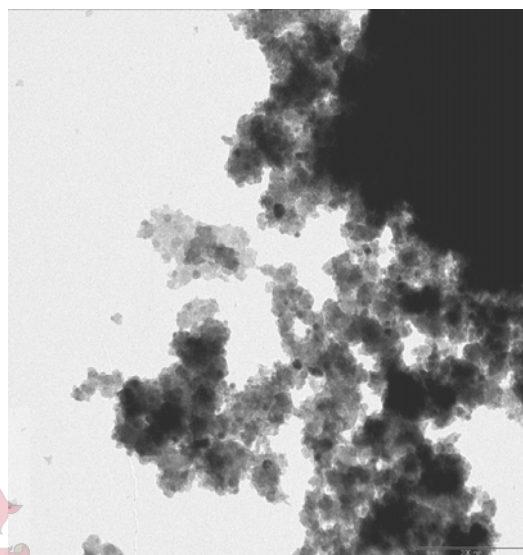
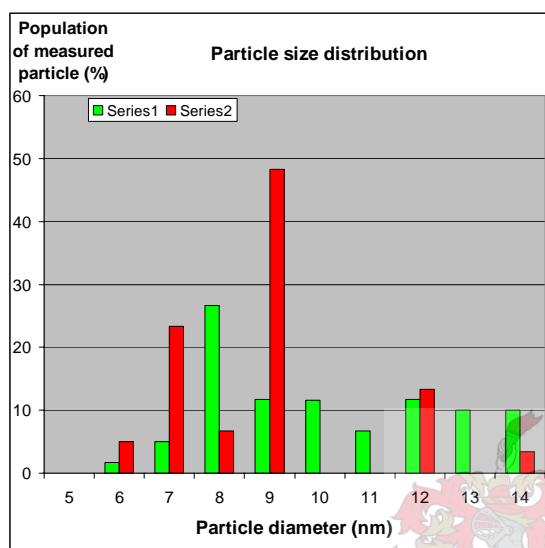


**Figure 4.3.7.1:** Particle size distribution for the investigation into the effect of salt ratio. Series 1 and 2 correspond to a catalyst particle with the bismuth molybdate salt ratio of 0.5 at 25vol. and 10 vol. % respectively.

**Figure 4.3.7.2 (Run B1Z):** TEM photograph of the catalyst prepared at a salt concentration of 0.2133 mol/L molybdate and 0.0533 mol/L bismuth; resulting in a Bi-Mo ratio of 0.5 for 25 vol. % surfactant concentration. The temperature of the mixture was kept at 35 °C.

In general, the above figures show that if one of the salt concentrations is increased far beyond the concentration of the other, with the experimental conditions kept as recorded in section 4.2.4, a slight increase in particle size occurs. The average particle size distribution is, however, wider. The summary of the specific experimental runs is presented in table 4.5 below.



**Table 4.5:** Summary for experimental runs for catalyst synthesis for investigation into the effect of stirring

Series	vol. % Brij35	Bismuth	Molybdate	Ratio	Temp.	Nucleation	Particle size range	Ave. particle size
		mol/L	mol/L		°C	min	(nm)	(nm)
1	25	0.2133	0.8532	0.5	35	20	6–14	8
2	10	0.0533	0.2133	0.5	35	20	5–14	9

### Discussion on the effect of salt ratio

The above observation indicates what happens when one of the salt concentrations is increased far beyond the concentration of the other. Gordad *et al.* (2000) were able to show that bismuth molybdate catalysts exhibit their highest performance when they are maintained in a slightly reduced state, which might significantly affect the phase of catalyst particle. As can be observed in the above figures and in comparison with the performance of catalyst particles described in section 4.2.4, which was performed under the same condition of nucleation, the average particle size distribution is broader (6–14 nm and 5–14 nm), with the average particle size being larger (8nm and 9 nm). However, the observation by Husein *et al.* (2003) contradicts this observation, as well as other observations that have shown that larger particles are obtained upon increasing the concentration of the precursor or the reducing agent far beyond that of the other, due to the generation of a more rigid surface, causing a lower solute exchange dynamic, resulting in fewer nuclei. Their experimental results showed that more reverse micelles with a monomer concentration higher than that of the critical nucleation centre formed, with the rate of nucleation becoming less dependant on the intermicellar exchange of the solubilisate. Further, more nuclei provide more seeds for particle growth, resulting in particles of smaller diameter. However, given that the system used by the authors made use of a single reverse micelle system, their results were rather to be expected, since such a system would not manifest the dynamic nature of the two-step reverse micelle system, in which the exchange of material depends on the success of the collision involved. Further, the final nanoparticle should follow the metal composition of the precursor for the latter system, as also shown by Fang and Yang (1999).

### 4.2.6 Effect of support and solvent used

The results obtained from the experimental runs performed to investigate the effect of support on particle size are presented in Figures 4.3.8.1 to 4.3.8.4.

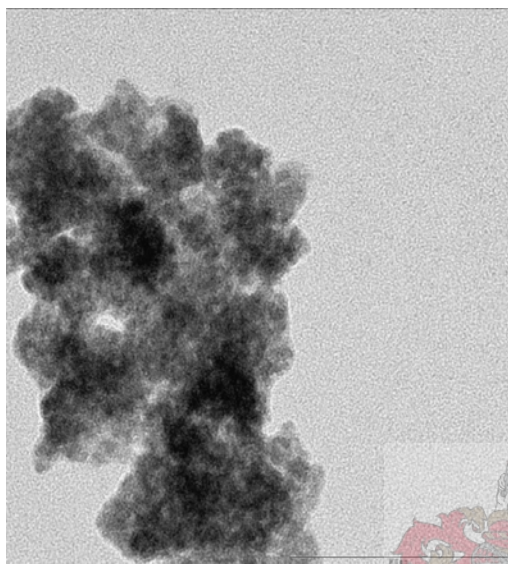


**Figure 4.3.8.1:** TEM photograph of the catalyst particles. The mixture of reverse micelles was washed with Tetrahydrofuran (THF) and the temperature of mixture kept at 35 °C for 25 vol. % surfactant concentration.

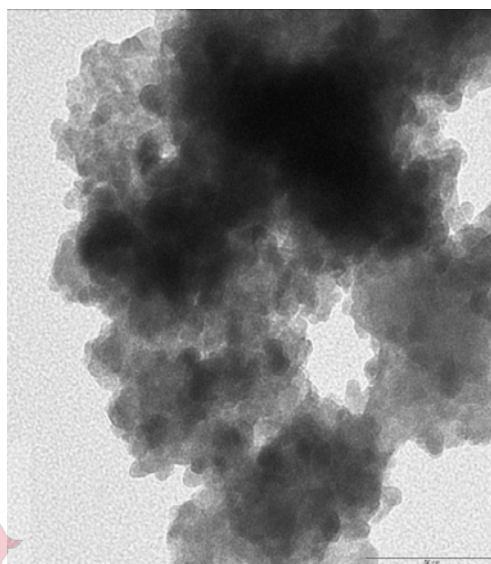


**Figure 4.3.8.2:** TEM photograph of the catalyst particles. The mixture of reverse micelles was washed with tetrahydrofuran (THF) and supported with silicon carbide. The temperature of the mixture was kept at 35 °C for 25 vol. % surfactant concentration.

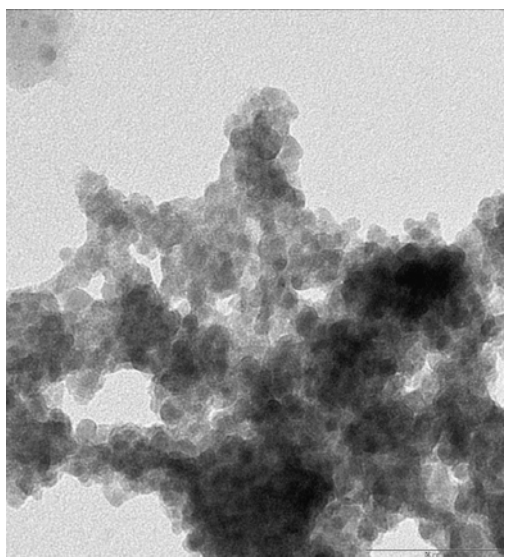


**Figure 4.3.8.3:** TEM photograph of the catalyst particles supported with silicon carbide for 25 vol. % surfactant concentration with the temperature of mixture kept at 35 °C.

Figures 4.3.8.1 to 4.3.8.3 show the images of individual particles for the same nucleation condition as that experienced by the catalyst particles shown in 4.3.6.2. Figure 4.3.8.1 reflects the imaging when the catalyst particles were washed with tetrahydrofuran (THF), showing that a change in solvent does not result in a reversal of particle agglomeration. However, when the reverse micelles were washed with THF whilst supported with silicon carbide (Figure 4.3.8.2) a small degree of liberation was present in the catalyst particles, although large agglomerates were still to be observed. Lastly, when the catalyst particles were supported only with silicon carbide, a significant degree of dissociation was observed, although aggregates still formed.

### **Discussion on the effect of support and solvent used**

The following investigation was performed to test whether the agglomeration observed in the catalyst particles could be reduced, although ultimately the particles were expected to form agglomerates. When the catalyst particle was calcined at an extremely high temperature (450 °C), particle sintering was observed. Further, Fang and Yang (1999) have shown that the aggregation of catalyst particles has a significant influence on the properties of the calcined particles, such as on the size and the strength of the aggregates and their morphological features. The test of agglomeration was undertaken by firstly testing the solvent used to wash the reverse micelles. When the inorganic substance was first introduced into the reverse micelle in a solid phase, it was insufficiently dispersed in the reverse micelle mixture. Hence, it was thought that the solvent probably played a significant role in particle agglomeration. As can be observed in Figure 4.3.8.1, changing the solvent does not seem to liberate the particle. The explanation for the observed pattern can be thought of in the way in which the solvent emulsifies the continuous phase, as shown by Bouchemal *et al.* (2004). The solvent must be completely miscible with the continuous phase. For a water continuous phase, THF will only be very soluble and not completely miscible. However, for the oil-continuous phase under study, THF was expected to be completely miscible with the continuous phase (oil) and, to a large extent, with the dispersed water droplets. Hence, the results were unexpected. Although the results of the support, when used together with THF, proved encouraging, little evidence suggests liberation of the catalyst particles concerned.

### 4.2.7 Operating window

The operating window for the synthesis of pure catalyst particles in which size and size distribution is defined is represented by the region indicated in the following figure.

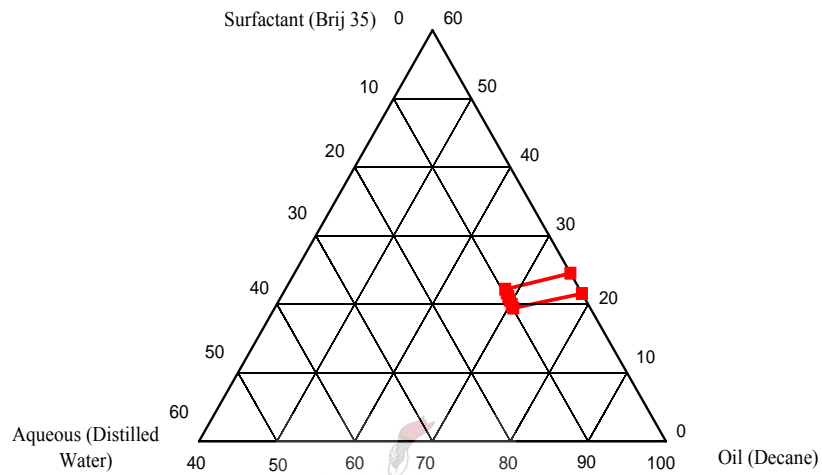


**Figure 4.3.9.1:** The operating region for the synthesis of pure  $\alpha$ -bismuth molybdate catalyst particles.



### 4.3 SYNTHESIS OF A PURE $\alpha$ - $\text{Bi}_2\text{Mo}_3\text{O}_{12}$

The following subchapter will give a detailed description of the catalyst particles by showing patterns of X-Ray diffraction and there by confirming in which the phase in which the catalyst exist. The results obtained from the experimental runs performed for the synthesis of the particles are presented in Figure 4.4.1 to 4.3.4.

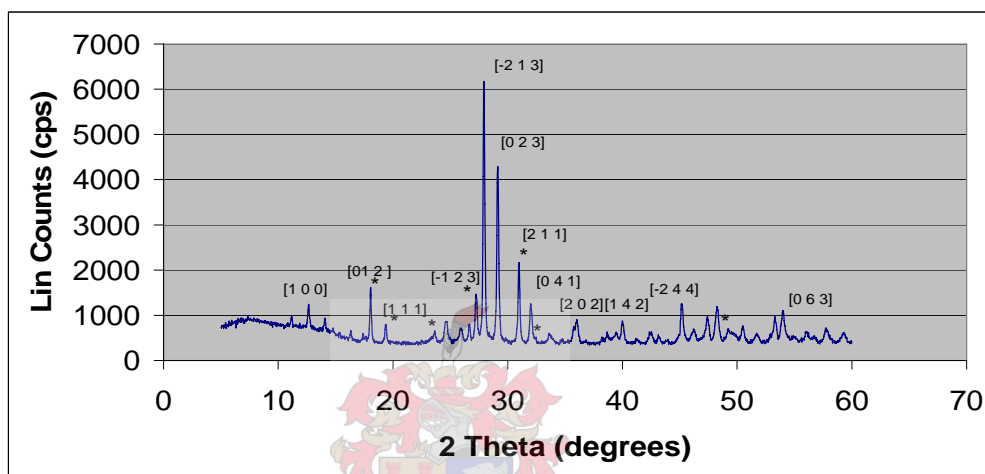


**Figure 4.4.1:** XRD patterns of calcined catalyst particles prepared after optimization of the reverse micelle technique, with the pH of the solution kept at 1.5, with asterisks corresponding to the ternary oxide phase ( $\alpha$ - $\text{Bi}_2\text{Mo}_3\text{O}_{12}$ ). Included is the d-spacing (the 'fingerprint') of the particles concerned.

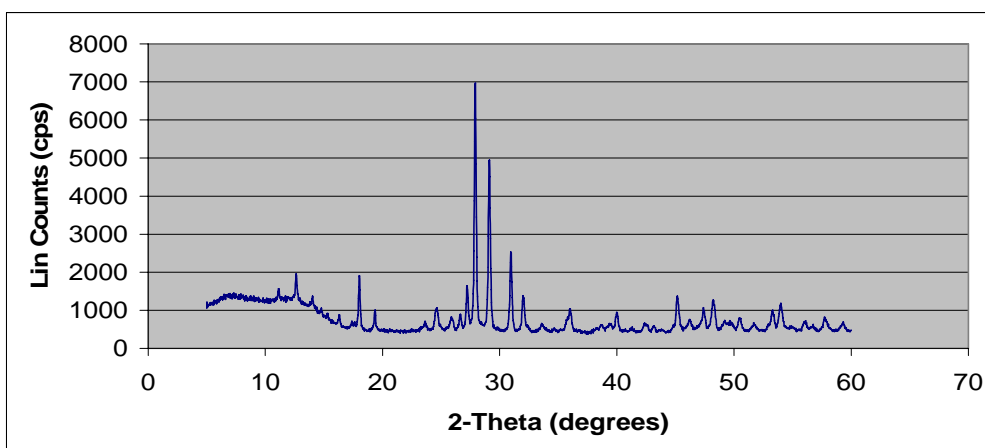


**Figure 4.4.2:** XRD patterns of a calcined catalyst, with particles prepared prior to optimization of the reverse micelle technique, with the pH of the solution kept at 1.5.

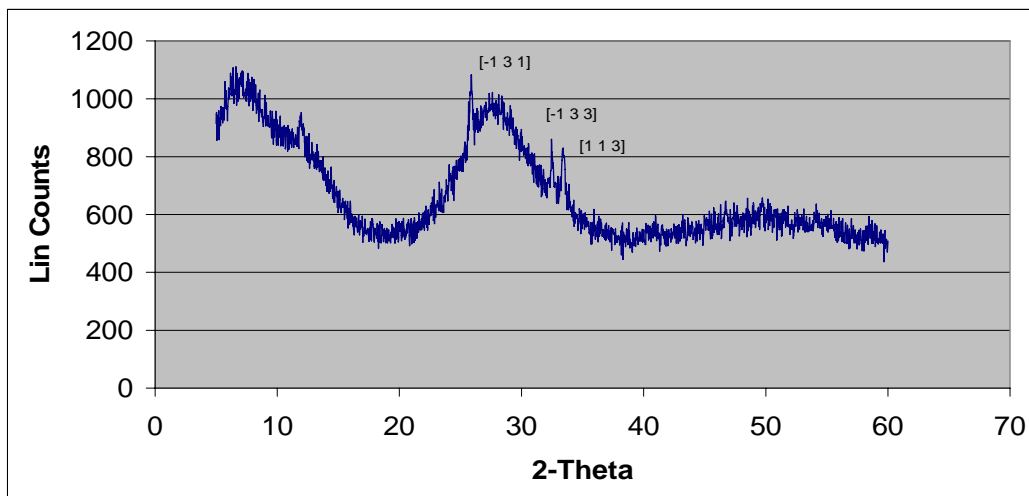


**Figure 4.4.3:** XRD patterns of an uncalcined catalyst, with particles prepared after optimization of the reverse micelle technique, with the pH of the solution kept at 1.5.

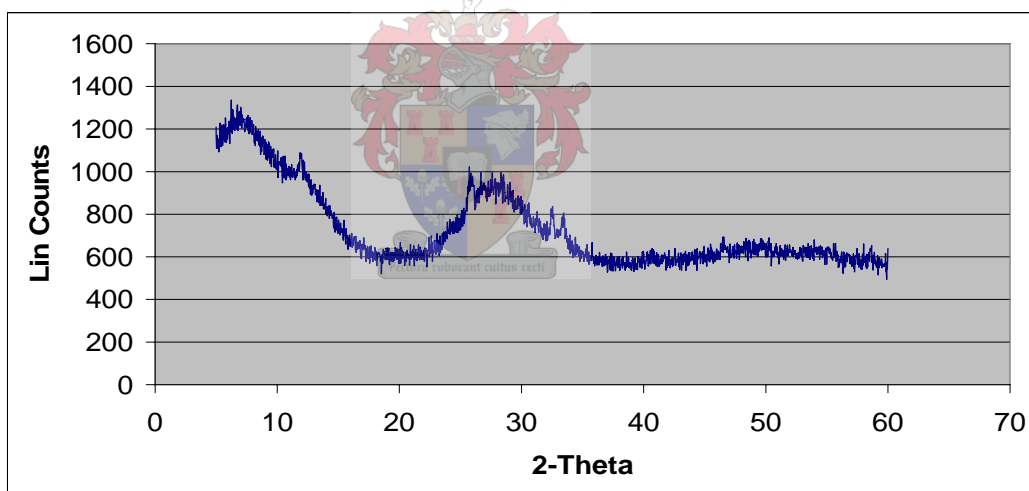


**Figure 4.4.4:** XRD patterns of an uncalcined catalyst, with particles prepared prior to optimization of the reverse micelle technique, with the pH of the solution kept at 1.5.

Figure 4.4.1 to Figure 4.4.4 show the diffractogram of the calcined and uncalcined catalyst. Figure 4.54 shows the patterns of the calcined catalyst particles prepared after the optimization of the reverse micelle technique, with the pH of the solution kept at 1.5, the asterisks correspond to pure  $\alpha\text{-Bi}_2\text{Mo}_3\text{O}_{12}$ , while their respective d-spacing is indicated in brackets. Figure 4.4.2 shows the patterns of calcined catalyst particles prepared prior to the optimization of the reverse micelle technique, with the pH of the solution maintained constant at 1.5. Figure 4.4.3 to 4.4.4 show the patterns of uncalcined catalyst particles prepared both before and after the optimization of the reverse micelle technique, with the pH of the solution kept at 1.5. The diffractogram in Figure 4.4.1 clearly shows the presence of pure  $\alpha\text{-Bi}_2\text{Mo}_3\text{O}_{12}$  with peaks observed at 18, 19, 24, 28, 31, 33 and 45 degrees.

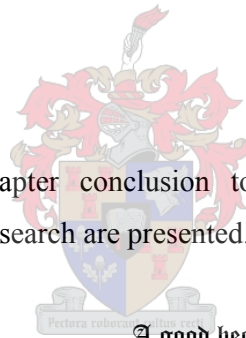
### Discussion on the results for the synthesis of catalyst particles

When compared with the respective diffractogram obtained by Devillers *et al.* (1996) (Figure A3 in appendix A), almost all the peaks of the pure  $\alpha\text{-Bi}_2\text{Mo}_3\text{O}_{12}$  obtained under the defined operating window correspond very well, with few peaks being unaccounted for. This might be due to the particle sintering observed at higher temperature, clearly indicating the effect of particle agglomeration, as observed in the Transmission Electron Microscopy (TEM) photographs. In relation to supporting the catalyst particles, Devillers *et al.* (1996) were able to confirm, on their comparing the XRD data collected on untreated and loaded specimens, that, after precursor deposition and calcination, peaks related to the molybdenum or tungsten oxide remained unchanged. Hence, it is recommended that such an observation needs further investigation. However, when compared with the calcined catalyst obtained before the optimization of reverse micelle (Figure 4.4.2), the catalyst particles after the optimization of the reverse micelles clearly show more improvement than do those of the catalyst prior to the optimization of the reverse micelles, with clear evidence of a broad peak visible for the latter between 6 and 9 degrees. The presence of such a peak is indicative of the uncalcined catalyst as shown in Figure 4.4.3 and 4.4.4 which clearly indicate the absence of pure  $\alpha\text{-Bi}_2\text{Mo}_3\text{O}_{12}$ .

# Chapter 5

## Conclusion and Recommendations

*Chapter layout:* In this chapter conclusion to the proof-of-principle research and recommendations for future research are presented.



A good beginning makes a good end [Louis L'Amour]



## 5.1 CONCLUSION

The conclusion concerning this study is as follows:

### 5.1.1 Optimization of the components of reverse micelles

#### Titration analysis

The formation and the stability of micelles for both surfactants (brij 35 and CTAB) and both oils (hexane and decane) is not affected by a change in temperature, stirring, aging of salts (bismuth and molybdate) or the pH of the aqueous content. However, such factors may have a limited effect, especially when CTAB is used as a surfactant. Further, the formation of stable micelles is achieved at an aqueous content of less than 20 vol. % for the addition of all aqueous phases and for both surfactants and oils. The surfactant Brij 35 forms micelles which are significantly more stable at low surfactant concentration for both oil-chain length, and the attendant stability increases slightly with increasing surfactant concentration. A clear distinction exists, however, between where micelles are stable and unstable, while the surfactant CTAB was found to form micelles which are significantly more stable at higher, in contrast to lower, surfactant concentration.

The addition of a co-surfactant to form a quaternary system, as well as the use of an ionic surfactant (CTAB), resulted in a rather more complex and complicated adsorption at the micelle interface. Further, the use of oil with long-chain length, decane, together with CTAB delivered inconsistent results. Lastly, the ternary system, consisting of brij 35 together with the longer chain length oil decane resulted in far more stable micelles, while the quaternary system was found to show higher stability at higher surfactant concentration for both short and long chain length oils.

#### Zetasizer analysis

For surfactant brij 35, growth was initially found to be purely catalytic, becoming growth by ripening after 200 seconds. However, growth by ripening appears higher at lower surfactant concentration and lower at higher surfactant concentration, while the inverse is true for catalytic growth. In addition, growth by ripening does not depend on the concentration of clustering. Nucleation also plays a crucial role in the tuning of particle sizes in the absence of Ostwald ripening, depending on the clustering of aggregates. In

addition, minimum clustering was found to be necessary for the formation of a stable nucleus. The control over nanodroplet diameter for a ternary system consisting of brij 35 was achieved by merely varying the water content. However, the final particle size will not be entirely dependent on the size of the water droplet, although it is expected to have a controlling influence.

As was seen with the titration analysis, for the CTAB surfactant, the addition of the co-surfactant to form a quaternary system leads to contradictory mechanism of micelle growth. Growth was found to be purely ripening for water (aqueous) and purely catalytic for a molybdate salt solution, showing previsible behavior for the addition of a bismuth salt solution. Further, the addition of a co-surfactant has two effects that can be described as both dynamic and microstructural. A ternary system consisting of a surfactant (brij 35) and a long oil-chain length (decane) resulted in far more stable micelles, which also agree with the titration analysis. Further, such stable micelles are formed at a very low aqueous content.

### 5.1.2 Synthesis of $\alpha$ -bismuth molybdate nanoparticles

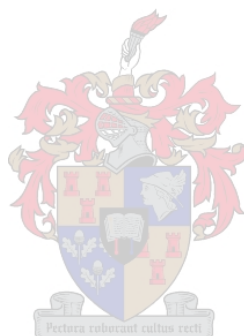
Increasing the reactant concentration resulted in larger particle sizes. Consistent with the Malvern Zetasizer results, particle size was found to decrease with an increase in surfactant concentration. Transmission Electron Microscopy (TEM) showed spherical particles which formed large agglomerates. Slow nucleation resulted in larger particle sizes, while fast nucleation resulted in smaller particles with narrow size distribution. In addition, slow nucleation resulted in a non-uniform average particle size distribution. Further, a collision between several atoms had to occur before nucleation. Hence, a minimum cluster of micelles was found to be required for the formation of a stable nucleus.

Increasing the thermal energy of a system was found to cause the micelles to aggregate together and thereby to increase the rate of collision, and, consequently, the rate of nucleation. Since nucleation is more sensitive to variations in temperature than is growth, particle size can be controlled by adjusting the temperature. However, further heating, approaching the critical temperature, resulted in supramicellar aggregates, with sphere-to-

rod transition being seen. Increasing the stirring rate resulted in kinetically controlled particle transfer, with smaller particles being formed as a result of slow nucleation and a moderate increase in temperature. Increasing the concentration of either the reducing agent or a precursor was found to result in a larger particle size, with broader particle size distribution.

### 5.1.3 Synthesis of pure $\alpha$ - $\text{Bi}_2\text{Mo}_3\text{O}_{12}$

The XRD diffractogram clearly shows the presence of pure  $\alpha$ - $\text{Bi}_2\text{Mo}_3\text{O}_{12}$  for the calcined catalyst and an improvement prior to the optimisation of reverse micelles.



## 5.2 RECOMMENDATIONS

The recommendations concerning to this research are as follows:

The surfactant brij 35 was found to be highly hydrophilic, meaning that, when left in the open for a considerable period of time, it was found to form bubbles at the surface. Therefore, although the method used in the current research proved effective, a still better method needs to be developed in order completely to eliminate the contact of brij 35 with the atmosphere. Synthesis should therefore be carried out in vacuum or in a dry area in the presence of as little moisture as possible.

Since particle size depends entirely on nucleation, an investigation into the influence of volume and vessel geometry is needed, since such influence might affect nucleation and, consequently, particle size and size distribution.

Research into particle agglomeration, especially when calcinating at higher temperature, offered small success. Future studies need to be devoted to investigating this phenomenon, especially as far as consideration of the solvent used to suspend the catalyst is concerned. Other heavier solvents than that used in this study may, in future, be recommended. Future studies should involve the use of mixed surfactant or of non-ionic surfactant containing small amounts of ionic surfactant.

Microemulsions form a highly dynamic system and, although a comprehensive study was conducted in the course of this research, research into the dynamics of microemulsion (which should possibly involve modelling) is needed in order to obtain a thorough understanding of the properties of the reverse micelles system at their air/water interface. Such a study would involve both the structure and dynamics of the layer in order to enable the complete control of particle sizes and the size distribution of the catalyst.

Microscopy needs to be developed still further. Since the particles investigated in such a study are extremely small, the beam of the microscope used for purposes of conducting the investigation tend to have a major influence on the catalyst particles, resulting in its melting the catalyst particles, and hence influencing the appearance of the crystallites concerned in cases of prolonged or high-intensity analysis.

---

# References

*Inspired by, Karl Ziegler*

---

Nobel prize winning chemist (1898-1973) who did a vast quantity of work on the catalysts allowing high density poly(ethene) and poly(propene) to be produced. Most of his work was done at the Max Planck Institute for Coal Research in Müllheim, Germany, and had nothing to do with coal, showing the economic benefits of pure research. Like Italy's Giulio Natta, he was a keen mountain climber. A quote: "*My only motivation has always been just to do what was fun.*" (Quoted in "*The Chain Straighteners*" by F. McMillan)



I was able to see ahead because I stood in the shoulder(s) of the(se) giant(s) [Linus Torvalds]

## 6.1 REFERENCES

Adair J. H, T. Li, Kido T, Havey K, Moon J, Mecholsky J, Morrone A, Talham D. R, Ludwig M. Wang L, *Recent developments in the preparation and properties of nanometer-size spherical and platelet-shaped particles and composite particles*, *Mater Science and Eng.*, R23 (1998) 139-242

Alexandridis P, Josef F. Holzwarth J. F and T. Alan Hatton A, *Thermodynamics of Droplet Clustering in Percolating AOT Water-in-Oil Microemulsions*, *J. Phys. Chem.*, 99 (1995) 8222-8232

Bai T, He P, Jia Z, Huang X, He Y, *Size-controlled preparation of monodispersed ZnO nanorods*, *Mater Letters*, 59 (2005) 1687– 1690

Bansal V.K, Shah D. O, and J. P. O'Connell J. P, *Influence of alkyl chain length compatibility on microemulsion structure and solubilization*, *J. of Colloid and Interf. Science*, 75 (1980) 462-475

Bonini M, Bardi U, Berti D, Neto C, and Baglioni P, *A New Way to Prepare Nanostructure Materials: Flame Spraying of Microemulsions*, *J. Phys. Chem., B* 106 (2002) 6178-6183

Bouchemal K, Briancon S, Perrier E, Fessi H, *Nano-emulsion formulation using spontaneous emulsification: solvent, oil and surfactant optimization*, *Int. J. of Pharm.*, 280 (2004) 241-251

Boutonnet M, Jerzy Kizling J and Maire P. S. G, *The preparation of monodisperse colloidal metal particles from microemulsions*, *Colloids and Surf.*, (1982) 209-225

Cason J, Miller M. E, Thompson J. B, Robert C. B, *Solvent effect on copper nanoparticles Growth behavior in AOT Reverse micelles System*, *J. Phys Chem., B* 105 (2001) 2297-302

Chen D-H, and Wu S-H, *Synthesis of Nickel Nanoparticles in Water-in-Oil Microemulsions*, *Chem. Mater*, 12 (2000), 1354-1360

Curri M. L, Agostiano A, Mavelli F, and Monica D. M, *Reverse micelle systems: self organized assembly as effective route for the synthesis of colloidal semiconductor nanocrystals*, *Material Science and Eng. C*, 22 (2002) 423-426

Curri M. L, Agostiano A, Manna L, Monica M. D, Catalano M, Chiavarone L, Spagnolo V, Lugara M, *Synthesis and Characterization of CdS Nanoclusters in a Quaternary Microemulsion: the Role of the Co-surfactant*, *J. Phys. Chem. B*, 104 (2000) 8391-8397

- Debuigne F, Jeunieau L, Wiame M, and J. B. Nagy J. B, ***Synthesis of Organic Nanoparticles in Different W/O Microemulsions***, *Langmuir*, 16 (2000) 7605-7611
- De Gennes P. G and Taupin C, ***Microemulsions and the Flexibility of oil in water Interfaces***, *J. Phys. Chem.*, 86 (1982) 2294-2304
- Devillers M, Tirions O, Cadus L, Ruiz P, and Delmon B, ***Bismuth Carboxylates as Precursors for the Incorporation of Bismuth in Oxide-based Materials***, *J. of solid state chem.*, 126 (1996) 152–160
- Eriksson S, Nylen U, Rojas S, Boutonet M, ***Preparation of catalyst from microemulsion and their application in heterogeneous catalysis***, *App. Cat. A: Gen.*, 265 (2004) 207-219
- Esquena J, Tadros T. F, Kostarelos K, and Solans C, ***Preparation of Narrow Size Distribution Silica Particles Using Microemulsions***, *Langmuir*, 13 (1997) 6400-6406
- Eastoe J, Warne B, ***Nanoparticle and polymer synthesis in microemulsion***, *Curr. Opin. Colloid Interf. Sciences*, 1 (1996) 800-5
- Fang X and Yang C, ***An Experimental Study on the Relationship between the Physical Properties of CTAB/Hexanol/Water Reverse Micelles and ZrO<sub>2</sub>-Y<sub>2</sub>O<sub>3</sub> Nanoparticles Prepared***, *J. of Colloid and Interf. Science*, 212 (1999) 242–251
- Feldman Y, Kozlovich N, Nir I, Garti N, Archipov V, Zamil, Zuev Y and Idiyatullin V. F, ***Mechanism of Transport of Charge Carriers in the Sodium Bis(2-ethylhexyl) Sulfosuccinate-Water-Decane Microemulsion near the Percolation Temperature Threshold***, *J. Phys. Chem.*, 100 (1996) 3745-3748
- Ghule A V, Ghule K A, Tzing S-H, chang J-Y, Chang H, Ling Y-C, ***Pyridine intercalative sonochemical synthesis and characterization of  $\alpha$ -Bi<sub>2</sub>Mo<sub>3</sub>O<sub>12</sub> phase nanorods***, *Chem. Phys. letter*, 383 (2004) 208-213
- Ghosh S and Moulik S. P, ***Interfacial and Micellization Behaviors of Binary and Ternary Mixtures of Amphiphiles (Tween-20, Brij-35, and Sodium Dodecyl Sulfate) in Aqueous Medium***, *J. of colloid and interf. science*, 208 (1998) 357–366
- Giustini M, Palazzo G, Colafemmina G, and Monica M. D, Giomini M, Ceglie A, ***Microstructure and Dynamics of the Water-in-Oil CTAB/n-Pentanol/n-Hexane/Water Microemulsion: A Spectroscopic and Conductivity Study***, *J. Phys. Chem.*, 100 (1996) 3190-3198

- Glatter O, Fritz G, Lindner H, Brunner-Popela J, Mittelbach R, Strey R and Egelhaaf S. U, *Nonionic Micelles near the Critical Point: Micellar Growth and Attractive Interaction*, *Langmuir*, 16 (2000) 8692-8701
- Gordard E, Gaigneaux E. M, Ruiz P, Delmon B, *New insights in the understanding of the behavior and performance of bismuth molybdate catalyst in the oxygen-assisted dehydration of 2 butanol*, *Cat. today*, 61 (2000) 279-285
- Grasselli R. K, *Selectivity issues in (amm)oxidation catalysis*, *Cat. Today*, 99 (2005) 23–31
- Grasselli R. K, *Advances and future trends in selective oxidation and ammoxidation catalysis*, *Cat. Today*, 49 (1999) 141-153
- Gutfelt S, Kizling J, Holmberg K, *Microemulsions as reaction medium for surfactant synthesis*, *Colloids and Surf. A: Physicochem. and Eng. Aspects*, 128 (1997) 265-271
- Hanna T A, *The role of bismuth in the SOHIO process*, *Coordination Chem. Reviews*, 248 (2004) 429-440
- Hansen J. R, *High-Resolution and Pulsed Nuclear Magnetic Resonance Studies of Microemulsions*, *J. of Phys. Chem.*, 78 (1974) 256-261
- Hamilton R. T, Billman J. F, *Measurements of interdroplets attraction and the onset of percolation in water-in-oil microemulsion*, *Langmuir*, 6 (1990) 1696-170
- Henon S, and Meunier J, *Ellipsometry and reflectivity at the Brewster angle: tools to study the bending elasticity and phase transitions in monolayers at liquid interfaces*, *Thin Solid Films*, 234 (1993) 471-474
- Holmberg K, *Surfactant-templated nanomaterials synthesis*, *J. of Colloid and Interf. Science*, 274 (2004) 355–364
- Hou M-J and Shah D. O, *Effects of the Molecular Structure of the Interface and Continuous Phase on Solubilization of Water in Water/Oil Microemulsions*, *Langmuir*, 3 (1987) 1086-1096
- Husein M, Rodil E and Vera J, *Formation of silver chloride nanoparticles in microemulsions by direct precipitation with the surfactant counterion*, *Langmuir*, 19 (2003) 8467-8474



- Islam M. D and Kato T, *Dependence of Phase Behavior of Some Non-ionic Surfactants at the Air–Water Interface on Micellization in the Bulk*, *J. of Colloid and Interf. Science*, 252 (2002) 365–372
- Izquierdo P, Esquena J, Th. F. Tadros Th. F, Federen C, Garcia M. J, Azemar N, and Solans C, *Formation and Stability of Nano-Emulsions Prepared Using the Phase Inversion Temperature Method*, *Langmuir*, 18 (2002) 26-30
- Jada A, Lang J and Zana R, *Relation between Electrical Percolation and Rate Constant for Exchange of Material between Droplets in Water in Oil Microemulsions*, *J. Phys. Chem.*, 93 (1989) 10-12
- Jana N. J, Gearheart L and Murphy C. J, *Seeding Growth for Size Control of 5-40 nm Diameter Gold Nanoparticles*, *Langmuir*, 17 (2001) 6782-6786
- Jonstromer M, Olsson M. U, and O'Neil Parker W, Jr., *A Self-Diffusion Study of Microemulsion Structure Using a Polar Solvent Mixture*, *Langmuir*, 11 (1995) 61-69
- Kabalnov A. S, *Can Micelles Mediate a Mass Transfer between Oil Droplets*, *Langmuir*, 10 (1994) 680-684
- Keulks G W, Hall J L, Daniel C, and Suzuki K, *The catalytic oxidation of propylene: IV. Preparation and characterization of Bismuth Molybdate*, *J. of cat.*, 34 (1974) 79-97
- Kitchens C, McLeod MC, Roberts B, *Solvents effects on the growth and steric stabilization of copper metallic nanoparticles in AOT micelle system*, *J. Phys. Chem., B* 107 (2003) 11331-8
- Kunieda H, Fukui Y, Uchiyama H, and Solans C, *Spontaneous Formation of Highly Concentrated Water-in-Oil Emulsions (Gel-Emulsions)*, *Langmuir*, 12 (1996) 2136-2140
- Leaver M, Fur I, and Olsson U, *Micellar Growth and Shape Change in an Oil-in-Water Microemulsion*, *Langmuir*, 11 (1995) 1524-1529
- Leaver M. S and Olsson U, *Viscosity of a Nonionic Microemulsion near Emulsification Failure*, *Langmuir*, 10 (1994) 3449-3454
- Li Y, Park C-W, *Particle size distribution in the synthesis of nanoparticle using microemulsion*, *Langmuir*, 15 (1999) 952-956

- Lisiecki I, ***Size control of spherical metallic nanocrystal***, *Colloids and surf. A: Physicochem. Eng. Aspects*, 250 (2004) 499-507
- Lisiecki I. and Pileni M. P, ***Synthesis of Copper Metallic Clusters Using Reverse Micelles as Microreactors***, *J. Am. Chem. Soc.*, 115 (1993) 3887-3896
- Liu D, Ma J, Cheng H, Zhao Z, ***Investigation on the conductivity and microstructure of AOT/non-ionic surfactants/water/n-heptane mixed reverse micelles***, *Colloids and Surf. A: Physicochem. and Eng. Aspects*, 135 (1998) 157-164
- Lopez-Quintela M. A, ***Synthesis of nanomaterials in microemulsion: formation mechanisms and growth control***, *Curr. opinions in Colloid and Surf. Science*, 8 (2003) 137-144
- Lopez-Quintela M A, Tojo C, Blanco M. C, Garcia Rio L, Leis J. R, ***Microemulsion dynamics and reaction in microemulsion***, *Curr. opinion in Colloid and Interf. Science*, 9 (2004) 264-278
- Lu J. R, Thomas R. K, Penfold J, ***Surfactant layers at the air water interface: structure and composition***, *Adv. in Colloid and Interf. Science*, 84 (2000) 143-304
- Maidment L. J, Chen V, and Warr G. G, ***Effect of added co-surfactant on ternary microemulsion structure and dynamics***, *Colloids and Surf. A: Physicochem. and Eng. Aspects*, 129-130 (1997) 311-319
- Merchand K. E, Tarret M, Lechaire J. P, Normand L, Kasztelan S, Cseri T. ***Investigation of AOT-based microemulsion for the controlled synthesis of MoS<sub>x</sub> nanoparticles: an electron microscopy study***. *Colloids and Surf. A: Physicochem. Aspect*, 214 (2003) 239-248
- Modes S, and Lianos P, ***Luminescence Probe Study of the Conditions Affecting Colloidal Semiconductor Growth in Reverse Micelles and Water-in-Oil Microemulsions***, *J. Phys. Chem.*, 93 (1989) 5854-5859
- Moulik S. P and Paul B. K, ***Structure, dynamics and transport properties of Microemulsions***, *Adv. in Colloid and Interf. Science*, 78 (1998) 99-195
- Nazario L. M. M, Hatton T. A, and Crespo J. P. S. G, ***Nonionic Co-surfactants in AOT Reversed Micelles: Effect on Percolation, Size, and Solubilization Site***, *Langmuir*, 12 (1996), 6326-6335

Panda A. K, Moulik S. P, Bhowmik B. B, Das A.R, ***Dispersed Molecular aggregates: II. Synthesis and characterization of nanoparticles of tungstic acid in H<sub>2</sub>O/ (TX100 + Alkanol)/n-heptane W/O microemulsion media***, *J. of Colloid and Interf. Science*, 235 (2001) 218-226

Pileni M. P, ***Colloid self assemblies used as templates to control the size, shape and self organization of nanoparticles***, *Supramolecular Science*, 5 (1998) 321-329

Pileni M.P, ***Nanosized Particles Made in Colloidal Assemblies***, *Langmuir*, 13 (1997) 3266-3276

Quintillan S, Tojo C, Blanco M. C, Lopez-Quintilla M A, ***Effects of intermicellar exchange on the size control of nanoparticles synthesized in microemulsion***, *Langmuir*, (2001) 17:7251-7254

Sajjadi S and Jahanza F, ***Nanoparticle formation by highly diffusion-controlled emulsion polymerization***, *Chem. Eng. Science*, 61 (2006) 3001 – 3008

Santra S, Tapeç R, Theodoropoulou N, Dobson J, Hebard A, and Tan\* W, ***Synthesis and Characterization of Silica-Coated Iron Oxide Nanoparticles in Microemulsion: The Effect of Nonionic Surfactants***, *Langmuir*, 17 (2001) 2900-2906

Shah PS, Holmes J. D, Jonston KP, Korgel BA, ***Size selective dispersion of dodecanethiol-coated nanocrystal in ligand and supercritical ethane by density tuning***, *J. of Phys. Chem. B*, 10 (2002) 2545-51

Shahidzadeh N, Bonn D, Aguerre-Charriol O, Meunier J, ***Spontaneous emulsification: relation to microemulsion phase behavior***, *Colloids and Surf. A: Physicochem. and Eng. Aspect*, 147 (1999) 375-380

Shevchenko E. V, Talapin D. V, Schnablegger H, Kornowski A, Festin O, Svedlindh P, Haase M, and Weller H, ***Study of Nucleation and Growth in the Organometallic Synthesis of Magnetic Alloy Nanocrystals: The Role of Nucleation Rate in Size Control of CoPt<sub>3</sub> Nanocrystals***, *J. Am. Chem. Soc.*, 125 (2003) 9090-9101

Tadros Th. F, Vandamme A, Levecké B, Booten K, Stevens C. V, ***Stabilization of emulsion using polymeric surfactant based on inulin***, *Adv. Colloids Interf. Sci.*, 108/109 (2004) 207-226

Tadros Th, Izquierdo P, Esquena J, Solans C, ***Formation and stability of nano-emulsions***, *Adv. in Colloid and Interf. Science*, 108/109 (2004) 303-318

Tamura K and Schelly Z A, *Reversed Micelle of Aerosol-OT in Benzene 3. Dynamics of the Solubilization of Picric Acid*, *J. Am. Chem. Soc.*, 103 (1980) 1018-1022

Toerne K, Rogers R, and von Wandruszka R, *Thermal Stability of Nonionic Surfactant Aggregates*, *Langmuir*, 17 (2001) 6119-6121

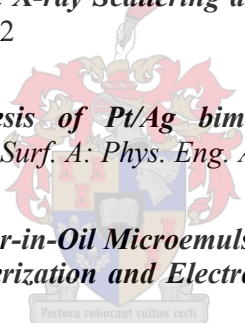
Tojo C, Barroso F, de Dios M, *Critical nucleus size effects on nanoparticle formation in microemulsions: A comparison study between experimental and simulation results*, *J. of Colloid and Interf. Science*, 296 (2006) 591–598

Tojo C, Blanco M. C and Lopez-Quintela M, A, *Preparation of Nanoparticles in Microemulsions: A Monte Carlo Study of the Influence of the Synthesis Variables*, *Langmuir*, 13 (1997) 4527-4534

Tomsic M, Bester-Rogac M, and Jamnik A, Kunz W, Touraud D, Bergmann A and Glatter O, *Nonionic Surfactant Brij 35 in Water and in Various Simple Alcohols: Structural Investigations by Small-Angle X-ray Scattering and Dynamic Light Scattering*, *J. Phys. Chem. B*, 108 (2004) 7021-7032

Wu M-L, Lai L-B, *Synthesis of Pt/Ag bimetallic nanoparticles in water-in-oil microemulsions*, *Colloids and Surf. A: Phys. Eng. Aspects*, 244 (2004) 149–157

Zhang X and Chan K-Y, *Water-in-Oil Microemulsion Synthesis of Platinum-Ruthenium Nanoparticle: Their Characterization and Electrocatalytic Properties*, *Chem. Mater*, 15 (2003) 451-459



## 6.2 INTERNET REFERENCE

<http://www.unl.edu/CMRAcfem/temoptic.htm>[2006/09/05]

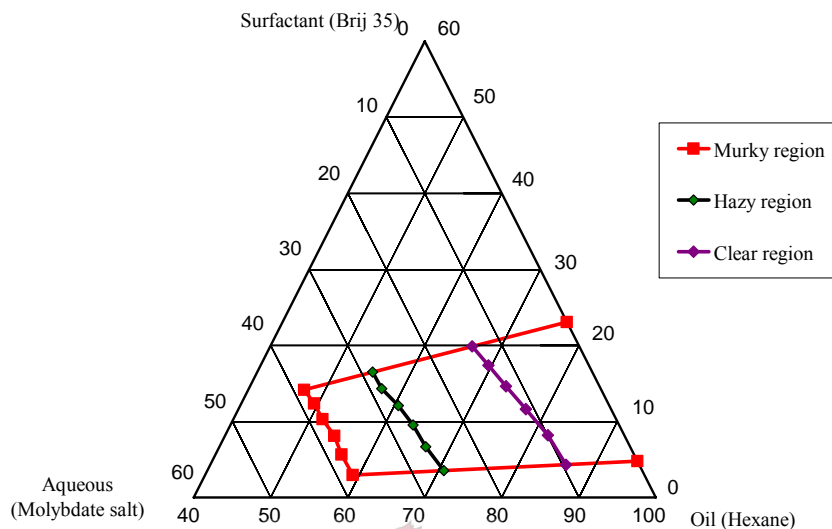
# Appendix

*Chapter layout:* Data obtained from all experiments including miscellaneous figures and tables.

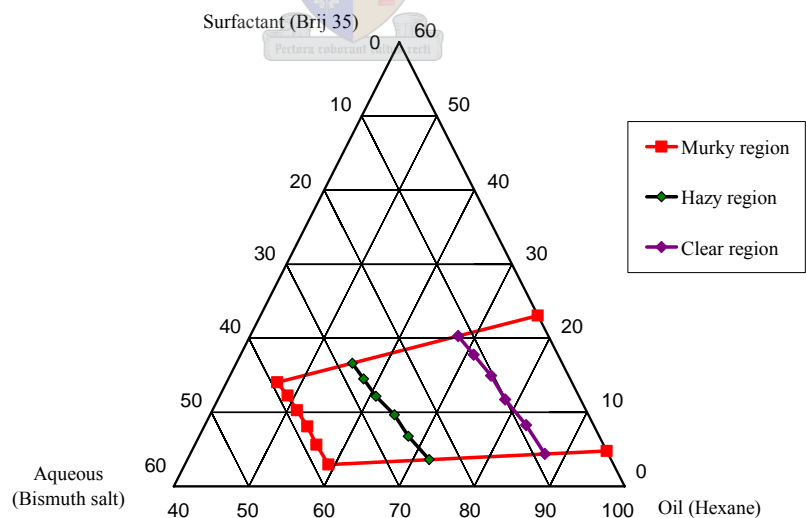
This is not the end. It is not even the beginning of the end, but it is the end of the beginning.  
[Winston Churchill]



### APPENDIX A1A: MISCELLANEOUS FIGURES (STABILITY IN A MIXTURE OF BRIJ 35 AND HEXANE)

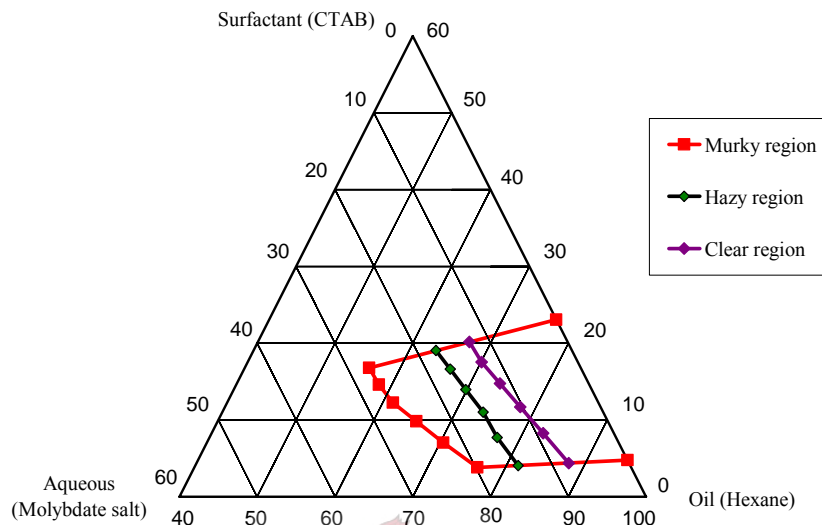


**Figure 7.1.1.1:** The stability region of micelles subject to the addition of molybdate salt solution to a mixture of hexane and Brij 35. The stability region shown corresponds to that of a clear, hazy and murky solution (with that of a milky solution not shown).

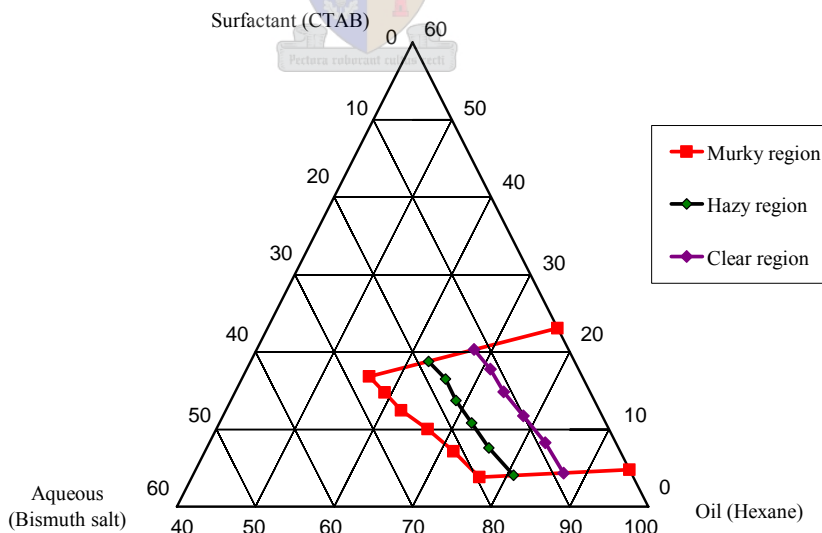


**Figure 7.1.1.2:** The stability region of micelles subject to the addition of bismuth salt solution to a mixture of hexane and Brij 35. The stability region shown corresponds to that of a clear, hazy and murky solution (with that of a milky solution not shown).

### APPENDIX A1B: STABILITY IN A MIXTURE OF CTAB IN PENTANOL AND HAXANE

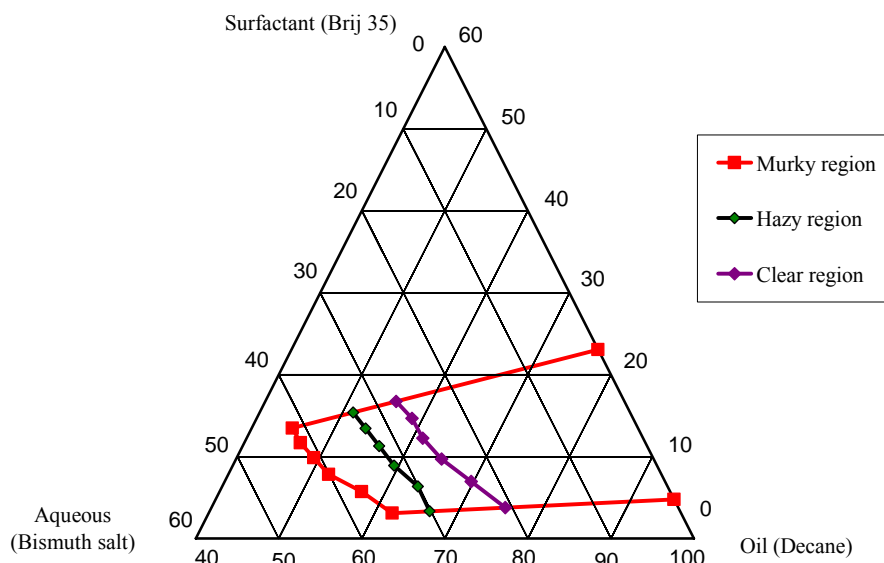


**Figure 7.1.2.1:** The stability region of micelles subject to the addition of molybdate salt solution to a mixture of hexane and CTAB, the latter was dissolved in pentanol. The stability region shown corresponds to that of a clear, hazy and murky solution (with that of a milky solution not shown).

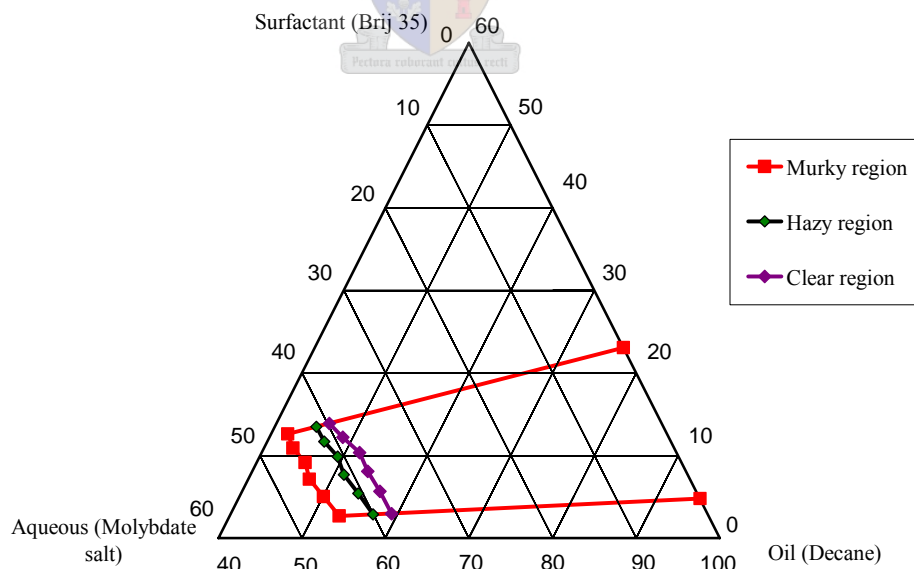


**Figure 7.1.2.2:** The stability region of micelles subject to the addition of bismuth salt solution to a mixture of hexane and CTAB. The stability region shown corresponds to that of a clear, hazy and murky solution (with that of a milky solution not shown).

## APPENDIX A1C: STABILITY IN A MIXTURE OF BRIJ 35 AND DECANE



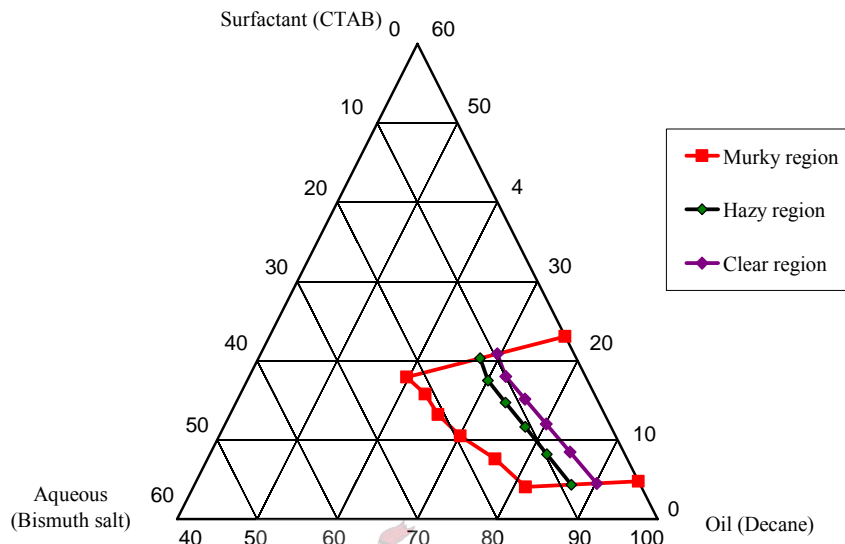
**Figure 7.1.3.1:** The stability region of micelles subject to the addition of bismuth salt solution to a mixture of decane and Brij35. The stability region shown corresponds to that of a clear, hazy and murky solution (with that of a milky solution not shown).



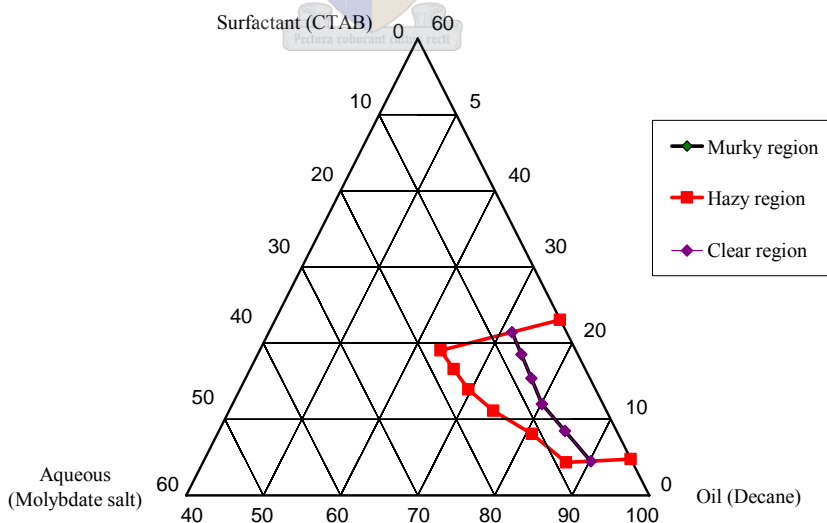
**Figure 7.1.3.2:** The stability region of micelles subject to the addition of molybdate salt solution to a mixture of decane and Brij35. The stability region shown corresponds to that of a clear, hazy and murky solution (with that of a milky solution not shown).



### APPENDIX A1D: STABILITY IN A MIXTURE OF CTAB IN PENTANOL AND DECANE

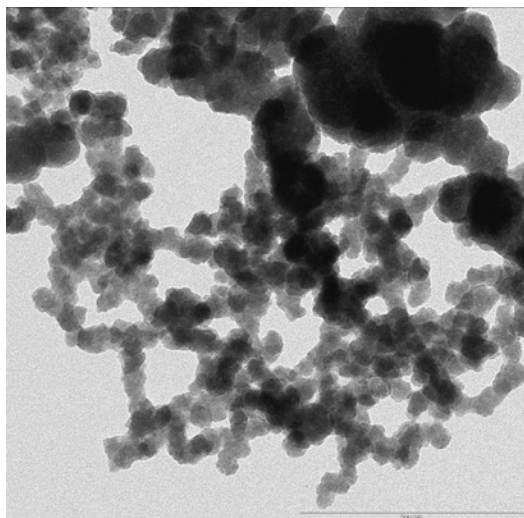


**Figure 7.1.4.1:** The stability region of micelles subject to the addition of bismuth salt solution to a mixture of decane and CTAB, the latter was dissolved in pentanol. The stability region shown corresponds to that of a clear, hazy and murky solution (with that of a milky solution not shown).

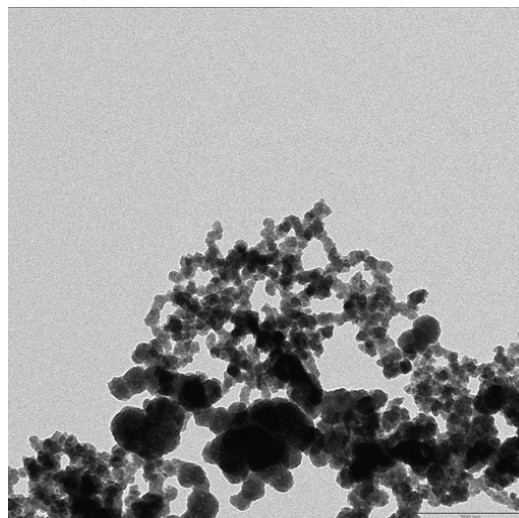


**Figure 7.1.4.2:** The stability region of micelles subject to the addition of molybdate salt solution to a mixture of decane and CTAB, the latter was dissolved in pentanol. The stability region shown corresponds to that of a clear, hazy and murky solution (with that of a milky solution not shown).

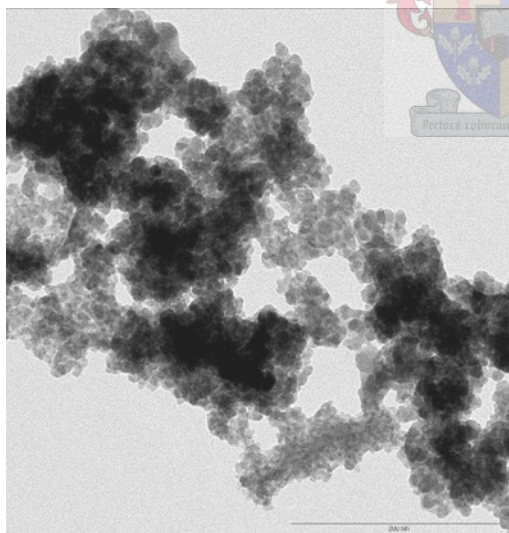
## APPENDIX A2A: EFFECT OF SALT CONCENTRATION



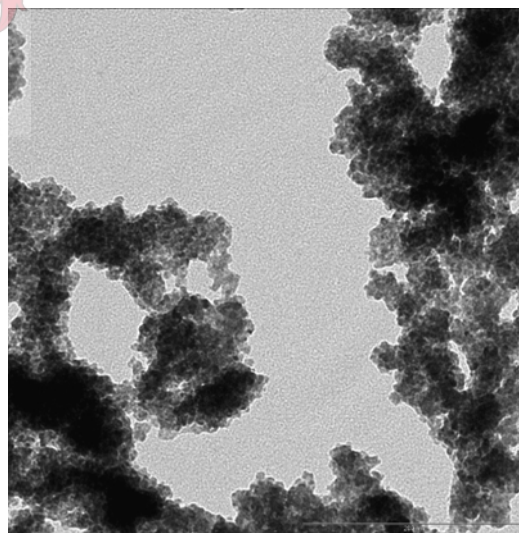
**Figure 7.3.1.1 (Series 1):** TEM photograph of the catalyst prepared at salt concentration of 0.64 mol/L molybdate and 0.2133 mol/L bismuth salts for 10 vol. % surfactant concentration.



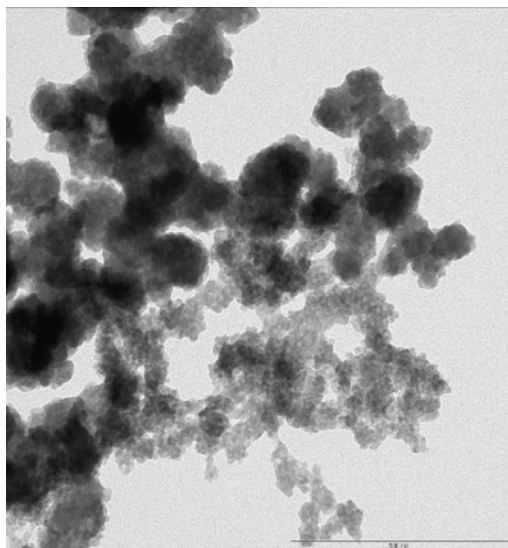
**Figure 7.3.1.2 (Series 2):** TEM photograph of the catalyst prepared at salt concentration of 0.32 mol/L molybdate and 0.1067 mol/L bismuth salts for 10 vol. % surfactant concentration.



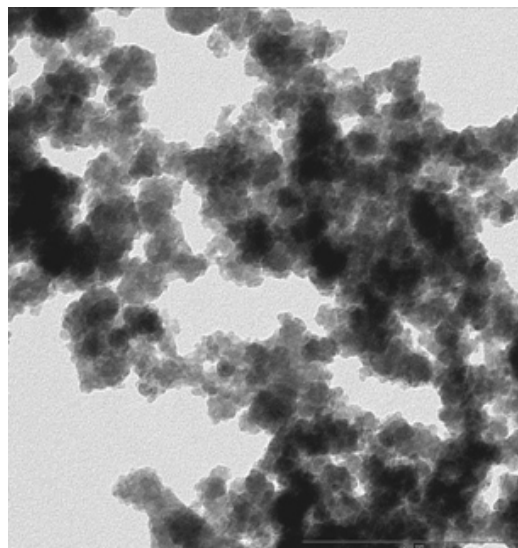
**Figure 7.3.1.3 (Series 3):** TEM photograph of the catalyst prepared at a salt concentration of 0.16 mol/L molybdate and 0.0533 mol/L bismuth salts for 10 vol. % surfactant concentration.



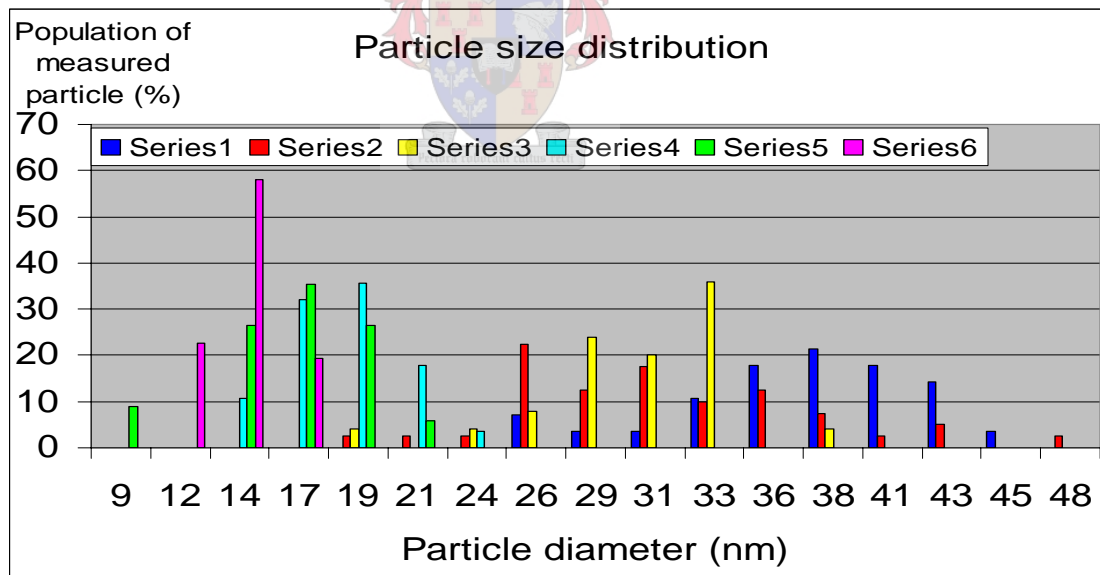
**Figure 7.3.2.4 (Series 4):** TEM photograph of the catalyst prepared at salt concentration of 0.064 mol/L molybdate and 0.2133 mol/L bismuth salts for 25 vol. % surfactant concentration.



**Figure 7.3.2.1 (Series 5):** TEM photograph of the catalyst prepared at a salt concentration of 0.32 mol/L molybdate and 0.1067 mol/L bismuth salts for 25 vol. % surfactant concentration.

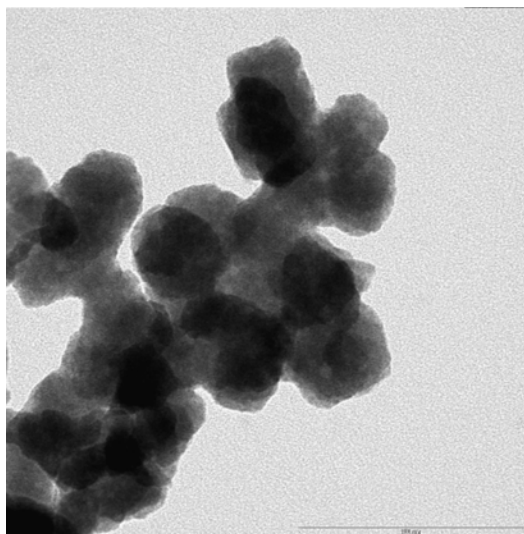


**Figure 7.3.2.2 (Series 6):** TEM photograph of the catalyst prepared at salt concentration of 0.16 mol/L molybdate and 0.0533 mol/L bismuth salts for 25 vol. % surfactant concentration.

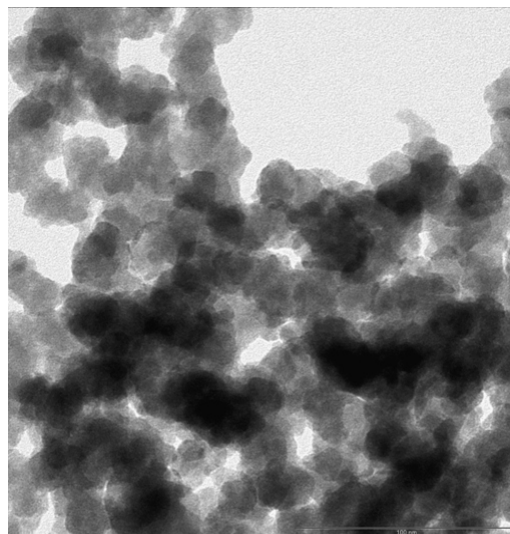


**Figure 7.3.2.3:** Particle size distribution for run to the investigation into the effect of salt concentration. Series 1, 2 and 3 are corresponding 0.64 mol/L molybdate and 0.2133 mol/L bismuth; 0.32 mol/L molybdate and 0.1067 mol/L bismuth and 0.16 mol/L molybdate and 0.0533 mol/L bismuth salts respectively at 10 vol. % surfactant. Series 4, 5 and 6 are corresponding and to 0.064 mol/L molybdate and 0.2133 mol/L bismuth; 0.32 mol/L molybdate and 0.1067 mol/L bismuth and 0.16 mol/L molybdate and 0.0533 mol/L bismuth salts respectively for 25 vol. % surfactant.

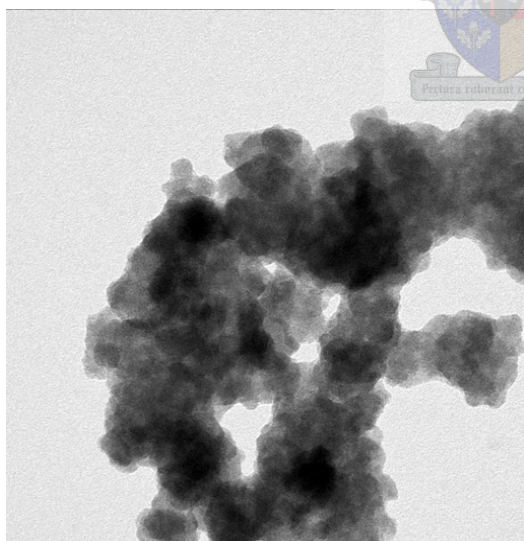
## APPENDIX A2B: EFFECT OF NUCLEATION AND GROWTH



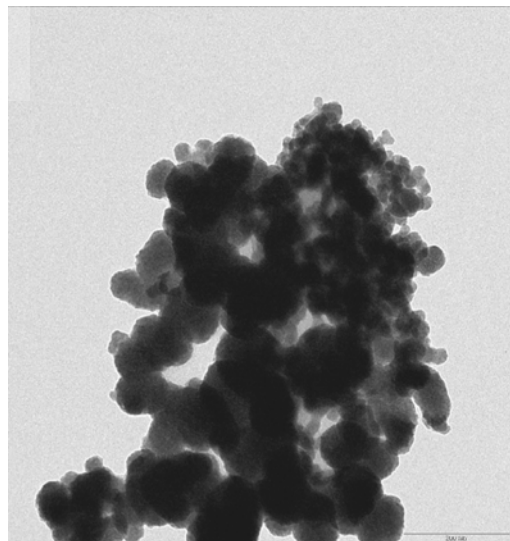
**Figure 7.3.3.1 (Series 4):** TEM photograph of the catalyst particles which were nucleated for a period of 120 minutes for 25 vol. % surfactant concentration.



**Figure 7.3.3.2 (Series 5):** TEM photograph of the catalyst particles which were nucleated for a period of 60 minutes for 25 vol. % surfactant concentration.

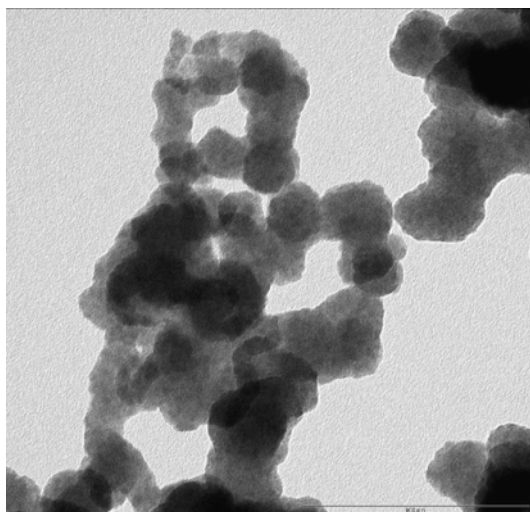


**Figure 7.3.3.3 (Series 6):** TEM photograph of the catalyst particles which were nucleated for a period 20 minutes for 25 vol. % surfactant concentration.

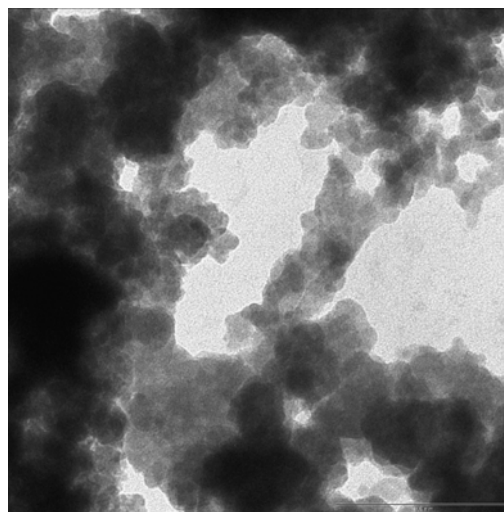


**Figure 7.3.3.4:** TEM photograph of the catalyst particles which were nucleated for a period 120 minutes for 10 vol. % surfactant concentration.

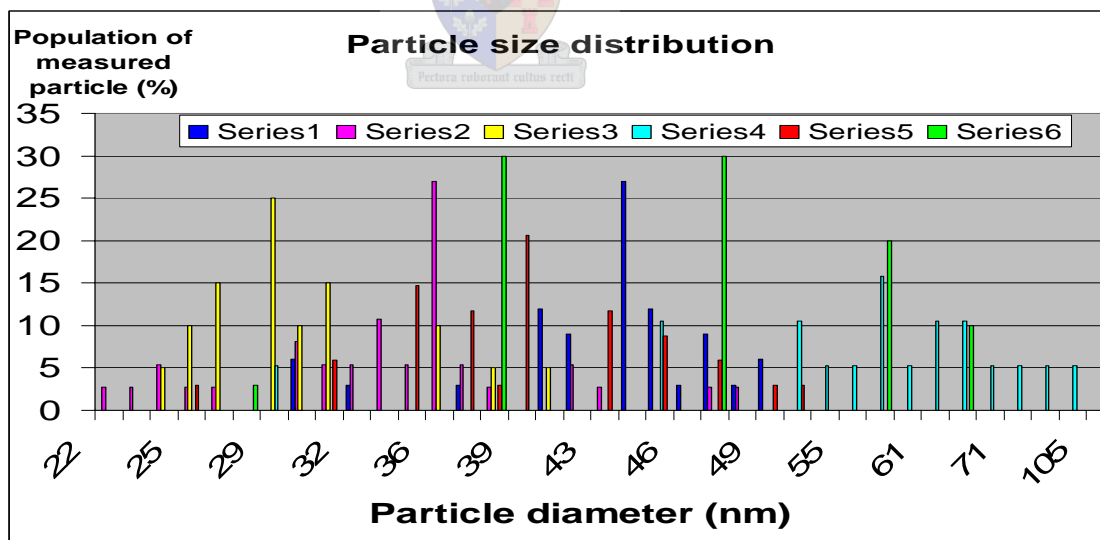
## APPENDIX A2C: EFFECT OF AGING



**Figure 7.3.4.1 (Series 1):** TEM photograph of the catalyst particles. The two reverse micelles allowed to stand separately for 24 hours and they were nucleated for a period 120 minutes for 25 vol. % surfactant concentration.

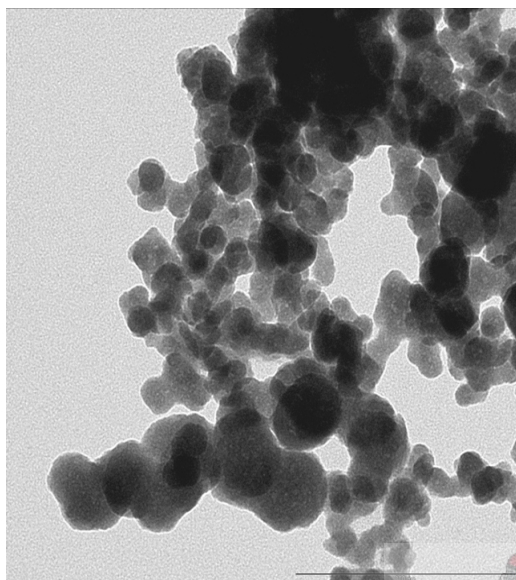


**Figure 7.3.4.2 (Series 2):** TEM photograph of the catalyst particles. The two reverse micelles allowed to stand separately for 24 hours and nucleated for a period 60 minutes for 25 vol. % surfactant concentration.

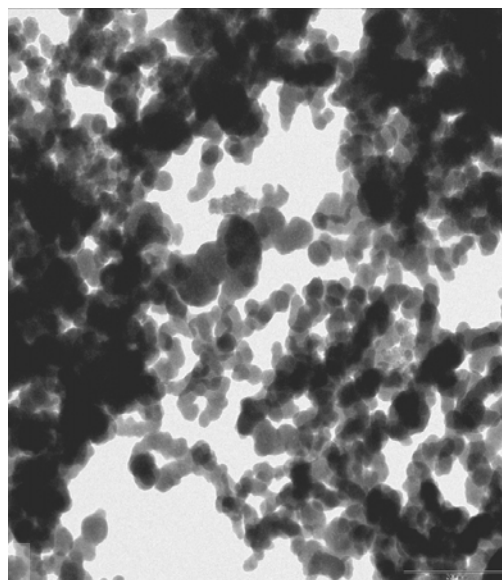


**Figure 7.3.2.3:** Particle size distribution for the investigation into the effect of nucleation and growth. Series 1, 2 and 3 were nucleated for 120, 60 and 20 minutes respectively with the two reverse micelles allowed to stand separately for 24 hours. Series 4, 5 and 6 were nucleated for 120, 60 and 20 minutes respectively.

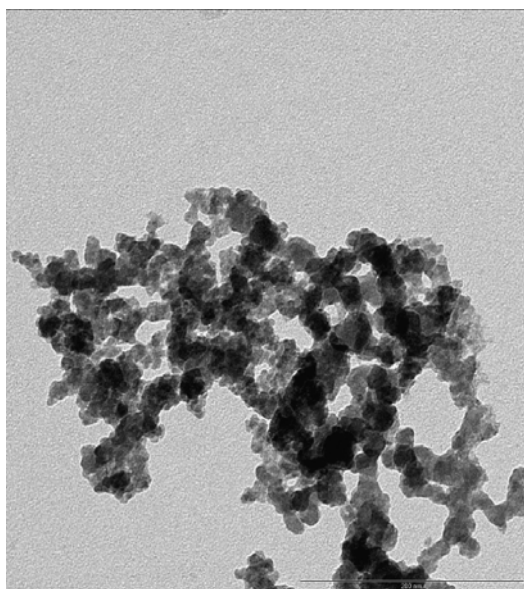
## APPENDIX A2D: EFFECT OF TEMPERATURE



**Figure 7.3.5.1 (Series 1):** TEM photograph of the catalyst prepared at a temperature of 30 °C and the reverse micelles were nucleated for 60 minutes for 25 vol. % surfactant concentration.

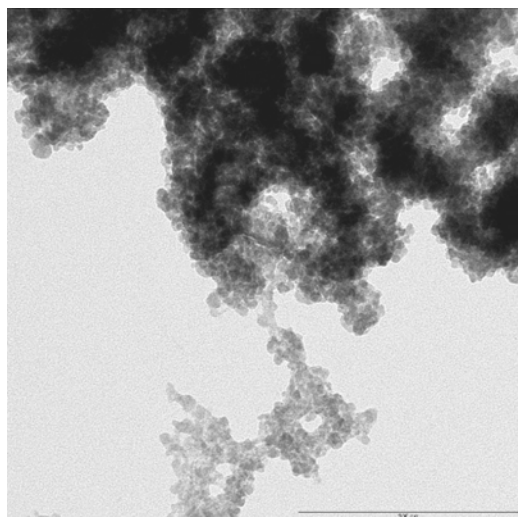


**Figure 7.3.5.2 (Series 2):** TEM photograph of the catalyst prepared at a temperature of 35 °C and nucleated for 60 minutes for 25 vol. % surfactant concentration.

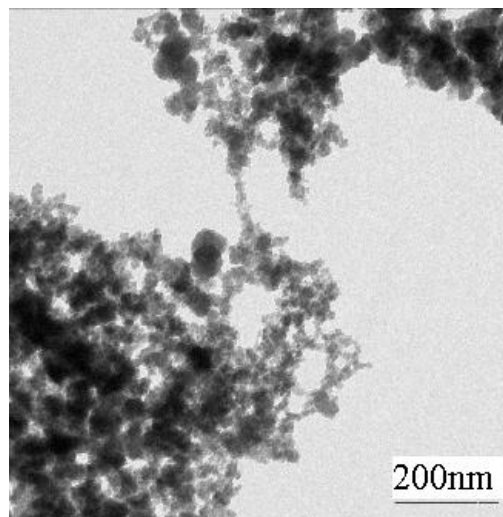


**Figure 7.3.5.3 (Series 3):** TEM photograph of the catalyst particle prepared at a temperature of 35 °C and was nucleated for 20 minutes at 25 vol. % surfactant concentration.

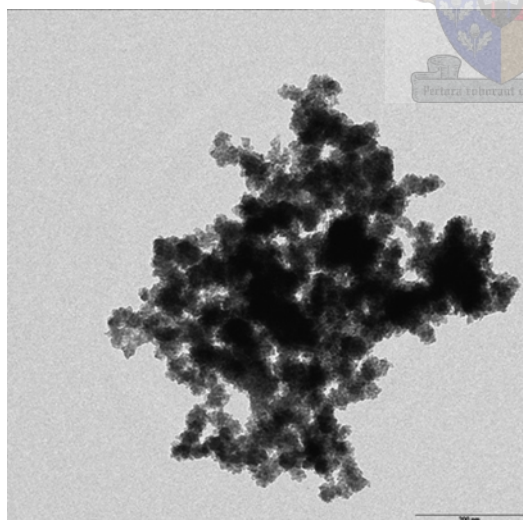
## APPENDIX A2E: EFFECT OF STIRRING



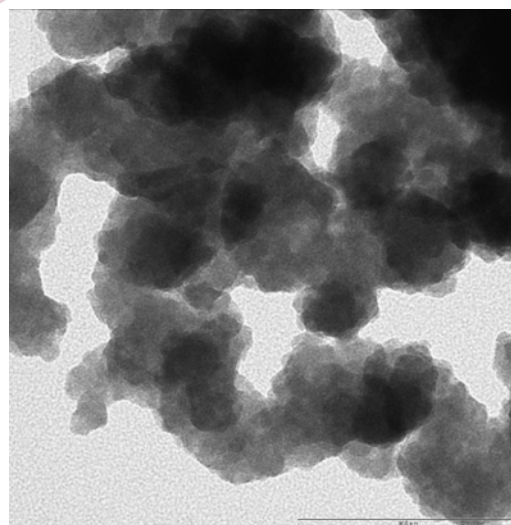
**Figure 7.3.6.1 (Series 1):** TEM photograph of the catalyst particles. The reverse micelles were stirred at 1.5 times the normal speed and nucleated for 20 minutes at 25 vol. % surfactant concentration.



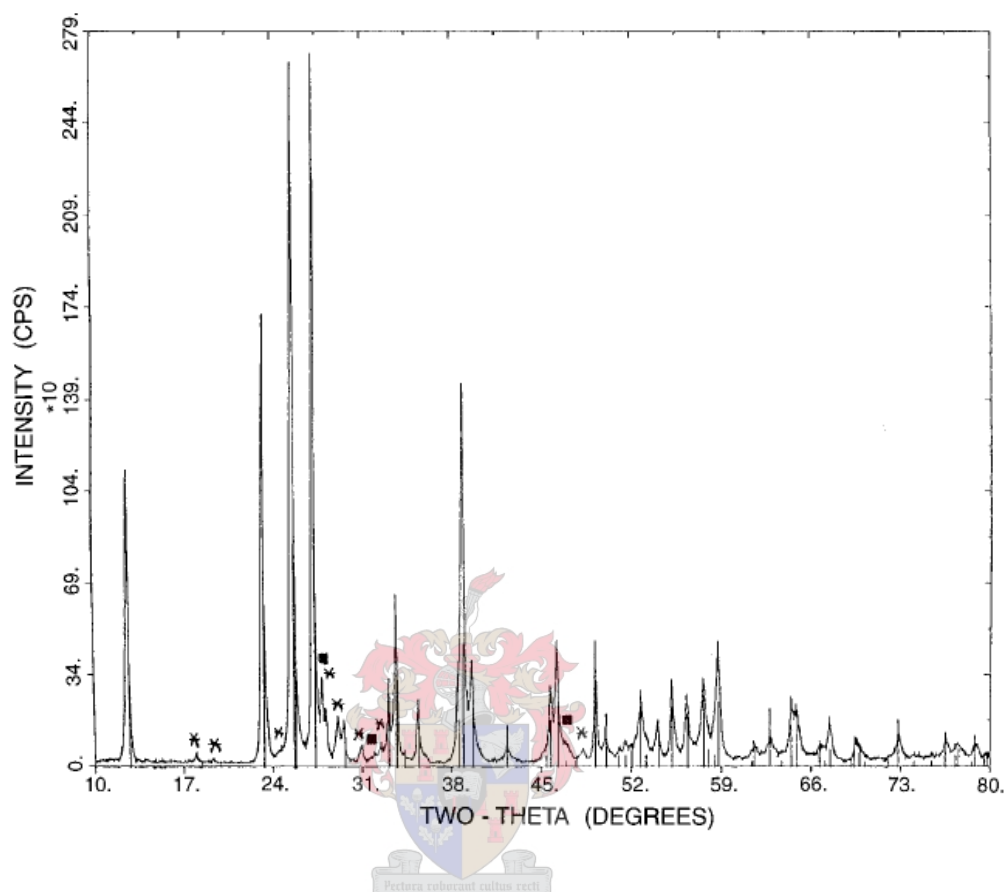
**Figure 7.3.6.2 (Series 2):** TEM photograph of the catalyst particles. The reverse micelles were stirred at 2.0 times the normal speed and nucleated for 20 minutes at 25 vol. % surfactant concentration.



**Figure 7.3.6.3 (Series 4):** TEM photograph of the catalyst particle. The reverse micelles stirred at 3.0 times the normal speed and nucleated for 20 minutes for 10 vol. % surfactant concentration.



**Figure 7.3.6.4 (Free run):** TEM photograph of the catalyst particle. The reverse micelles were sonicated for 1 minute and 30 seconds for 25 vol. % surfactant concentration. The temperature of mixture was kept at 35 °C.

APPENDIX A3: SYNTHESIS OF A PURE  $\alpha$ - $\text{Bi}_2\text{Mo}_3\text{O}_{12}$ 

**Figure A1:** X-ray powder diffractogram of  $\text{MoO}_3/1.9/\text{Bi}(\text{lact})_2(6 \text{ wt.}\%)$ . Vertical lines correspond to  $\text{MoO}_3$ . Ternary oxide phases are labeled with asterisks ( $\alpha$ - $\text{Bi}_2\text{Mo}_3\text{O}_{12}$ ) and squares ( $\gamma$ - $\text{Bi}_2\text{MoO}_6$ ) [Devillers et al., (1996)].



## APPENDIX D1: EXPERIMENTAL DATA (TITRATION ANALYSIS)

*Table D1A: Mass of aqueous added to a brij35-hexane mixture to turn the appearance of the mixture from clear to hazy, murky corresponding to R1, R2 and R3 respectively.*

<i>SURF.</i> <i>Brij 35</i>	<i>OIL</i> <i>n-hexane</i>	<i>AQUEOUS</i>								
		<i>Distilled water</i>			<i>Acid. Dist. water</i>			<i>Molybdate salt</i>		
		<i>R1</i>	<i>R2</i>	<i>R3</i>	<i>R1</i>	<i>R2</i>	<i>R3</i>	<i>R1</i>	<i>R2</i>	<i>R3</i>
<i>g</i>	<i>g</i>	<i>g</i>	<i>g</i>	<i>g</i>	<i>g</i>	<i>g</i>	<i>g</i>	<i>g</i>	<i>g</i>	
0.50	10	2.10	4.59	6.79	1.97	4.34	6.51	1.10	3.64	6.40
1.10	10	2.20	4.79	7.09	2.20	4.63	6.90	1.21	3.97	6.73
1.75	10	2.40	5.09	7.29	2.47	4.93	7.40	1.44	4.20	6.96
2.50	10	2.60	5.39	7.78	2.70	5.23	7.90	1.66	4.53	7.40
3.30	10	2.70	3.59	8.28	2.89	5.52	8.59	1.87	4.97	7.73
4.25	10	2.89	5.89	8.88	3.06	5.72	9.07	2.10	5.19	8.17

*Continuation of table D1A: Mass of aqueous added to a brij35-hexane mixture to turn the appearance of the mixture from clear to hazy, murky corresponding to R1, R2 and R3 respectively.*

<i>SURF.</i> <i>Brij 35</i>	<i>OIL</i> <i>n-hexane</i>	<i>AQUEOUS</i>								
		<i>Aged molybd salt</i>			<i>Bismuth salt</i>			<i>Aged bismuth salt</i>		
		<i>R1</i>	<i>R2</i>	<i>R3</i>	<i>R1</i>	<i>R2</i>	<i>R3</i>	<i>R1</i>	<i>R2</i>	<i>R3</i>
<i>g</i>	<i>g</i>	<i>g</i>	<i>g</i>	<i>g</i>	<i>g</i>	<i>g</i>	<i>g</i>	<i>g</i>	<i>g</i>	
0.50	10	1.21	3.86	6.62	0.97	3.35	6.41	1.18	3.55	6.71
1.10	10	1.44	4.20	7.07	1.09	3.75	6.80	1.38	3.85	7.10
1.75	10	1.46	4.42	7.29	1.28	3.99	7.10	1.49	4.14	7.40
2.50	10	1.77	4.75	7.62	1.38	4.44	7.49	1.67	4.54	7.79
3.30	10	1.99	5.08	7.95	1.59	4.73	7.89	1.79	4.83	8.18
4.25	10	2.21	5.41	8.28	1.77	5.03	8.38	1.97	5.13	8.58

**Table D1B:** Mass of aqueous added to a CTAB-hexane mixture to turn the appearance of the mixture from clear to hazy, murky corresponding to R1, R2 and R3 respectively.

<i>SURF.</i> <i>CTAB</i>	<i>OIL</i> <i>n-hexane</i>	<i>AQUEOUS</i>								
		<i>Distilled water</i>			<i>Acid. Dist. water</i>			<i>Molybdate salt</i>		
		<i>R1</i>	<i>R2</i>	<i>R3</i>	<i>R1</i>	<i>R2</i>	<i>R3</i>	<i>R1</i>	<i>R2</i>	<i>R3</i>
<i>g</i>	<i>g</i>	<i>g</i>	<i>g</i>	<i>g</i>	<i>g</i>	<i>g</i>	<i>g</i>	<i>g</i>	<i>g</i>	
0.50	10	0.50	0.90	1.50	0.6	1.0	2.00	0.88	1.78	2.59
1.10	10	0.60	1.00	2.00	0.6	1.1	2.20	1.10	1.99	3.20
1.75	10	0.60	1.10	2.20	0.7	1.2	2.70	1.33	2.10	3.75
2.50	10	0.70	1.20	2.49	0.7	1.3	2.99	1.54	2.32	4.31
3.30	10	0.80	1.40	2.70	0.8	1.4	3.09	1.78	2.54	4.64
4.25	10	0.80	1.50	3.09	0.9	1.5	3.49	1.88	2.76	4.86

**Continuation of Table D1B:** Mass of aqueous added to a CTAB-hexane mixture to turn the appearance of the mixture from clear to hazy, murky and corresponding to R1, R2 and R3 respectively.

<i>SURF.</i> <i>CTAB</i>	<i>OIL</i> <i>n-hexane</i>	<i>AQUEOUS</i>								
		<i>Aged molybd salt</i>			<i>Bisuth salt</i>			<i>Aged bismuth salt</i>		
		<i>R1</i>	<i>R2</i>	<i>R3</i>	<i>R1</i>	<i>R2</i>	<i>R3</i>	<i>R1</i>	<i>R2</i>	<i>R3</i>
<i>g</i>	<i>g</i>	<i>g</i>	<i>g</i>	<i>g</i>	<i>g</i>	<i>g</i>	<i>g</i>	<i>g</i>	<i>g</i>	
0.50	10	0.88	1.77	2.76	1.00	1.87	2.56	0.99	2.00	2.86
1.10	10	1.10	1.99	3.42	1.09	2.16	2.96	1.09	2.26	3.25
1.75	10	1.33	2.10	4.09	1.28	2.38	3.45	1.18	2.47	3.65
2.50	10	1.55	2.32	4.42	1.47	2.56	4.04	1.38	2.66	4.14
3.30	10	1.76	2.54	4.64	1.59	2.67	4.44	1.59	2.85	4.73
4.25	10	1.89	2.76	4.97	1.80	2.98	4.83	1.67	3.07	5.13

**Table DIC:** Mass of aqueous added to a brij35-decane mixture to turn the appearance of the mixture from clear to hazy, murky corresponding to R1, R2 and R3 respectively.

<i>SURF.</i> <i>Brij35</i>	<i>OIL</i> <i>n-decane</i>	<i>AQUEOUS</i>								
		<i>Distilled water</i>			<i>Acid. Dist. water</i>			<i>Molybdate salt</i>		
		<i>R1</i>	<i>R2</i>	<i>R3</i>	<i>R1</i>	<i>R2</i>	<i>R3</i>	<i>R1</i>	<i>R2</i>	<i>R3</i>
<i>g</i>	<i>g</i>	<i>g</i>	<i>g</i>	<i>g</i>	<i>g</i>	<i>g</i>	<i>g</i>	<i>g</i>	<i>g</i>	
0.50	10	6.27	7.32	8.97	6.27	7.39	8.86	6.37	7.02	8.32
1.10	10	6.66	7.76	9.13	6.66	7.78	9.13	6.70	7.51	8.96
1.75	10	7.04	8.09	9.41	7.00	8.06	9.19	7.07	8.05	9.61
2.50	10	7.32	8.25	9.63	7.67	8.74	9.57	7.33	8.26	9.83
3.30	10	7.98	8.75	10.2	8.06	9.13	9.96	7.99	8.86	10.48
4.25	10	8.64	9.24	10.7	8.51	9.58	10.62	8.59	9.23	10.80

**Continuation of Table DIC:** Mass of aqueous added to a brij35-decane mixture to turn the appearance of the mixture from clear to hazy, murky corresponding to R1, R2 and R3 respectively.

<i>SURF.</i> <i>Brij35</i>	<i>OIL</i> <i>n-decane</i>	<i>AQUEOUS</i>								
		<i>Aged molybd salt</i>			<i>Bisuth salt</i>			<i>Aged bismuth salt</i>		
		<i>R1</i>	<i>R2</i>	<i>R3</i>	<i>R1</i>	<i>R2</i>	<i>R3</i>	<i>R1</i>	<i>R2</i>	<i>R3</i>
<i>g</i>	<i>g</i>	<i>g</i>	<i>g</i>	<i>g</i>	<i>g</i>	<i>g</i>	<i>g</i>	<i>g</i>	<i>g</i>	
0.50	10	5.99	6.48	7.67	1.38	2.27	2.80	1.48	2.47	2.96
1.10	10	6.73	6.97	7.99	1.68	2.37	3.25	1.68	2.66	3.35
1.75	10	6.75	7.34	8.32	1.97	2.66	3.85	1.87	2.76	3.85
2.50	10	7.18	7.99	8.64	2.17	2.86	4.14	2.07	2.96	4.24
3.30	10	7.61	8.37	9.07	2.27	3.06	4.44	2.37	3.25	4.44
4.25	10	8.10	8.75	9.77	2.47	3.25	4.63	2.56	3.45	4.73

**Table DID:** Mass of aqueous added to a CTAB-decane mixture to turn the appearance of the mixture from clear to hazy, murky corresponding to R1, R2 and R3 respectively.

<b>SURF.</b> <b>CTAB</b>	<b>OIL</b> <b>n-decane</b>	<b>AQUEOUS</b>								
		<b>Distilled water</b>			<b>Acid. Dist. water</b>			<b>Molybdate salt</b>		
		<b>R1</b>	<b>R2</b>	<b>R3</b>	<b>R1</b>	<b>R2</b>	<b>R3</b>	<b>R1</b>	<b>R2</b>	<b>R3</b>
<b>g</b>	<b>g</b>	<b>g</b>	<b>g</b>	<b>g</b>	<b>g</b>	<b>g</b>	<b>g</b>	<b>g</b>	<b>g</b>	
0.25	5	0.83	1.09	2.08	1.10	1.25	2.13	0.29	0.29	0.49
0.55	5	0.99	1.30	2.18	1.25	1.51	2.29	0.39	0.39	0.69
0.88	5	1.20	1.61	2.29	1.46	1.72	2.50	0.49	0.49	0.99
1.25	5	1.35	1.88	2.60	1.61	1.87	2.81	0.49	0.49	1.18
1.65	5	1.66	1.98	2.91	1.82	2.21	3.12	0.49	0.49	1.28
2.13	5	1.92	2.29	3.12	2.03	2.34	3.33	0.49	0.49	1.38

**Continuation of Table DID:** Mass of aqueous added to a CTAB-decane mixture to turn the appearance of the mixture from clear to hazy, murky corresponding to R1, R2 and R3 respectively.

<b>SURF.</b> <b>CTAB</b>	<b>OIL</b> <b>n-decane</b>	<b>AQUEOUS</b>								
		<b>Aged molybdat salt</b>			<b>Bismuth salt</b>			<b>Aged bismuth salt</b>		
		<b>R1</b>	<b>R2</b>	<b>R3</b>	<b>R1</b>	<b>R2</b>	<b>R3</b>	<b>R1</b>	<b>R2</b>	<b>R3</b>
<b>g</b>	<b>g</b>	<b>g</b>	<b>g</b>	<b>g</b>	<b>g</b>	<b>g</b>	<b>g</b>	<b>g</b>	<b>g</b>	
0.25	5	0.29	0.29	0.49	0.30	0.49	0.89	0.49	0.59	0.99
0.55	5	0.39	0.39	0.69	0.39	0.59	1.09	0.59	0.69	1.48
0.88	5	0.49	0.49	0.99	0.49	0.69	1.38	0.69	0.79	1.87
1.25	5	0.49	0.49	1.18	0.59	0.79	1.58	0.79	0.89	2.07
1.65	5	0.49	0.49	1.28	0.69	0.89	1.68	0.79	0.89	2.17
2.13	5	0.49	0.49	1.38	0.69	0.89	1.87	0.89	0.99	2.37

## APPENDIX D2: EXPERIMENTAL DATA (MALVERN ZETASIZER)

**Table D2.1:** Sizes of the particle taken at an indicated time for distilled water added to a constant brij35-decane mixture at 10 vol. % vol. brij35.

Time	Volume of distilled water added			
	5 vol. %	10 vol. %	15 vol. %	20 vol. %
sec	Sizes (nm)			
0				
34	109.4	107.9	105.6	114.9
67	119.3	170.5	145.5	173.6
101	161.9	163.4	164.2	186.6
134	173.5	177.9	186.2	168.8
168	169.9	177.9	180.9	194.2
202	169.8	187.2	185.4	205.8
235	174.1	171	187	193.2
269	178.7	176.7	182	201.3
302	170.5	183.5	193.4	202.6
336	175.5	174.9	188.2	203.6
371	165	182.1	201.2	210.3
404	187.7	181.3	192.1	200.2
438	175	179	202.8	204.5
471	185.8	182.6	193.5	209.3
505	183.7	184	194.5	222.4
538	173.5	185	202.9	208
572	171.8	195.1	193.5	202.6
606	187	190.8	202.3	200.8
639	185.5	180.4	196.2	202.9
673	172	193	199	205
708	181.6	184.7	194.5	207.2
741	177.4	190.2	207.8	215.9
775	180.7	189.4	203.7	225
808	182.9	187.6	214.6	260.3
842	177.3	184	200.1	224.6
875	187	193.8	201.2	205.8
909	191.6	185.8	212.4	213
943	185.6	191.8	199.9	207.5
976	171.9	190.6	219	210.7
1010	180.4	202.1	211.4	217.5
1045	196.3	186.9	204.4	224.4
1078	195.4	178.2	212.9	222.1
1112	184.2	184.3	200.4	216.2
1145	178	181.6	219.5	215.8
1179	173.7	193.3	210.3	203.9
1212	176	184.5	209.2	211
1246	188.7	194.5	211.5	225.4
1280	178.5	191.9	207.7	226.5
1313	172.4	184.7	206.6	218.2
1347	187	183.8	199.9	220.7

1382	183	186.6	199	210.8
1415	186.7	188.6	219.3	229.6
1449	174.1	193	197	222.2
1482	200.6	205.1	212.4	232.6
1516	196.3	183.4	216.4	216.7
1549	194.2	192.3	206.7	210.2
1583	187.3	187.1	224.8	230.5
1617	175.6	187.5	215.3	209
1650	185.9	187.5	209	210.6
1684	196.7	185.7	209	225.6

**Table D2.2:** Sizes of the particle taken at an indicated time for distilled water added to a constant brij35-decane mixture at 25 vol. % vol. brij35

Time	Volume of distilled water added			
	5 vol. %	10 vol. %	15 vol. %	20 vol. %
sec	Sizes (nm)			
0				
34	83.5	93.9	64	71.2
67	90.2	96.4	68.8	77.9
101	95.5	99.6	98.7	102.9
134	103	103.1	108.3	109.2
168	101.6	101.1	114	110.8
202	104.8	105.5	116.8	113.7
235	101	105.2	117	119
269	103	108.3	115.3	117.6
302	106.2	103.5	118.2	122
336	109.5	108.6	120.3	123.7
371	106.9	111.7	122.7	120.3
404	111.6	109.2	124.2	124.5
438	114.9	105.2	125.1	122.9
471	106.8	110.4	127.3	131.3
505	108.6	118.3	126.5	129.2
538	114.6	113	129.6	126.9
572	106.2	112.4	125.8	139.2
606	108.6	113.6	128.3	138.3
639	117	114.7	133.8	135.4
673	108.1	116	129.6	133.1
708	108.8	114.7	130.9	135.5
741	110.3	116.4	135.3	137.6
775	107.9	118.7	132.2	138.8
808	111	120.8	128.7	141.1
842	114.3	115.8	133.7	139.1
875	112.7	120.9	142.2	137.9
909	115	118.4	131.5	140.1
943	115.1	113.4	136.8	144.1

976	117.3	122.3	139.9	145.2
1010	119.4	120.9	136.5	146
1045	114.9	124.5	136.7	146.1
1078	115.7	122	135.7	145
1112	124.5	125.7	143.6	148
1145	116.5	129.6	142.1	151.5
1179	122.1	121.9	147.2	144.2
1212	115.5	125.6	138.8	150.3
1246	117.3	123.3	135.1	145.7
1280	123.9	127.9	141.4	158.9
1313	115.1	129.5	145.1	147.7
1347	113.2	120.9	138.6	155.1
1382	123.3	127.3	143.4	152.4
1415	118.7	120.4	146.6	151.8
1449	116.9	126.3	144.5	151.2
1482	111.5	126.7	143	153.6
1516	124.2	127.2	141.5	155.2
1549	122.1	127.2	143.8	153.7
1583	121.1	129.9	149.1	152.8
1617	117	124.4	146	163.7
1650	122.6	134.4	143.7	149.9
1684	120.6	123.3	145.6	150

**Table D2.3:** Sizes of the particle taken at an indicated time for a molybdate salt solution added to a constant brij35-decane mixture at 10 vol. % vol. brij35.

Time	Volume of molybdate salt added			
	5 vol. %	10 vol. %	15 vol. %	20 vol. %
sec	Sizes (nm)			
0				
34	90.7	111.3	78.7	101.8
67	112.8	156.7	97.1	152
101	148	176.4	140.7	199
134	183.4	192.4	182.4	228.5
168	177.8	187	226.4	235.5
202	203.6	183.8	206	240
235	192.5	190.4	204.6	241
269	182.7	204	211.3	235.4
302	186.1	172.6	239.4	255.7
336	185.1	195.3	238.8	250.9
371	181.4	192.8	217.7	234
404	192.4	191.9	214.1	248.6
438	162.4	201.9	212.9	251
471	174	186.6	213.3	230.5
505	177.1	186.7	224.5	246.1
538	177.7	192.6	210.6	244.4
572	197.6	201.7	236.9	254.8
606	163.8	209.4	217.6	252

639	179	198.8	243.4	230.1
673	170.2	191.8	236.7	242
708	164.5	193.2	224.2	254
741	169.8	196.2	227	249.7
775	174.3	192.3	228	246.8
808	168.6	202.8	224.6	262.1
842	176.4	198.4	219.4	222.3
875	174.3	188.6	220.5	242.4
909	160	189.3	238.9	251.3
943	149.6	199.8	226.5	230.7
976	173.6	196.1	215.2	258.2
1010	168.6	199.7	231	232.8
1045	183.2	208.8	249.9	221.2
1078	190.2	192.3	217.4	262.8
1112	161.7	205.9	239.5	247
1145	169.6	190.7	232.8	252.7
1179	171.5	198.6	213.4	250
1212	172.6	196.1	203.6	248.8
1246	155.9	201.6	225.4	269.6
1280	164.9	210.5	216.5	244.7
1313	167.3	184	211.8	261.3
1347	172.4	198	231.8	249
1382	155	197.2	221.5	255.8
1415	163.7	209.6	236.2	249.5
1449	153.8	207.3	228.7	229.8
1482	194.2	202.9	223.1	233.8
1516	174	206.6	227.8	263.8
1549	162.8	190.1	236.4	227.4
1583	147.9	200	225.3	219.7
1617	186.8	188.8	240	215
1650	188.1	202.5	216.7	242.8
1684	192.8	195.4	229.2	248.3

**Table D2.4:** Sizes of the particle taken at an indicated time for a molybdate salt solution added to a constant brij35-decane mixture at 25 vol. % vol. brij35.

Time	Volume of molybdate salt added			
	5 vol. %	10 vol. %	15 vol. %	20 vol. %
sec	Sizes (nm)			
0				
34	79.7	68.4	71.7	106.9
67	74.1	72.6	71.1	110.6
101	71.4	67.8	69.5	111.6
134	80.1	71	71.6	111.5
168	81.1	73.6	79.3	118.4
202	80.6	75.6	81.9	123
235	84.2	81.7	85.8	131.1
269	83.6	91.8	90.2	123.7



302	88.5	87.2	83.8	124.8
336	89.1	89.2	94	137.5
371	86.3	90.7	97.4	132.2
404	88.2	86.5	107.8	132
438	91.3	88.6	109.1	145.9
471	92.9	85.1	93.5	128.8
505	91.9	86.4	102.2	131.9
538	90.1	88.4	100	139
572	93.2	99.2	105.8	137
606	92.9	97.3	110.9	122.1
639	93.1	92.4	109.9	147.9
673	90.1	91.1	102.2	138.1
708	94.1	94.8	119.6	154.2
741	97.3	90.6	113.8	156
775	98.5	92.6	113.4	165.1
808	94.9	108.5	116.3	172.8
842	95.6	100	108	154.2
875	100.6	102.1	109.4	151.7
909	101.3	99.7	116.3	185.5
943	99.5	100.8	118.5	166.7
976	100.1	98.4	134.7	174
1010	103.4	106.5	122.3	161.8
1045	108.6	103.9	126.3	191.6
1078	105	105.8	122.6	190.4
1112	103.3	106.1	147.7	201.6
1145	112.7	115.8	136.2	182.6
1179	108.2	113.4	130.8	208.5
1212	106.5	112.1	131.1	161.1
1246	109.6	109.8	130	193.6
1280	111.1	123.5	140.2	180.5
1313	106.5	114.9	125.9	192.5
1347	106.5	114.9	125.9	192.5
1382	108.9	110	133.3	190.1
1415	117.6	114.5	154.6	195.2
1449	117.3	122.5	141.3	203.3
1482	114.2	104.6	168.8	186.4
1516	112.6	121.5	150.9	201.6
1549	116.1	124.1	139.4	182.8
1583	116.3	123.1	151.4	216
1617	119.3	131.4	159.7	191.6
1650	119.4	131	149.5	169.5
1684		130.4	126.3	187.8

1112	198.2	218	233.3	260.6
1145	193.9	214.3	215.6	253.1
1179	191	216.2	254.8	288.8
1212	198.6	214.4	239.4	286.4
1246	200.7	217.8	239.3	261
1280	194.7	221.6	248.2	267.4
1313	205	218	241.8	277.3
1347	201.3	223.2	242.4	260.7
1382	206.2	225.1	246.7	269.9
1415	205	214.4	255.3	257.1
1449	201.3	213.5	230	294.6
1482	206.1	220.2	261	286.9
1516	208.6	218.8	249.9	257.3
1549	208.8	222.4	246.5	267.9
1583	194.9	213.8	249.8	296.8
1617	205.8	234.2	247.9	263.7
1650	212.2	234.9	261.9	287
1684	208.5	215	264.1	287.1

**Table D2.7:** Sizes of the particle taken at an indicated time for distilled water added to a constant CTAB-decane mixture at 10 vol. % vol. CTAB.

Time	Volume of distilled water added			
	2.5 vol. %	5.0 vol. %	7.5 vol. %	10 vol. %
sec	Sizes (nm)			
0				
34	48.2	61.4	115.5	284.5
67	63.2	73.8	220.3	378.9
101	75	86	236	399.5
134	79.4	93.8	342.4	407.9
168	83.8	104	311.7	422.9
202	75.9	98.1	322	431
235	77	95.6	351.9	442.4
269	93.6	112.4	374.4	417.8
302	84	97.8	365.6	470.5
336	73.6	97.4	345.6	437.7
371	89.2	108.9	412.7	455.8
404	94.5	110.5	364.4	509.1
438	83.3	114.3	390.3	486.5
471	86.6	104.1	366.1	498
505	77.3	101.5	348.7	459.9
538	79.7	101.7	374.2	503.4
572	86.5	126.4	380.9	498
606	94.3	102.8	446.3	477.6
639	104.2	96.2	394.2	482.7
673	97.7	113.3	328.3	469.5
708	84.7	84.6	374.6	519.5
741	85.2	102.6	378.1	513.6

775	91.5	104.8	367.4	391.8
808	77.3	106.1	515.6	501.8
842	94	102.1	374.1	465.8
875	106.9	120.7	452.6	537.1
909	89.8	102.2	390.3	586.3
943	106.7	111.5	355.4	440
976	106.5	118.5	352.9	435.5
1010	112.6	102.3	315.9	419.8
1045	98.8	110	373.6	495.4
1078	102	95.4	470.6	535.6
1112	114.1	97.1	322.6	503.6
1145	134.8	100.9	493	562.6
1179	149.4	108.4	289	471.3
1212	113.7	101.8	328	578.8
1246	92.8	101.9	434.5	525.5
1280	152.5	123.2	428.4	506.7
1313	112.7	100.9	418.3	462.3
1347	104.5	90.5	446.5	451.5
1382	111.6	94.5	319	475.4
1415	118.7	97.9	468.4	449.6
1449	101.2	95.7	443.4	450.9
1482	138.3	122.5	374	473.1
1516	112	115.1	301.6	526
1549	135.8	95.7	386.9	501.6
1583	176.5	129.7	301.6	590
1617	136.9	116.1	323.5	471.6
1650	121.7	148.1	321.3	555
1684	159.2	115	380.8	418.5

**Table D2.8:** Sizes of the particle taken at an indicated time for distilled water added to a constant CTAB-decane mixture at 25 vol. % vol. CTAB.

Time	Volume of distilled water added			
	2.5 vol. %	5.0 vol. %	7.5 vol. %	10 vol. %
sec	Sizes (nm)			
0				
34	3.4	3.5	3.6	4.9
67	3.1	3.3	3.4	5
101	3.1	3.3	3.5	5
134	3.3	3.1	3.5	5.1
168	2.8	3.1	3.5	5.1
202	3.1	3	3.5	5.5
235	3.3	3	3.6	5.4
269	2.9	3.2	3.5	5.3
302	3	3.1	3.8	5.5
336	2.7	3.1	3.5	5.3
371		3.1	3.5	5.4
404	2.4	2.9	3.5	5.4

438	2.8	3.3	3.4	5.4
471	2.4	3.1	3.6	5.6
505	3.1	3.1	3.7	5.4
538	3	3.2	3.6	5.4
572	2.4	3.2	3.5	5.4
606	3.3	3.2	3.6	5.4
639	3.2	3.1	3.5	5.3
673	3	3.3	3.5	5.4
708	3.2	3.2	3.5	5.6
741	3.2	3.1	3.4	5.3
775	3.1	3.2	3.6	5.5
808	3.3	3.2	3.4	5.4
842	3.7	3.1	3.4	5.6
875	2.6	3.4	3.5	5.3
909	2.8	3.3	3.6	5.5
943	2.4	3.2	3.4	5.4
976	2.6	3.3	3.5	5.5
1010	3.5	3.3	3.4	5.4
1045	3.1	3.2	3.6	5.5
1078	2.8	3.1	3.4	5.5
1112	3.7	3.1	3.4	5.4
1145	3.3	3	3.5	5.3
1179	2.7	3.3	3.6	5.6
1212	2.4	3	3.5	5.3
1246	2.6	3.1	3.4	5.4
1280	2.5	3.1	3.5	5.4
1313	2.8	3	3.5	5.6
1347	2.7	3.1	3.6	5.4
1382	2.5	3.1	3.5	5.2
1415	3.3	3	3.7	5.3
1449	3	3.2	3.5	5.6
1482	2.3	3.1	3.5	5.7
1516	2.4	3	3.4	5.5
1549		3	3.5	5.3
1583	3.2	3	3.5	5.5
1617	2.8	3	3.4	5.4
1650	2.4	3	3.4	5.4
1684	2.6	3.2	3.4	5.4

**Table D2.9:** Sizes of the particle taken at an indicated time for a molybdate salt solution added to a constant CTAB-decane mixture at 10 % vol. CTAB.

Time	Volume of molybdate salt added		
	2.5 vol. %	5.0 vol. %	
sec	Sizes (nm)		
0			
34	69.3	70.7	
67	75.5	75.8	
101	78.6	78.7	
134	77.8	86.5	
168	87.3	90.9	
202	97.1	101.1	
235	98.8	111.9	
269	106.3	118.4	
302	113.7	126.3	
336	115.7	139.6	
371	121.5	155.3	
404	133	165.8	
438	135.8	184.7	
471	139.7	216.5	
505	145.8	217.4	
538	158.5	245.4	
572	168.8	266.7	
606	169.4	295.5	
639	200.3	291.4	
673	194.6	321	
708	212.5	363.4	
741	220.6	376.2	
775	228.3	431.4	
808	224.2	372.1	
842	244.3	514.2	
875	260	482	
909	275.3	471.2	
943	300.4	550.4	
976	295.4	497.7	
1010	299.8	499.5	
1045	325.2	662.4	
1078	321	611.9	
1112	374.2	615	
1145	409.6	526.9	
1179	437.9	643.8	
1212	390.8	568.7	
1246	451.9		
1280	469.9	754.1	
1313	510.8	697.9	
1347	464	756.4	
1382	572.4	838.6	
1415	506	678.8	
1449	592.1	900.1	

1482	563.9	756		
1516	619.9	920.2		
1549	572.4	829.4		
1583	608.1	752.7		
1617	657.7	1018.1		
1650	571.8	728.9		
1684	714	947.5		

**Table D2.10:** Sizes of the particle taken at an indicated time for a molybdate salt solution added to a constant CTAB-decane mixture at 25 % vol. CTAB.

Time	Volume of molybdate salt added		
	2.5 vol. %	5.0 vol. %	
<i>sec</i>	<i>Sizes (nm)</i>		
0			
34	91.5	77.7	
67	162	196.2	
101	251.6	238.6	
134	308.2	249	
168	328.3	392.9	
202	364.3	394.4	
235	310.4	457	
269	324.7	422.9	
302	364	553.9	
336	376.1	402.6	
371	393	519.4	
404	412.8	567.8	
438	439.4	523.2	
471		510.9	
505	480.5	541.7	
538	492.5	630.6	
572	443.2	622.7	
606	516.9	637.1	
639	480.3	587	
673	499	694	
708	430.4	636	
741	352	653.5	
775	411.6	666.9	
808	504.8	837.6	
842	483.4	721.6	
875	505.6	830.5	
909	491.5	574.5	
943	521.6	658.8	
976	471.4	619.1	
1010	520.6	642.4	
1045	469	546.7	

1078	488.7	701.2	
1112	568.7	807.9	
1145	483.1	796.9	
1179	542.1	700.3	
1212	523.6	576.3	
1246	477	624.3	
1280	586.2	540.5	
1313	589.4	740.3	
1347	411.9	729.4	
1382		618.7	
1415	604.4	571.9	
1449	548.6	540.9	
1482	619.7		
1516	506.4	607.1	
1549	455.3	651.5	
1583	498.3	695	
1617	545.4	494.7	
1650	532.7	847	
1684	705.2	601.1	

**Table D2.11:** Sizes of the particle taken at an indicated time for a bismuth salt solution added to a constant CTAB-decane mixture at 10 vol. % CTAB.

Time	Volume of bismuth salt added		
	2.5 vol. %	5.0 vol. %	7.5 vol. %
sec	Sizes (nm)		
0			
34	87.6	65.6	27.9
67	96.3	72.6	33.1
101	104.9	76	39.3
134	113.8	82.4	49.2
168	125.1	81.6	62.8
202	129.4	91.3	78.4
235	140.3	96.3	94.9
269	138.6	96.2	112.5
302	145.1	99.8	142.3
336	156	106.7	165.1
371	158.2	112	185.9
404	161.3	119.2	217.8
438	190.2	122.8	242.1
471	195.5	122.8	279.8
505	205.4	132.8	298.5
538	215.6	137.9	348.7
572	241.5	149	349.6
606	242.3	148.2	425.9
639	236	157.9	475.7
673	257	153.5	452.5

708	281.4	172.6	552.6
741	266.4	171	598.1
775	279.4	176.4	653.1
808	296.9	187.2	608.7
842	293.1	183.1	666.1
875	310.6	205.1	734.1
909	326.5	215	943.8
943	323.4	218.6	900.7
976	319.3	217.6	902.5
1010	298	225	895.9
1045	291.7	232.2	1197.8
1078	264.2	240.8	1234.8
1112	255.1	268.3	1230.1
1145	224.1	266.6	1244.3
1179	213.3	293.3	1539.6
1212	212.3	324.5	1725.2
1246	206.8	303.3	1553.4
1280	194	348	1872
1313	197.6	371.6	1852.2
1347	199.3	376.4	1780.9
1382	199.4	387.8	1589.1
1415	211.2	418.3	1435.8
1449	201.1	453.9	1697.1
1482	211.1	413.3	1841.8
1516	212.2	428	
1549	226	464.6	1439.6
1583	216.6	439.3	1889
1617	220.3	477.9	1527.5
1650	222.8	460.6	1615.3
1684	240.1	486.5	1579.2



**Table D2.12:** Sizes of the particle taken at an indicated time for a bismuth salt added to a constant CTAB-decane mixture at 25 vol. % CTAB.

Time	Volume of bismuth salt added		
	2.5 vol. %	5.0 vol. %	
sec	Sizes (nm)		
0			
34	87.6	65.6	
67	96.3	72.6	
101	104.9	76	
134	113.8	82.4	
168	125.1	81.6	
202	129.4	91.3	
235	140.3	96.3	
269	138.6	96.2	



302	145.1	99.8		
336	156	106.7		
371	158.2	112		
404	161.3	119.2		
438	190.2	122.8		
471	195.5	122.8		
505	205.4	132.8		
538	215.6	137.9		
572	241.5	149		
606	242.3	148.2		
639	236	157.9		
673	257	153.5		
708	281.4	172.6		
741	266.4	171		
775	279.4	176.4		
808	296.9	187.2		
842	293.1	183.1		
875	310.6	205.1		
909	326.5	215		
943	323.4	218.6		
976	319.3	217.6		
1010	298	225		
1045	291.7	232.2		
1078	264.2	240.8		
1112	255.1	268.3		
1145	224.1	266.6		
1179	213.3	293.9		
1212	212.3	324.5		
1246	206.8	303.3		
1280	194	348		
1313	197.6	371.6		
1347	199.3	376.4		
1382	199.4	387.8		
1415	211.2	418.3		
1449	201.1	453.9		
1482	211.1	413.3		
1516	212.2	428		
1549	226	464.6		
1583	216.6	439.3		
1617	220.3	477.9		
1650	222.8	460.6		
1684	240.1	486.5		

## APPENDIX D3: EXPERIMENTAL DATA (PARTICLE SIZE DISTRIBUTION)

*Table D3.1: Particle size diameter for measuring sizes distribution for the investigation into the effect of salt concentration, the particle size distribution is measured for the indicated run in chapter 4.2.*

Sizes (nm)						
Series 4	Series 5	Series 6	Series 1	Series 2	Series 3	
52	36	31	21	17	14	
50	26	43	19	17	14	
45	48	29	19	19	17	
50	33	31	19	14	14	
38	29	24	19	17	14	
47	29	33	17	17	14	
45	24	31	14	14	17	
26	52	33	17	17	12	
52	29	33	21	17	14	
43	43	26	19	19	14	
45	43	31	21	14	14	
50	24	33	14	19	14	
50	24	29	14	21	12	
52	24	33	19	17	17	
26	26	33	17	14	14	
45	24	33	17	9	14	
41	33	29	21	14	12	
50	24	33	21	21	14	
48	29	31	19	19	14	
48	26	29	17	17	17	
45	26	29	19	14	12	
48	24	24	19	19	14	
43	31	29	16	9	12	
48	31	19	17	17	14	
48	24	24	17	17	17	
52	33		17	19	12	
43	19		24	14	17	
57	24		19	21	12	
	38		14	19	14	
	29			17	14	
	33			17	14	
	26			19		
	24			9		
	57			19		
	36					
	29					
	43					
	43					
	43					

**Table D3.2:** Particle size diameter for measuring sizes distribution for the investigation into the effect into nucleation and growth, the particle size distribution is measured for the indicated run in chapter 4.2.

<i>Sizes (nm)</i>						
<i>Series 6</i>	<i>Series 5</i>	<i>Series 4</i>	<i>Series 1</i>	<i>Series 2</i>	<i>Series 3</i>	<i>Series 7</i>
57	48	33	76	42	14	22
50	39	38	36	39	36	36
88	40	48	67	48	31	31
57	43	33	43	57	30	67
82	37	38	48	63	60	33
72	32	38	52	55	30	42
61	38	57	52	51	36	36
86	42	38	76	52	25	36
43	35	48	38	95	29	30
69	26	38	33	51	25	24
76	42	48	26	56	41	37
52	49	38	48	83	29	25
50	45	48	26	52	26	33
60	40	67	24	61	26	38
57	43	38	24	51	29	32
45	40	38	24	47	27	36
55	44	57	31	54	41	48
62	51	38	31	60	38	45
45	48	48	48	62	26	35
	37	48	57	60	31	48
	31	33	36	62		31
	38	67	57	52		30
	35	48	76	48		36
	26	38	76	58		36
	33	38	105			37
	43	57	105			30
	48	67				36
	49	38				36
	46	48				33
	38	48				42
	45					36
	35					43
	27					26
	36					32
						36
						33
						34

**Table D3.3:** Particle size diameter for measuring sizes distribution for the investigation into the effect into temperature, the particle size distribution is measured for the indicated run in chapter 4.2.

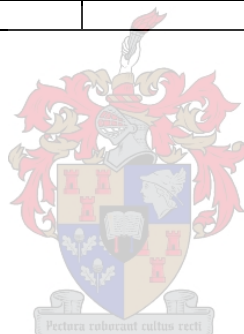
<i>Sizes (nm)</i>		
<i>Series 1</i>	<i>Series 2</i>	<i>Series 3</i>
36	17	33
31	17	29
24	23	45
30	20	38
22	21	33
23	15	31
26	17	33
26	17	26
31	15	24
23	14	29
31	15	33
24	17	29
32	23	31
40	17	33
41	21	33
37	17	29
29	15	19
24	17	33
31	14	24
33	21	21
37	21	29
33	20	33
33	17	31
33	17	31
27	14	24
26	15	33
27	17	29
30	19	38
33		26
31		24
		29
		31
		28
		28
		24
		36
		38
		33
		33
		26



**Table D3.4:** Particle size diameter for measuring sizes distribution for the investigation into the effect into stirring and salt ratio, the particle size distribution is measured for the indicated run in chapter 4.2.

<i>Sizes (nm)</i>					
<i>Series 1</i>	<i>Series 2</i>	<i>Series 3</i>	<i>Series 4</i>	<i>Series 1</i>	<i>Series 2</i>
33	17	8	8	7	7
29	12	6	10	9	10
45	14	7	8	10	10
38	14	8	7	13	5
33	14	6	8	12	12
31	14	9	10	9	10
33	17	10	7	9	8
26	12	9	8	10	10
24	14	12	8	14	12
29	14	6	11	8	10
33	14	6	8	10	12
29	12	7	8	10	10
31	14	6	11	8	12
33	17	9	10	7	5
33	14	7	8	12	10
29	12	10	10	11	10
19	14	5	11	12	7
33	17	8	12	8	7
24	12	7	8	9	10
21	14	9	6	10	10
29	14	7	12	11	10
33	12	7	11	7	7
31	14	8	10	11	10
31	14	7	7	12	7
24	17	6	12	9	7
33	2	9	8	8	12
29	17	10	6	12	7
38	12	10	5	13	10
26	14	9	11	10	10
24	14	7	8	11	10
29	14	7	8	6	7
31	14	6	12	12	10
28	12	8	7	6	5
28	17	7	12	8	12
24	14	6	10	8	10
36	14	9	6	10	12
38	14	7	13	10	7
33	17	9	8	12	10
33	17	9	7	13	7
26	12	7	10	13	10
8	14	10	8	7	8

10	12	7	10	10	10
10	14	6	13	13	10
8	14	8	8	8	12
8	14	9	8	8	10
11	17	8	11	8	7
10	12	8	10	10	7
8	14	9	8	11	10
11	14	7	11	13	10
8	17	7	8	12	7
	14			10	10
	14			8	8
	14			8	10
	12			8	7
	14			9	10
	14			8	8
	17			8	10
	14			8	5
	14			11	10
	14			9	7
	14				
	12				



APPENDIX D4: EXPERIMENTAL DATA (SYNTHESIS OF PURE  $\alpha$ - $\text{Bi}_2\text{Mo}_3\text{O}_{12}$ )*Table D4: Measurements for measuring the XRD pattern of a pure catalyst particle, the measurement correspond to an indicated figure in chapter 4.3.*

Intensity (Cps)	2 Theta (degrees)			
	Figure 4.4.1	Figure 4.4.2	Figure 4.4.3	Figure 4.4.4
5	734	1053	914	1209
5.03	736	1215	951	1109
5.06	718	1099	857	1115
5.09	771	1095	929	1170
5.12	766	1120	886	1112
5.15	777	1123	943	1149
5.18	760	1135	922	1151
5.21	781	1134	958	1093
5.24	712	1187	859	1149
5.27	774	1186	933	1153
5.3	780	1157	907	1164
5.33	788	1139	933	1227
5.36	728	1204	908	1142
5.39	772	1167	973	1117
5.42	838	1156	944	1150
5.45	714	1154	931	1217
5.48	748	1170	969	1216
5.51	789	1144	965	1123
5.54	800	1154	917	1123
5.57	760	1223	967	1138
5.6	780	1149	969	1221
5.63	744	1264	964	1150
5.66	758	1178	927	1192
5.69	795	1248	994	1209
5.72	871	1222	1060	1139
5.75	792	1212	968	1248
5.78	775	1245	971	1222
5.81	812	1240	1028	1173
5.84	776	1170	981	1138
5.87	826	1224	965	1155
5.9	777	1277	970	1200
5.93	889	1279	924	1154
5.96	847	1277	973	1207
5.99	860	1270	1000	1176
6.02	804	1265	1037	1201
6.05	841	1217	1017	1235
6.08	837	1313	1000	1216
6.11	842	1255	1018	1132
6.14	837	1277	1015	1209
6.17	871	1349	1088	1242
6.2	866	1287	1035	1191
6.23	829	1350	1075	1335
6.26	823	1337	1043	1192
6.29	870	1352	1010	1212
6.32	723	1296	1051	1181

6.35	880	1273	1052	1289
6.38	834	1357	1107	1231
6.41	885	1295	1070	1200
6.44	803	1355	985	1256
6.47	927	1421	993	1254
6.5	916	1317	1031	1197
6.53	833	1410	1015	1193
6.56	879	1389	1021	1227
6.59	874	1286	1044	1230
6.62	866	1328	1110	1241
6.65	900	1404	1092	1250
6.68	881	1388	978	1201
6.71	937	1399	1087	1284
6.74	845	1406	1030	1311
6.77	938	1364	991	1208
6.8	845	1413	1065	1193
6.83	884	1344	1052	1247
6.86	915	1364	1002	1260
6.89	915	1434	1072	1280
6.92	929	1378	1068	1263
6.95	877	1407	1050	1217
6.98	829	1438	1064	1217
7.01	845	1322	1071	1301
7.04	838	1412	1089	1241
7.07	823	1381	1044	1281
7.1	902	1388	1058	1204
7.13	875	1377	1096	1264
7.16	912	1301	1074	1247
7.19	892	1417	1013	1233
7.22	866	1425	1093	1241
7.25	901	1361	1006	1247
7.28	915	1369	1019	1244
7.31	890	1451	1013	1216
7.34	909	1339	1014	1187
7.37	999	1321	1022	1219
7.4	925	1335	1033	1218
7.43	928	1384	1023	1218
7.46	908	1325	993	1245
7.49	892	1428	1060	1251
7.52	905	1364	1015	1207
7.55	935	1350	1013	1253
7.58	915	1364	1066	1196
7.61	917	1326	1085	1263
7.64	886	1345	990	1230
7.67	882	1299	1068	1204
7.7	883	1323	976	1179
7.73	897	1409	1032	1244
7.76	900	1304	1038	1183
7.79	886	1341	1055	1253
7.82	861	1407	992	1213
7.85	868	1298	1035	1227
7.88	936	1299	1001	1219
7.91	920	1428	1073	1237
7.94	909	1328	1060	1177



7.97	907	1367	1051	1187
8	879	1337	960	1212
8.03	880	1358	1020	1195
8.06	887	1349	1002	1221
8.09	857	1402	1067	1174
8.12	910	1368	1024	1135
8.15	863	1298	1034	1163
8.18	925	1339	994	1177
8.21	869	1326	987	1122
8.24	902	1249	1048	1211
8.27	866	1358	978	1155
8.3	910	1370	950	1192
8.33	889	1291	963	1146
8.36	829	1381	997	1186
8.39	876	1269	966	1162
8.42	865	1344	963	1145
8.45	872	1323	1019	1196
8.48	880	1241	923	1129
8.51	865	1303	963	1177
8.54	846	1314	1011	1121
8.57	866	1278	1029	1169
8.6	863	1305	967	1188
8.63	855	1275	962	1082
8.66	872	1358	955	1134
8.69	840	1282	962	1159
8.72	859	1298	938	1095
8.75	863	1383	961	1128
8.78	827	1258	962	1122
8.81	875	1353	920	1166
8.84	839	1300	937	1159
8.87	878	1300	904	1149
8.9	832	1255	931	1134
8.93	836	1294	933	1081
8.96	863	1305	946	1081
8.99	847	1332	1012	1151
9.02	817	1378	990	1085
9.05	862	1236	907	1101
9.08	836	1232	914	1059
9.11	819	1246	986	1137
9.14	851	1243	909	1076
9.17	847	1328	941	1126
9.2	823	1252	926	1054
9.23	818	1289	907	1117
9.26	783	1317	941	1071
9.29	784	1279	907	1139
9.32	798	1305	912	1065
9.35	829	1257	903	1129
9.38	854	1296	904	1117
9.41	778	1337	903	1038
9.44	852	1210	958	1097
9.47	834	1305	910	1117
9.5	741	1295	932	1071
9.53	841	1254	873	1024

9.56	832	1247	866	1104
9.59	813	1264	956	1073
9.62	820	1234	917	1068
9.65	795	1245	899	1093
9.68	845	1261	843	1075
9.71	828	1247	904	1106
9.74	785	1234	928	1022
9.77	772	1224	868	1056
9.8	838	1323	923	1022
9.83	784	1279	927	1036
9.86	750	1273	891	1079
9.89	798	1269	957	1041
9.92	835	1195	856	1012
9.95	791	1216	840	1032
9.98	801	1261	927	1025
10.01	816	1217	873	1009
10.04	779	1264	876	1097
10.07	802	1217	878	974
10.1	767	1283	840	994
10.13	774	1316	909	1047
10.16	777	1194	868	1046
10.19	818	1289	907	1046
10.22	808	1248	902	1042
10.25	755	1276	939	1032
10.28	800	1300	838	1028
10.31	764	1186	892	1065
10.34	775	1283	884	1024
10.37	798	1282	842	1027
10.4	794	1261	902	981
10.43	772	1188	842	948
10.46	774	1295	890	1030
10.49	705	1236	837	1071
10.52	736	1237	848	991
10.55	775	1256	904	972
10.58	765	1263	907	998
10.61	777	1291	870	973
10.64	732	1290	897	1072
10.67	746	1285	828	999
10.7	781	1239	871	962
10.73	803	1291	901	1035
10.76	788	1215	896	973
10.79	814	1261	880	1005
10.82	761	1283	895	984
10.85	835	1310	819	1015
10.88	772	1249	906	1013
10.91	785	1275	890	984
10.94	786	1343	826	1000
10.97	748	1282	853	1024
11	799	1306	894	976
11.03	809	1344	844	1018
11.06	827	1380	876	1000
11.09	895	1482	860	962
11.12	925	1569	857	1000

11.15	957	1563	886	980
11.18	978	1478	833	1033
11.21	898	1408	877	990
11.24	840	1361	896	1001
11.27	736	1318	858	973
11.3	792	1346	882	1000
11.33	779	1287	832	996
11.36	760	1255	836	1014
11.39	786	1343	860	999
11.42	777	1339	851	974
11.45	769	1298	843	994
11.48	758	1337	866	962
11.51	766	1305	876	996
11.54	801	1303	860	989
11.57	774	1248	860	976
11.6	766	1323	858	1008
11.63	758	1294	837	983
11.66	737	1337	901	1030
11.69	740	1307	873	1008
11.72	780	1376	855	1018
11.75	753	1216	839	1009
11.78	762	1307	829	1041
11.81	719	1300	922	1002
11.84	765	1248	903	1085
11.87	824	1356	934	1088
11.9	741	1311	942	1074
11.93	766	1309	920	1064
11.96	713	1360	952	1067
11.99	748	1330	927	1085
12.02	712	1314	893	1047
12.05	748	1327	900	1012
12.08	760	1323	874	1008
12.11	733	1295	886	961
12.14	779	1263	913	1053
12.17	781	1315	885	1007
12.2	723	1335	898	987
12.23	753	1319	853	1044
12.26	753	1289	842	991
12.29	764	1265	800	972
12.32	760	1337	856	962
12.35	749	1345	840	997
12.38	748	1344	869	967
12.41	790	1401	787	956
12.44	734	1334	830	972
12.47	772	1404	868	952
12.5	833	1394	841	959
12.53	901	1535	781	988
12.56	960	1591	791	932
12.59	1129	1789	880	988
12.62	1197	1952	794	942
12.65	1242	1888	760	922
12.68	1195	1815	801	954
12.71	1008	1652	776	895

12.74	933	1453	808	896
12.77	919	1418	790	961
12.8	854	1421	796	903
12.83	803	1279	849	891
12.86	747	1268	793	932
12.89	764	1295	795	915
12.92	700	1250	817	900
12.95	723	1320	785	928
12.98	701	1289	807	940
13.01	769	1203	768	919
13.04	730	1209	759	940
13.07	728	1188	762	938
13.1	747	1155	796	938
13.13	681	1236	814	892
13.16	712	1168	797	915
13.19	718	1209	765	901
13.22	686	1223	757	914
13.25	698	1180	840	858
13.28	694	1178	842	902
13.31	667	1144	765	908
13.34	669	1158	776	912
13.37	648	1197	818	884
13.4	661	1149	777	855
13.43	692	1177	775	899
13.46	700	1164	748	881
13.49	670	1135	786	936
13.52	677	1121	781	844
13.55	641	1148	765	878
13.58	722	1155	751	882
13.61	703	1117	785	844
13.64	661	1127	748	862
13.67	670	1100	757	880
13.7	727	1130	738	843
13.73	697	1117	724	902
13.76	699	1172	800	862
13.79	686	1157	718	826
13.82	645	1229	724	841
13.85	741	1144	721	825
13.88	668	1163	751	841
13.91	694	1161	761	848
13.94	750	1183	738	843
13.97	775	1303	701	873
14	839	1293	720	804
14.03	868	1373	736	812
14.06	937	1321	681	832
14.09	836	1193	680	793
14.12	832	1132	737	834
14.15	714	1125	750	804
14.18	716	1131	685	833
14.21	726	1056	705	838
14.24	678	1122	674	822
14.27	634	1066	715	780
14.3	666	1033	720	839

14.33	704	1037	680	809
14.36	654	990	721	794
14.39	624	1082	713	816
14.42	676	986	764	800
14.45	621	919	698	804
14.48	633	974	691	791
14.51	605	961	700	780
14.54	645	987	657	785
14.57	650	988	667	796
14.6	660	910	660	763
14.63	632	918	645	737
14.66	638	954	718	808
14.69	665	970	643	793
14.72	658	1011	666	716
14.75	687	962	666	780
14.78	719	1058	676	769
14.81	659	956	677	770
14.84	620	966	697	780
14.87	640	922	663	786
14.9	616	871	670	726
14.93	599	856	624	758
14.96	600	823	680	714
14.99	597	875	608	710
15.02	549	830	639	771
15.05	552	840	654	753
15.08	554	860	627	728
15.11	559	859	684	718
15.14	584	852	651	704
15.17	559	784	622	732
15.2	565	817	619	758
15.23	563	820	607	715
15.26	507	917	638	726
15.29	601	902	624	731
15.32	621	922	629	717
15.35	620	885	656	713
15.38	599	816	630	719
15.41	551	750	625	679
15.44	539	805	645	766
15.47	506	749	631	771
15.5	484	743	583	716
15.53	543	729	604	710
15.56	529	741	624	699
15.59	490	722	646	673
15.62	517	664	611	661
15.65	510	741	608	732
15.68	506	663	629	687
15.71	513	740	611	698
15.74	543	706	587	700
15.77	504	687	645	699
15.8	467	708	554	636
15.83	492	680	590	686
15.86	512	654	583	675
15.89	505	667	621	652

15.92	504	663	566	702
15.95	519	664	608	664
15.98	512	662	646	660
16.01	495	637	611	672
16.04	492	655	573	649
16.07	500	659	573	681
16.1	442	649	601	709
16.13	512	680	593	647
16.16	508	669	589	646
16.19	506	743	561	682
16.22	507	737	577	656
16.25	577	742	548	666
16.28	575	855	591	686
16.31	657	889	530	694
16.34	654	852	582	681
16.37	559	763	593	682
16.4	550	693	558	634
16.43	514	635	586	696
16.46	449	642	578	622
16.49	485	586	588	671
16.52	470	567	558	641
16.55	459	572	550	662
16.58	439	569	540	636
16.61	478	558	542	663
16.64	438	589	573	670
16.67	451	564	600	666
16.7	461	562	558	640
16.73	446	569	530	651
16.76	425	549	545	676
16.79	456	545	579	656
16.82	433	537	549	623
16.85	405	549	562	595
16.88	432	521	575	612
16.91	436	563	560	593
16.94	461	525	557	657
16.97	397	532	593	639
17	421	514	505	638
17.03	439	572	544	633
17.06	435	549	538	661
17.09	414	557	526	688
17.12	403	524	557	642
17.15	431	540	537	637
17.18	442	549	584	641
17.21	455	562	552	652
17.24	454	567	535	604
17.27	454	605	544	580
17.3	467	597	532	630
17.33	496	657	535	638
17.36	543	669	546	626
17.39	596	715	552	649
17.42	548	653	547	596
17.45	533	622	540	610
17.48	468	601	522	609

17.51	485	593	508	592
17.54	489	618	553	646
17.57	494	663	514	570
17.6	497	647	524	636
17.63	541	693	575	602
17.66	525	618	523	599
17.69	446	582	548	651
17.72	427	604	509	611
17.75	478	576	585	600
17.78	474	612	580	624
17.81	507	630	581	578
17.84	486	702	567	579
17.87	557	775	555	615
17.9	572	874	527	606
17.93	700	1065	514	621
17.96	840	1311	506	589
17.99	1108	1605	552	642
18.02	1460	1907	534	616
18.05	1610	1778	539	585
18.08	1446	1536	534	625
18.11	1108	1112	530	614
18.14	867	901	519	559
18.17	674	760	568	617
18.2	557	593	565	591
18.23	516	609	507	616
18.26	464	584	546	616
18.29	462	537	483	617
18.32	411	531	563	612
18.35	414	504	503	618
18.38	449	541	569	613
18.41	389	518	575	604
18.44	410	460	506	591
18.47	414	477	524	578
18.5	424	494	502	599
18.53	429	500	529	521
18.56	400	481	528	590
18.59	410	477	564	609
18.62	402	487	546	570
18.65	411	444	545	598
18.68	385	463	511	633
18.71	376	470	506	616
18.74	397	461	520	625
18.77	386	449	552	616
18.8	423	489	522	608
18.83	377	467	533	590
18.86	405	507	519	592
18.89	380	484	502	586
18.92	392	433	544	639
18.95	399	462	524	626
18.98	395	493	552	589
19.01	389	517	502	624
19.04	384	468	503	640
19.07	434	527	519	590

19.1	401	501	532	606
19.13	435	534	547	640
19.16	425	549	510	590
19.19	458	587	530	564
19.22	506	603	530	611
19.25	477	644	506	610
19.28	597	780	502	599
19.31	689	846	539	621
19.34	775	963	533	581
19.37	798	1006	521	607
19.4	781	862	565	588
19.43	696	662	549	620
19.46	561	593	523	604
19.49	493	568	556	577
19.52	475	567	520	598
19.55	426	535	522	620
19.58	443	526	524	597
19.61	411	489	551	584
19.64	387	506	501	606
19.67	404	509	554	642
19.7	379	492	518	625
19.73	438	462	585	602
19.76	367	489	515	596
19.79	385	482	548	637
19.82	402	482	538	588
19.85	415	459	550	623
19.88	411	504	571	592
19.91	432	502	506	608
19.94	419	478	520	569
19.97	398	466	576	635
20	405	452	544	572
20.03	404	501	569	607
20.06	381	497	543	614
20.09	386	457	567	668
20.12	394	514	562	571
20.15	378	469	528	643
20.18	406	427	511	594
20.21	374	442	575	633
20.24	399	450	521	613
20.27	426	496	537	593
20.3	386	440	554	625
20.33	363	435	587	607
20.36	398	442	558	599
20.39	404	462	522	600
20.42	391	482	550	560
20.45	366	442	514	577
20.48	416	410	542	621
20.51	374	452	521	611
20.54	377	461	529	591
20.57	401	450	533	578
20.6	383	505	546	611
20.63	371	505	567	630
20.66	369	454	536	619



20.69	359	457	572	596
20.72	389	437	556	603
20.75	349	449	582	612
20.78	398	475	566	591
20.81	381	479	528	603
20.84	413	480	492	562
20.87	354	466	501	592
20.9	375	454	570	657
20.93	375	443	527	590
20.96	424	433	586	606
20.99	392	419	547	595
21.02	386	453	499	624
21.05	389	435	536	622
21.08	379	455	563	599
21.11	346	435	552	635
21.14	409	452	570	598
21.17	392	440	577	651
21.2	389	485	503	588
21.23	391	448	588	559
21.26	391	457	581	597
21.29	363	448	511	611
21.32	415	474	558	622
21.35	363	425	564	634
21.38	388	447	570	589
21.41	364	466	571	620
21.44	399	459	519	582
21.47	349	453	551	619
21.5	396	398	576	617
21.53	400	467	565	635
21.56	382	476	540	654
21.59	358	461	605	599
21.62	380	443	594	598
21.65	372	462	548	591
21.68	388	459	567	586
21.71	364	467	576	644
21.74	380	465	569	624
21.77	358	403	546	599
21.8	372	413	584	629
21.83	374	471	549	589
21.86	382	471	579	609
21.89	384	431	600	615
21.92	357	476	592	619
21.95	358	422	605	587
21.98	381	413	557	630
22.01	391	409	590	623
22.04	380	424	546	579
22.07	420	438	611	595
22.1	408	464	575	641
22.13	379	441	583	638
22.16	360	443	629	627
22.19	361	440	567	616
22.22	345	432	599	636
22.25	378	476	555	602

22.28	407	467	600	553
22.31	378	463	546	622
22.34	384	456	613	628
22.37	387	419	616	628
22.4	362	477	589	643
22.43	357	474	566	692
22.46	433	507	589	601
22.49	450	440	596	634
22.52	438	462	596	656
22.55	411	494	631	643
22.58	401	502	597	618
22.61	397	436	639	697
22.64	388	443	632	645
22.67	374	473	609	665
22.7	417	454	659	580
22.73	392	448	641	620
22.76	389	443	619	632
22.79	402	482	579	632
22.82	427	470	599	619
22.85	431	429	686	673
22.88	379	476	569	676
22.91	391	471	632	646
22.94	443	491	604	638
22.97	431	451	590	639
23	428	457	607	614
23.03	403	483	635	676
23.06	445	492	625	649
23.09	455	470	628	708
23.12	441	520	648	624
23.15	427	433	635	660
23.18	474	508	628	666
23.21	471	549	613	677
23.24	453	491	621	643
23.27	508	498	711	608
23.3	510	566	661	696
23.33	468	526	670	666
23.36	506	537	611	620
23.39	527	530	657	637
23.42	495	550	610	638
23.45	497	550	687	646
23.48	483	581	655	634
23.51	535	559	610	700
23.54	562	609	628	709
23.57	585	641	607	666
23.6	576	668	631	660
23.63	656	717	608	673
23.66	617	691	658	716
23.69	585	646	665	682
23.72	507	603	664	706
23.75	518	556	644	673
23.78	502	587	680	716
23.81	481	573	671	694
23.84	422	486	721	698

23.87	430	493	686	700
23.9	409	510	700	686
23.93	412	521	689	761
23.96	434	485	647	730
23.99	406	500	683	726
24.02	415	493	689	710
24.05	437	468	705	709
24.08	400	512	772	723
24.11	388	487	716	737
24.14	441	478	742	775
24.17	446	527	734	707
24.2	429	520	735	740
24.23	447	513	734	745
24.26	445	512	683	722
24.29	470	500	713	733
24.32	428	560	743	762
24.35	491	574	751	709
24.38	499	646	670	762
24.41	530	704	765	729
24.44	616	733	649	764
24.47	627	861	699	711
24.5	722	928	686	756
24.53	810	988	766	754
24.56	854	1034	756	718
24.59	853	1001	726	723
24.62	849	1049	745	760
24.65	856	1064	750	784
24.68	856	971	787	784
24.71	867	922	723	715
24.74	806	867	751	795
24.77	705	812	764	786
24.8	587	700	753	738
24.83	575	648	789	716
24.86	553	595	767	778
24.89	509	639	762	754
24.92	472	613	751	724
24.95	513	618	793	777
24.98	508	561	753	745
25.01	472	563	781	729
25.04	471	552	802	779
25.07	440	527	793	794
25.1	379	494	751	742
25.13	435	510	754	817
25.16	371	520	750	802
25.19	438	496	810	745
25.22	464	500	749	813
25.25	405	474	803	805
25.28	385	519	795	827
25.31	413	463	813	758
25.34	475	507	836	775
25.37	426	510	850	803
25.4	446	553	802	801
25.43	446	510	781	815

25.46	455	529	838	816
25.49	446	525	820	877
25.52	449	567	789	816
25.55	443	558	795	839
25.58	460	531	904	891
25.61	475	525	873	929
25.64	464	544	859	896
25.67	504	610	989	953
25.7	507	595	892	907
25.73	519	647	943	1022
25.76	527	690	959	914
25.79	586	744	1023	941
25.82	672	738	1012	965
25.85	671	791	1022	968
25.88	721	826	1082	992
25.91	716	761	1082	932
25.94	691	786	1026	938
25.97	675	774	1017	978
26	693	743	930	961
26.03	612	723	963	933
26.06	568	666	895	930
26.09	578	630	893	935
26.12	517	564	903	917
26.15	474	535	841	871
26.18	454	494	949	821
26.21	476	477	886	854
26.24	422	523	933	834
26.27	422	478	899	882
26.3	456	472	910	909
26.33	452	517	896	910
26.36	466	528	967	876
26.39	436	552	893	854
26.42	460	556	958	885
26.45	474	618	885	921
26.48	486	589	928	909
26.51	535	636	906	914
26.54	538	731	895	854
26.57	607	744	921	909
26.6	747	852	889	928
26.63	788	898	918	903
26.66	798	891	975	994
26.69	729	776	900	893
26.72	675	772	967	952
26.75	617	686	957	893
26.78	539	622	947	909
26.81	501	593	931	933
26.84	451	575	909	919
26.87	491	528	947	914
26.9	482	597	959	940
26.93	491	596	959	946
26.96	498	564	970	939
26.99	522	597	977	922
27.02	509	637	968	912

27.05	589	689	936	926
27.08	653	757	988	933
27.11	747	951	964	876
27.14	893	1166	927	920
27.17	1206	1417	938	861
27.2	1349	1642	958	909
27.23	1463	1593	958	923
27.26	1414	1508	952	920
27.29	1354	1325	967	955
27.32	1160	1198	957	883
27.35	989	959	1018	917
27.38	870	850	990	911
27.41	701	757	974	894
27.44	670	758	959	887
27.47	616	645	976	962
27.5	606	664	964	906
27.53	592	676	981	903
27.56	562	737	971	930
27.59	584	743	965	957
27.62	666	773	1022	994
27.65	682	841	957	913
27.68	749	956	968	927
27.71	802	1118	941	892
27.74	956	1434	984	926
27.77	1235	1789	960	925
27.8	1729	2559	945	963
27.83	2586	3875	978	931
27.86	4071	5439	931	965
27.89	5788	6899	971	849
27.92	6171	6973	994	949
27.95	5591	6044	944	889
27.98	4749	4840	944	918
28.01	3458	3450	949	919
28.04	2411	2394	981	916
28.07	1597	1765	913	922
28.1	1253	1360	945	948
28.13	956	1099	1014	884
28.16	814	945	978	944
28.19	732	822	967	934
28.22	637	739	959	899
28.25	618	732	945	943
28.28	585	706	952	911
28.31	534	664	947	994
28.34	546	699	949	922
28.37	629	667	1008	976
28.4	575	633	990	940
28.43	524	694	955	905
28.46	529	670	991	853
28.49	520	631	931	882
28.52	542	606	895	983
28.55	517	623	986	950
28.58	490	613	984	932
28.61	475	606	958	950

28.64	519	596	927	901
28.67	466	619	922	859
28.7	475	597	913	884
28.73	521	644	909	878
28.76	479	654	936	875
28.79	588	681	904	882
28.82	563	690	893	874
28.85	641	754	951	939
28.88	696	922	908	924
28.91	770	1001	925	852
28.94	863	1281	929	846
28.97	1095	1608	931	869
29	1390	2128	873	880
29.03	2063	2953	938	948
29.06	2763	3915	925	938
29.09	3928	4927	977	927
29.12	4281	4944	899	858
29.15	4224	4512	961	889
29.18	3690	3679	921	903
29.21	3018	2890	905	871
29.24	2140	2097	896	887
29.27	1600	1542	885	828
29.3	1188	1204	934	899
29.33	969	990	876	912
29.36	793	866	895	851
29.39	652	712	890	811
29.42	554	666	843	864
29.45	556	561	888	853
29.48	527	619	886	822
29.51	478	539	842	874
29.54	523	549	902	850
29.57	487	526	829	824
29.6	455	536	829	840
29.63	468	507	892	841
29.66	456	539	870	840
29.69	458	488	874	826
29.72	416	501	869	885
29.75	431	557	844	843
29.78	462	497	826	876
29.81	505	515	859	841
29.84	457	557	788	844
29.87	446	482	833	862
29.9	469	541	855	806
29.93	456	513	882	811
29.96	417	482	818	882
29.99	427	476	894	835
30.02	434	470	822	799
30.05	375	455	868	806
30.08	417	503	841	862
30.11	389	465	834	833
30.14	442	479	827	817
30.17	427	448	805	814
30.2	399	467	823	818

30.23	382	448	837	754
30.26	405	491	812	843
30.29	356	478	829	800
30.32	386	455	795	761
30.35	405	441	802	822
30.38	436	473	811	768
30.41	413	470	793	769
30.44	414	455	780	741
30.47	417	504	830	786
30.5	418	518	800	844
30.53	437	492	769	807
30.56	430	493	844	789
30.59	473	494	832	852
30.62	458	531	779	823
30.65	426	546	792	765
30.68	477	550	778	759
30.71	495	651	808	796
30.74	567	708	769	748
30.77	615	791	781	781
30.8	715	961	789	773
30.83	797	1146	809	743
30.86	1044	1382	813	737
30.89	1280	1775	741	754
30.92	1648	2247	804	745
30.95	1993	2526	768	741
30.98	2164	2489	751	788
31.01	2071	2145	713	749
31.04	1730	1741	806	753
31.07	1430	1337	810	748
31.1	1080	1025	758	714
31.13	840	819	768	778
31.16	639	735	728	749
31.19	564	642	743	754
31.22	538	592	706	776
31.25	496	536	767	791
31.28	469	507	716	813
31.31	447	477	700	766
31.34	432	466	768	766
31.37	442	443	700	746
31.4	430	498	696	715
31.43	407	487	724	727
31.46	428	494	763	779
31.49	394	445	771	744
31.52	420	487	717	768
31.55	371	484	738	765
31.58	423	478	703	712
31.61	390	520	769	739
31.64	425	475	663	702
31.67	419	499	707	717
31.7	419	513	668	690
31.73	466	508	734	733
31.76	435	573	730	682
31.79	522	612	756	725

31.82	509	622	728	704
31.85	594	698	689	754
31.88	663	856	676	714
31.91	860	1011	684	742
31.94	1046	1227	720	751
31.97	1165	1314	695	704
32	1252	1385	666	675
32.03	1240	1310	683	692
32.06	1120	1323	710	751
32.09	1032	1163	658	765
32.12	935	1026	683	677
32.15	809	874	710	686
32.18	708	742	725	701
32.21	597	687	719	715
32.24	571	628	709	711
32.27	534	589	726	737
32.3	484	588	718	704
32.33	502	562	694	726
32.36	495	607	712	757
32.39	489	602	752	752
32.42	470	558	753	824
32.45	486	563	859	790
32.48	516	502	818	822
32.51	448	522	814	808
32.54	379	525	786	836
32.57	404	520	760	781
32.6	391	472	779	798
32.63	384	456	745	795
32.66	424	444	697	748
32.69	393	455	696	736
32.72	396	417	694	725
32.75	399	471	708	686
32.78	399	432	711	687
32.81	381	464	707	698
32.84	376	450	696	704
32.87	371	467	639	719
32.9	382	431	684	730
32.93	402	472	681	719
32.96	431	443	644	699
32.99	390	433	732	692
33.02	403	459	639	704
33.05	383	428	652	721
33.08	404	452	681	726
33.11	385	495	663	699
33.14	421	423	704	713
33.17	405	493	720	721
33.2	420	456	729	703
33.23	383	505	682	731
33.26	400	490	686	739
33.29	414	459	751	758
33.32	429	504	788	782
33.35	409	496	825	786
33.38	443	531	826	738



33.41	431	521	829	791
33.44	434	509	797	805
33.47	471	543	799	797
33.5	466	568	803	752
33.53	502	616	788	776
33.56	588	614	756	687
33.59	590	655	671	699
33.62	603	608	680	711
33.65	562	629	709	732
33.68	575	604	679	695
33.71	536	582	617	697
33.74	544	568	662	669
33.77	506	568	678	684
33.8	499	526	638	640
33.83	545	535	631	685
33.86	481	525	618	643
33.89	478	490	703	657
33.92	483	534	671	636
33.95	483	540	627	702
33.98	473	490	645	615
34.01	446	472	625	671
34.04	441	466	611	631
34.07	440	502	622	624
34.1	416	444	611	640
34.13	426	454	592	674
34.16	382	461	628	673
34.19	368	480	599	597
34.22	413	477	633	641
34.25	414	428	578	654
34.28	384	447	649	620
34.31	376	430	561	633
34.34	383	438	587	625
34.37	396	451	569	606
34.4	386	448	607	681
34.43	378	422	594	692
34.46	348	505	602	614
34.49	390	495	588	612
34.52	389	463	589	634
34.55	364	470	600	658
34.58	450	482	584	653
34.61	438	505	545	620
34.64	438	534	583	635
34.67	438	512	566	605
34.7	407	515	575	638
34.73	460	497	619	648
34.76	482	469	616	628
34.79	421	475	610	579
34.82	468	444	595	625
34.85	383	491	534	611
34.88	419	465	568	593
34.91	405	459	613	629
34.94	403	464	553	625
34.97	390	414	568	615

35	380	440	585	616
35.03	406	430	601	610
35.06	408	483	585	623
35.09	407	480	568	578
35.12	401	470	602	607
35.15	409	496	550	598
35.18	396	503	576	610
35.21	420	495	606	607
35.24	449	494	575	628
35.27	454	494	571	601
35.3	438	486	557	638
35.33	422	469	589	593
35.36	381	484	565	657
35.39	439	493	564	582
35.42	425	497	574	602
35.45	424	511	559	609
35.48	429	482	576	597
35.51	428	496	564	623
35.54	426	552	538	565
35.57	492	563	533	600
35.6	495	627	540	606
35.63	532	627	558	583
35.66	598	673	571	582
35.69	659	752	498	583
35.72	710	724	549	596
35.75	711	753	498	619
35.78	755	798	554	666
35.81	688	821	573	605
35.84	696	758	548	602
35.87	676	790	532	584
35.9	741	847	527	592
35.93	818	866	618	569
35.96	837	1019	548	597
35.99	840	1035	544	558
36.02	899	1040	563	589
36.05	891	996	515	582
36.08	837	911	538	584
36.11	760	862	531	607
36.14	715	736	525	567
36.17	622	674	553	584
36.2	559	623	565	562
36.23	526	583	574	595
36.26	514	538	506	575
36.29	427	506	542	601
36.32	451	495	593	583
36.35	432	450	570	563
36.38	375	510	525	620
36.41	404	450	555	592
36.44	401	447	536	575
36.47	387	451	584	591
36.5	377	448	546	597
36.53	388	506	571	589
36.56	425	472	568	588

36.59	386	454	529	565
36.62	396	431	524	556
36.65	417	471	524	593
36.68	399	450	545	604
36.71	406	460	548	582
36.74	427	482	522	558
36.77	404	464	544	596
36.8	429	473	514	560
36.83	454	489	538	578
36.86	409	464	563	609
36.89	406	458	512	611
36.92	396	401	526	566
36.95	371	432	570	577
36.98	368	438	542	599
37.01	383	451	546	563
37.04	387	392	532	529
37.07	408	406	544	541
37.1	362	435	517	579
37.13	346	422	562	584
37.16	368	423	513	586
37.19	393	419	533	571
37.22	367	447	513	602
37.25	370	411	506	541
37.28	368	458	545	556
37.31	393	422	525	617
37.34	370	420	553	536
37.37	369	438	476	616
37.4	377	375	550	558
37.43	383	422	534	554
37.46	398	412	548	566
37.49	360	445	548	534
37.52	402	374	541	600
37.55	368	425	535	565
37.58	391	435	532	574
37.61	358	433	536	595
37.64	341	424	496	559
37.67	388	401	523	560
37.7	382	406	551	535
37.73	374	450	514	573
37.76	394	410	527	564
37.79	401	388	505	585
37.82	377	423	525	562
37.85	396	438	503	600
37.88	367	487	521	551
37.91	402	420	516	562
37.94	397	439	528	597
37.97	396	404	523	579
38	348	511	519	601
38.03	403	466	495	537
38.06	418	465	512	563
38.09	419	469	520	543
38.12	415	475	515	563
38.15	470	478	543	561

38.18	469	496	461	591
38.21	517	544	558	566
38.24	496	532	526	577
38.27	492	504	569	548
38.3	420	520	445	599
38.33	509	539	533	574
38.36	438	508	539	569
38.39	442	498	504	561
38.42	483	498	521	572
38.45	417	480	529	570
38.48	414	497	505	538
38.51	443	532	489	572
38.54	494	558	506	563
38.57	514	576	507	550
38.6	507	608	551	621
38.63	584	615	515	577
38.66	629	609	516	557
38.69	572	614	547	573
38.72	573	591	496	564
38.75	513	606	545	597
38.78	554	601	572	589
38.81	518	557	520	551
38.84	471	524	543	558
38.87	487	526	485	548
38.9	511	535	514	571
38.93	465	514	498	564
38.96	473	510	503	568
38.99	445	457	496	539
39.02	469	539	490	548
39.05	464	535	475	583
39.08	500	523	469	584
39.11	459	564	527	595
39.14	510	571	537	578
39.17	502	566	518	533
39.2	501	584	493	568
39.23	515	553	499	534
39.26	533	562	506	558
39.29	531	567	519	594
39.32	541	626	511	550
39.35	535	654	490	564
39.38	588	639	537	541
39.41	582	609	514	555
39.44	609	640	553	567
39.47	626	633	512	554
39.5	600	651	541	541
39.53	587	647	522	602
39.56	551	575	496	575
39.59	537	576	519	583
39.62	505	564	509	572
39.65	496	516	512	576
39.68	479	552	540	593
39.71	497	533	508	552
39.74	480	565	533	578

39.77	475	580	511	566
39.8	530	567	519	595
39.83	559	608	509	567
39.86	574	702	520	548
39.89	627	823	549	623
39.92	759	828	505	570
39.95	781	894	528	575
39.98	874	954	522	624
40.01	855	942	547	610
40.04	780	910	513	579
40.07	800	842	506	583
40.1	755	779	509	543
40.13	650	694	496	566
40.16	599	592	497	567
40.19	582	570	568	583
40.22	506	559	537	590
40.25	463	528	538	615
40.28	450	458	551	619
40.31	453	488	538	623
40.34	447	471	543	591
40.37	392	474	562	560
40.4	377	462	512	558
40.43	385	481	551	609
40.46	405	423	546	603
40.49	415	484	519	578
40.52	382	490	560	571
40.55	408	444	518	630
40.58	397	469	549	568
40.61	372	439	506	595
40.64	408	476	538	595
40.67	384	469	550	591
40.7	389	451	538	638
40.73	404	509	568	586
40.76	415	448	520	572
40.79	396	470	534	632
40.82	371	447	574	600
40.85	361	463	553	625
40.88	404	434	567	569
40.91	396	431	542	606
40.94	416	435	527	568
40.97	381	459	595	582
41	410	452	588	561
41.03	401	460	558	598
41.06	407	459	510	620
41.09	378	492	534	610
41.12	449	487	526	557
41.15	403	522	566	568
41.18	490	474	546	572
41.21	442	530	518	608
41.24	460	504	525	598
41.27	453	483	535	555
41.3	470	560	473	587
41.33	453	473	526	566

41.36	440	491	513	590
41.39	409	488	495	568
41.42	432	462	531	575
41.45	448	449	549	603
41.48	425	508	562	609
41.51	396	437	548	569
41.54	406	466	564	600
41.57	364	440	527	605
41.6	376	443	548	580
41.63	395	413	539	600
41.66	410	451	519	592
41.69	399	438	541	607
41.72	396	416	498	618
41.75	378	457	540	609
41.78	374	453	537	598
41.81	395	441	537	566
41.84	393	420	491	538
41.87	389	447	549	597
41.9	400	424	542	598
41.93	379	433	524	551
41.96	383	423	526	577
41.99	355	467	493	593
42.02	422	449	505	561
42.05	366	448	547	629
42.08	405	438	522	593
42.11	424	464	529	584
42.14	422	490	534	589
42.17	444	504	532	549
42.2	486	539	520	568
42.23	503	545	506	580
42.26	483	568	550	566
42.29	481	610	541	591
42.32	549	655	516	567
42.35	628	650	538	596
42.38	572	664	531	556
42.41	584	599	537	581
42.44	608	629	536	561
42.47	580	637	567	593
42.5	564	636	527	593
42.53	636	600	520	596
42.56	602	621	520	638
42.59	556	592	524	605
42.62	522	600	558	561
42.65	494	608	521	577
42.68	504	555	500	586
42.71	484	516	528	576
42.74	412	476	559	589
42.77	460	480	512	592
42.8	435	455	561	576
42.83	383	451	501	592
42.86	396	447	501	617
42.89	401	470	564	557
42.92	439	431	539	580

42.95	386	498	538	540
42.98	382	484	508	596
43.01	472	526	554	586
43.04	421	524	548	618
43.07	484	554	527	602
43.1	507	572	520	537
43.13	568	588	577	610
43.16	504	593	540	582
43.19	504	580	600	571
43.22	516	549	564	597
43.25	492	550	556	563
43.28	491	547	541	613
43.31	462	494	519	577
43.34	429	433	571	584
43.37	422	487	581	614
43.4	410	448	569	604
43.43	395	426	537	624
43.46	416	427	521	538
43.49	367	437	492	579
43.52	417	455	511	610
43.55	389	452	512	597
43.58	393	471	528	603
43.61	389	485	588	558
43.64	392	482	554	588
43.67	377	476	570	617
43.7	396	469	530	564
43.73	428	465	539	576
43.76	451	464	557	618
43.79	434	497	562	602
43.82	437	504	524	581
43.85	437	479	560	588
43.88	424	473	534	584
43.91	423	483	544	595
43.94	420	470	574	585
43.97	467	459	564	623
44	440	470	561	588
44.03	360	460	557	588
44.06	418	447	514	585
44.09	383	440	538	607
44.12	391	433	528	565
44.15	387	428	535	620
44.18	396	404	553	634
44.21	353	409	538	583
44.24	380	431	502	606
44.27	368	437	519	566
44.3	415	446	576	618
44.33	364	436	551	631
44.36	371	429	566	537
44.39	372	474	509	637
44.42	379	417	545	594
44.45	387	438	547	600
44.48	376	448	545	591
44.51	376	420	579	602

44.54	421	469	534	598
44.57	389	424	564	622
44.6	431	481	513	626
44.63	402	478	549	614
44.66	443	495	535	569
44.69	458	524	567	594
44.72	442	532	550	617
44.75	499	546	534	597
44.78	477	609	549	605
44.81	500	577	549	611
44.84	505	560	495	623
44.87	536	564	511	568
44.9	565	642	525	613
44.93	560	593	541	639
44.96	554	632	595	648
44.99	562	733	585	581
45.02	641	876	572	597
45.05	863	930	580	576
45.08	921	1141	546	602
45.11	1130	1300	574	605
45.14	1245	1347	586	611
45.17	1215	1371	589	557
45.2	1249	1296	564	596
45.23	1162	1176	578	599
45.26	1102	1129	581	641
45.29	976	1025	546	600
45.32	809	906	580	581
45.35	745	818	545	589
45.38	660	736	611	629
45.41	619	628	569	577
45.44	567	589	535	603
45.47	547	606	516	659
45.5	556	598	533	627
45.53	506	555	574	596
45.56	488	509	600	641
45.59	476	572	518	590
45.62	453	551	560	630
45.65	475	464	526	603
45.68	485	473	552	580
45.71	430	518	578	570
45.74	479	540	623	582
45.77	438	531	573	622
45.8	436	532	540	619
45.83	441	518	609	578
45.86	495	556	550	600
45.89	477	581	566	610
45.92	517	542	551	605
45.95	518	572	566	635
45.98	554	582	541	636
46.01	588	601	566	588
46.04	564	646	531	608
46.07	613	621	589	628
46.1	613	664	562	617



46.13	621	726	602	610
46.16	650	705	535	604
46.19	701	753	531	589
46.22	662	761	569	621
46.25	653	735	546	587
46.28	678	722	570	609
46.31	626	707	634	662
46.34	610	645	575	639
46.37	532	588	517	641
46.4	578	626	550	632
46.43	546	618	563	624
46.46	460	592	552	692
46.49	475	523	578	686
46.52	465	496	589	623
46.55	489	550	590	692
46.58	444	531	555	664
46.61	431	553	608	636
46.64	472	496	606	636
46.67	465	519	606	653
46.7	484	536	642	643
46.73	445	530	646	635
46.76	487	553	603	644
46.79	490	518	617	634
46.82	470	587	602	621
46.85	502	524	597	638
46.88	469	582	599	648
46.91	507	550	575	631
46.94	513	569	589	622
46.97	483	607	590	606
47	551	608	569	573
47.03	527	572	571	610
47.06	523	622	510	660
47.09	521	651	616	603
47.12	595	667	573	613
47.15	616	650	585	596
47.18	612	716	585	611
47.21	663	717	526	607
47.24	663	747	567	617
47.27	697	734	555	636
47.3	781	813	559	622
47.33	818	919	591	648
47.36	920	1030	585	606
47.39	965	1071	640	596
47.42	962	994	590	595
47.45	894	975	607	655
47.48	890	902	560	627
47.51	800	836	599	630
47.54	774	827	584	622
47.57	708	729	608	614
47.6	609	671	560	593
47.63	543	620	597	630
47.66	564	522	631	664
47.69	459	570	603	640

47.72	452	573	569	644
47.75	454	537	598	612
47.78	471	525	581	656
47.81	461	578	583	654
47.84	472	578	527	588
47.87	507	592	546	618
47.9	501	617	569	627
47.93	534	615	591	619
47.96	562	621	581	627
47.99	606	708	559	650
48.02	676	787	593	619
48.05	764	817	548	625
48.08	830	944	550	628
48.11	871	1035	605	649
48.14	954	1063	602	649
48.17	1059	1217	561	615
48.2	1092	1266	601	670
48.23	1189	1268	539	660
48.26	1162	1245	571	637
48.29	1123	1143	589	646
48.32	1121	1144	602	626
48.35	1016	1002	585	601
48.38	857	1006	581	686
48.41	829	847	621	635
48.44	717	769	573	644
48.47	649	734	525	655
48.5	619	628	654	649
48.53	567	548	608	668
48.56	516	539	544	582
48.59	533	536	617	660
48.62	473	541	558	678
48.65	465	472	609	639
48.68	436	509	585	621
48.71	450	546	598	669
48.74	432	480	564	612
48.77	429	515	529	631
48.8	433	500	590	596
48.83	447	522	554	611
48.86	513	493	577	627
48.89	500	558	583	619
48.92	469	566	630	671
48.95	519	617	569	631
48.98	481	573	640	629
49.01	506	583	629	682
49.04	514	618	569	611
49.07	562	622	581	633
49.1	600	651	569	660
49.13	595	689	612	665
49.16	677	681	556	615
49.19	680	731	570	642
49.22	705	721	588	609
49.25	653	699	607	659
49.28	676	661	579	616

49.31	638	644	612	643
49.34	600	652	604	603
49.37	611	624	620	621
49.4	621	639	625	655
49.43	595	652	559	625
49.46	603	646	612	661
49.49	628	665	548	639
49.52	630	657	597	649
49.55	586	604	637	641
49.58	584	687	621	684
49.61	601	683	610	669
49.64	604	727	624	631
49.67	609	648	645	683
49.7	558	612	632	634
49.73	595	693	657	644
49.76	596	631	636	675
49.79	591	654	625	636
49.82	574	645	635	643
49.85	531	661	557	665
49.88	573	595	623	641
49.91	551	635	623	637
49.94	543	590	544	657
49.97	536	558	594	615
50	516	580	571	602
50.03	484	517	582	663
50.06	459	525	588	600
50.09	471	544	617	613
50.12	441	533	582	645
50.15	516	474	584	602
50.18	438	546	653	614
50.21	459	527	550	672
50.24	536	562	569	652
50.27	492	567	587	689
50.3	547	622	584	631
50.33	554	619	564	632
50.36	601	691	638	630
50.39	689	726	580	624
50.42	676	792	603	661
50.45	725	781	628	559
50.48	762	789	598	600
50.51	734	791	577	626
50.54	699	789	539	619
50.57	687	780	566	600
50.6	625	695	600	626
50.63	599	636	581	619
50.66	525	625	556	614
50.69	502	552	615	603
50.72	514	532	594	610
50.75	452	543	616	646
50.78	484	528	598	619
50.81	438	499	600	649
50.84	437	501	591	629
50.87	459	469	616	662

50.9	397	459	512	613
50.93	413	460	578	646
50.96	386	496	619	596
50.99	387	453	580	599
51.02	412	482	556	614
51.05	418	462	602	621
51.08	404	443	590	567
51.11	382	469	548	591
51.14	402	466	564	644
51.17	461	473	590	651
51.2	429	486	548	612
51.23	407	439	551	605
51.26	386	486	604	627
51.29	456	462	525	638
51.32	395	474	563	607
51.35	447	503	530	631
51.38	454	513	614	604
51.41	445	507	602	629
51.44	453	520	570	630
51.47	467	544	602	588
51.5	504	575	617	628
51.53	487	551	597	607
51.56	519	566	579	610
51.59	558	596	610	655
51.62	553	579	557	583
51.65	568	610	581	628
51.68	548	677	564	608
51.71	608	607	584	623
51.74	578	604	607	638
51.77	546	619	578	653
51.8	559	611	562	606
51.83	544	612	629	619
51.86	524	561	567	632
51.89	516	549	556	634
51.92	495	510	564	626
51.95	468	554	561	656
51.98	457	534	531	622
52.01	449	506	564	631
52.04	431	509	548	621
52.07	413	497	553	624
52.1	407	469	575	624
52.13	393	469	581	608
52.16	381	483	550	632
52.19	406	455	560	615
52.22	444	482	565	644
52.25	418	482	519	602
52.28	430	492	528	621
52.31	394	474	552	630
52.34	449	480	542	610
52.37	438	493	607	629
52.4	409	476	561	628
52.43	375	449	576	612
52.46	427	483	560	593

52.49	405	469	589	614
52.52	424	490	573	597
52.55	392	468	576	612
52.58	464	459	616	598
52.61	421	445	602	589
52.64	419	438	540	615
52.67	454	493	597	619
52.7	410	486	570	593
52.73	457	506	581	614
52.76	508	495	549	620
52.79	488	497	590	643
52.82	465	583	565	638
52.85	564	552	568	625
52.88	533	631	569	606
52.91	584	628	563	621
52.94	596	633	597	639
52.97	509	597	573	601
53	535	606	588	588
53.03	559	627	577	580
53.06	614	622	547	651
53.09	610	687	564	647
53.12	645	711	619	629
53.15	670	764	560	622
53.18	714	830	554	640
53.21	797	912	540	645
53.24	852	973	576	606
53.27	971	989	551	637
53.3	903	1002	578	631
53.33	851	925	593	643
53.36	851	845	543	599
53.39	823	881	571	643
53.42	759	871	569	599
53.45	682	731	541	611
53.48	632	669	552	662
53.51	602	643	556	613
53.54	533	645	543	596
53.57	476	537	585	648
53.6	482	553	589	603
53.63	498	573	558	589
53.66	557	566	547	635
53.69	523	640	552	606
53.72	578	666	546	651
53.75	638	724	564	643
53.78	729	743	566	628
53.81	768	833	553	634
53.84	812	910	578	593
53.87	878	1018	544	636
53.9	925	1020	553	617
53.93	1037	1120	570	585
53.96	1091	1147	608	677
53.99	1066	1188	583	649
54.02	1098	1135	600	626
54.05	1015	1065	593	641

54.08	889	996	600	643
54.11	824	937	573	633
54.14	774	893	636	620
54.17	763	795	574	645
54.2	673	717	596	612
54.23	660	700	612	626
54.26	617	616	555	615
54.29	595	584	581	635
54.32	575	570	588	644
54.35	576	568	600	647
54.38	524	589	604	638
54.41	516	571	560	588
54.44	508	552	553	647
54.47	502	536	567	651
54.5	543	548	573	617
54.53	519	546	570	613
54.56	504	517	586	614
54.59	460	546	573	646
54.62	452	520	531	624
54.65	457	526	562	596
54.68	458	541	524	626
54.71	473	503	572	608
54.74	536	563	562	630
54.77	513	583	582	611
54.8	496	521	575	619
54.83	475	557	580	564
54.86	510	530	559	625
54.89	548	590	582	631
54.92	527	572	593	637
54.95	521	576	568	641
54.98	517	542	557	566
55.01	501	561	545	631
55.04	526	551	567	640
55.07	507	551	600	645
55.1	527	518	541	643
55.13	473	530	562	636
55.16	471	530	566	646
55.19	471	494	585	618
55.22	478	501	565	636
55.25	458	495	551	637
55.28	450	522	577	635
55.31	408	448	580	599
55.34	414	440	613	620
55.37	440	457	554	609
55.4	413	484	563	595
55.43	419	488	553	593
55.46	454	478	562	585
55.49	444	497	553	590
55.52	445	473	560	602
55.55	459	503	587	662
55.58	458	470	544	606
55.61	503	483	564	599
55.64	415	494	521	605

55.67	444	467	537	608
55.7	434	484	534	663
55.73	483	516	512	624
55.76	476	462	574	580
55.79	462	547	549	583
55.82	476	566	549	626
55.85	453	584	504	586
55.88	520	630	534	586
55.91	528	604	566	609
55.94	626	681	510	552
55.97	607	659	528	568
56	614	694	589	553
56.03	638	673	524	570
56.06	636	700	539	591
56.09	613	722	539	578
56.12	593	726	525	575
56.15	586	626	536	602
56.18	528	677	577	601
56.21	616	563	519	623
56.24	527	590	507	588
56.27	501	586	561	565
56.3	498	524	586	572
56.33	487	527	525	524
56.36	484	516	505	589
56.39	462	514	535	622
56.42	462	500	535	611
56.45	483	548	504	551
56.48	514	523	501	584
56.51	481	534	543	601
56.54	468	568	571	556
56.57	468	570	541	608
56.6	481	561	535	603
56.63	508	543	500	618
56.66	538	565	507	577
56.69	500	560	563	615
56.72	548	587	523	606
56.75	529	632	519	611
56.78	483	544	509	607
56.81	511	555	482	611
56.84	468	549	550	604
56.87	453	505	496	570
56.9	512	492	485	604
56.93	431	515	521	605
56.96	431	534	516	577
56.99	452	492	560	566
57.02	412	458	586	601
57.05	382	503	533	555
57.08	409	486	519	596
57.11	386	494	550	590
57.14	422	470	530	570
57.17	426	441	562	614
57.2	367	463	538	548
57.23	435	456	502	603

57.26	405	456	522	530
57.29	401	489	504	579
57.32	463	496	546	579
57.35	427	508	521	567
57.38	449	489	502	603
57.41	425	496	527	609
57.44	460	520	529	604
57.47	462	558	482	638
57.5	482	564	502	595
57.53	494	567	536	591
57.56	537	552	533	564
57.59	577	607	524	585
57.62	585	678	545	552
57.65	635	725	495	613
57.68	685	761	539	587
57.71	704	827	515	556
57.74	719	786	550	578
57.77	700	807	539	588
57.8	639	740	511	543
57.83	677	723	499	566
57.86	663	749	507	541
57.89	648	688	475	572
57.92	632	699	515	612
57.95	562	645	543	561
57.98	580	622	501	576
58.01	550	574	511	660
58.04	509	636	474	574
58.07	555	569	544	579
58.1	466	548	504	602
58.13	498	530	510	593
58.16	483	524	528	602
58.19	462	519	556	599
58.22	472	536	560	551
58.25	457	501	511	611
58.28	475	503	530	545
58.31	390	492	551	608
58.34	427	482	560	554
58.37	430	471	497	599
58.4	447	446	556	594
58.43	440	474	550	599
58.46	418	468	593	620
58.49	383	487	543	579
58.52	397	478	565	625
58.55	420	435	519	636
58.58	388	483	560	640
58.61	397	455	544	630
58.64	380	469	564	632
58.67	407	473	501	651
58.7	395	505	578	576
58.73	437	447	564	595
58.76	425	463	543	607
58.79	423	461	500	539
58.82	410	457	539	568



58.85	441	459	541	568
58.88	426	503	512	621
58.91	468	476	550	583
58.94	429	512	566	578
58.97	494	534	490	589
59	491	538	519	562
59.03	505	533	525	575
59.06	490	563	506	552
59.09	525	595	561	551
59.12	512	572	505	579
59.15	564	575	516	606
59.18	577	616	516	571
59.21	603	621	498	516
59.24	572	643	516	569
59.27	616	652	515	549
59.3	607	632	517	595
59.33	610	697	539	574
59.36	569	630	503	562
59.39	584	616	502	563
59.42	549	593	546	574
59.45	494	535	518	586
59.48	521	538	504	590
59.51	496	549	518	549
59.54	497	543	501	570
59.57	494	512	502	566
59.6	417	489	532	564
59.63	417	466	516	559
59.66	401	451	482	559
59.69	421	493	437	554
59.72	411	446	511	557
59.75	415	453	544	568
59.78	414	483	484	561
59.81	399	449	487	616
59.84	371	466	505	535
59.87	428	432	514	529
59.9	395	441	511	495
59.93	406	450	503	570
59.96	430	465	471	544
59.99	376	480	508	639